Aus dem
Department für Diagnostische Labormedizin der
Universität Tübingen
Institut für Pathologie und Neuropathologie
Abteilung Allgemeine und Molekulare Pathologie
Und Pathologische Anatomie

Molecular analysis of extranodal NK/T-cell lymphoma, nasal type in Latin America

Inaugural-Dissertation
zur Erlangung des Doktorgrades
der Medizin

der Medizinischen Fakultät
der Eberhard-Karls-Universität
zu Tübingen

vorgelegt von

Montes-Mojarro, Ivonne Aidee

2023

Gedruckt mit Genehmigung der Fakultät der Medizinischen Eberhard-Karls-Universität Tübingen.

Dekan:	Professor Dr. B. Pichler
1. Berichterstatter:	Professorin Dr. L. Quintanilla-Martinez de Fend
2. Berichterstatter:	Professorin Dr. B Schittek
3. Berichterstatter:	Professor Dr. H-G Kopp
4. Berichterstatter:	Professor DR. T. Menter
Tag der Disputation	25.10.2023

Parts of the results presented in this dissertation have already been published elsewhere

Montes-Mojarro IA, Chen BJ, Ramirez-Ibarguen AF, Quezada-Fiallos CM, Pérez-Báez WB, Dueñas D, Casavilca-Zambrano S, Ortiz-Mayor M, Rojas-Bilbao E, García-Rivello H, Metrebian MF, Narbaitz M, Barrionuevo C, Lome-Maldonado C, Bonzheim I, Fend F, Steinhilber J, Quintanilla-Martinez L. Mutational profile and EBV strains of extranodal NK/T-cell lymphoma, nasal type in Latin America. *Mod Pathol* **2020** May; 33(5):781-791. doi: 10.1038/s41379-019-0415-5.

Montes-Mojarro IA, Fend F, Quintanilla-Martinez L. EBV and the Pathogenesis of NK/T Cell Lymphoma. *Cancers (Basel)* 2021 Mar 19; **13**(6).

I. Dedications

This dissertation is especially dedicated to my mother, my brother and my nephews Mateo and Nicolas, who are the most important supporters of my personal and academic life. My lovely mother, who taught me that great things in life, can only be achieved with perseveranc0e and hard work. To Pablo Napal, for being by my side, pushing me forward and being so patient.

I also dedicate this work to Dr. Carlos Ortiz-Hidalgo, who introduced me the academic pathology world and has always been and will always be a role model for me.

II. *Table of Contents*

III. List of abbreviations

ALCL:	Anaplastic Large Cell Lymphoma
ALK:	Anaplastic Lymphoma Kinase
AWD:	Alive with disease
BART:	*Bam*HI-A region rightward transcript
CHL:	Classic Hodgkin Lymphoma
DOD:	Dead of disease
EBER:	EBV-encoded nuclear antigen
ECOG,	Eastern Cooperative Oncology Group
IPI:	International Prognostic Index
LMP1:	Latent Membrane Protein-1
NGS:	Next generation sequencing
PCR:	Polymerase chain reaction
EBNA:	Epstein-Barr nuclear antigen
EBV:	Epstein Barr Virus
ERK:	Extracellular signal-regulated kinase
JAK:	Janus kinase
JNK:	c-Jun N-Terminal kinase
LDH:	Lactate dehydrogenase
LGL:	T-cell large granular lymphocytic
LP:	Leader protein
LPD:	Lymphoproliferative disorders (LPD
MAPK:	Mitogen-activated protein kinase
NED:	no evidence of disease
NF-κB:	Nuclear factor-κB
PDL1:	Programmed death-ligand 1
STAT:	signal transducer and activator of transcription
TCR:	T-cell receptor
T-LGL:	T-cell large granular lymphocytic
UAT:	Upper aerodigestive tract
VAF:	Variant allele frequency
WHO:	World Health Organization

IV. List of figures

V. List of tables

1. Introduction

1.1 Definition and Epidemiology

Extranodal Natural killer/T (NK/T)-cell lymphoma, nasal type (ENKTCL) comprises a highly aggressive group of clonal proliferations predominantly of NK cell lineage and rarely of T-cell origin, with distinctive clinicopathological features associated with Epstein Virus Bar (EBV) infection. This lymphoma commonly arises in the upper aerodigestive tract (UAT), being the nasal cavity the distinctive site of involvement [1]. ENKTCL accounts for 6-15% of all non-Hodgkin lymphomas in East Asian countries, 2-8% in Latin-American countries and less than 0.1% in Europe and North America [2-5]. In East Asia countries, ENKTCL is more frequent in Thailand (34%), China (21%), Japan (12%) and South Korea (9%) [6]. The incidence of ENKTCL in Latin America is frequent and higher in native populations from Guatemala, Mexico, Peru, Bolivia and Ecuador, while in other countries with a high proportion of European migration, such as Argentina and Uruguay, is relatively less common. Among the different series of ENKTCL reported from Latin America, the highest frequency is seen in Peru (131 cases, 29.2%) [7-10] followed by Brazil (114 cases, 25.4%) [9,11-13], Guatemala (125 cases, 27.8%) [9,14], Chile (31 cases, 6.9%) [13,15] and Mexico (48 cases, 10.7%) [5,16]. For instance, in Mexico ENKTCL accounts for approximately 10% of all malignant lymphomas and 40% of all T-cell lymphomas [17].

1.2 History

In the past, this neoplasm was known as "lethal midline granuloma", referring to the aggressive course and to the rapid destruction of the midline structures of the face, which leads relentlessly to death [18]. Likewise, this neoplasm was also called "polymorphic reticulosis". This term denoted the morphology of this neoplasm composed of a polymorphic population of lymphoid, neutrophil and eosinophil cells, imitating a reactive infiltrate [19]. Successively, the REAL classification of lymphoid malignancies enlisted these group as “angiocentric T-cell lymphomas”,

because of their constant propensity to infiltrate blood vessels and its origin on T-cells, recognized by the expression of the T-cell receptor (TCR) antigen (CD3), which was detected by immunohistochemistry (IHC) using polyclonal antibodies [20]. Later, with the emergence of monoclonal antibodies, it was recognized that CD3 expression is mainly present on the cytoplasm of the neoplastic cells, which is a unique feature of NK cells since they do not express the epsilon chain of CD3 (CD3ε) on their surface. Molecular analysis by Southern Blot also supported the origin of this lymphoma in NK-cells by demonstrating the germline configuration of the TCR gene. In the updated 2017 World Health Organization (WHO) classification of lymphoid neoplasms, these lymphomas are referred to as extranodal NK/T cell lymphoma, to reflect their NK and T-cell origin acknowledgement [1].

1.3 Clinical features

ENKTCL in earlier stages most commonly presents with nasal obstruction, epistaxis, purulent nasal discharge and facial swelling; whereas in later stages this lymphoma can extend to surrounding tissues, originating extensive necrotic lesions and destruction of the hard palate [21,22] (Figure 1).

Figure 1. **Clinical presentation in a Mexican patient with natural killer/T-cell lymphoma, nasal type.**
A child exhibiting an extended ulcerative necrotizing lesion involving the nose, extending onto the cheek, lips and destroying adjacent tissues. Courtesy of Dr Toussaint / Dr Ortiz-Hidalgo, Mexico City.

This lymphoma has a predilection (>80% of the cases) to involve the upper aerodigestive tract (UAT), most frequently the nasal cavity followed by nasopharynx,

paranasal sinuses, hypopharynx and larynx [23-25]. In less than 20% of the cases, this lymphoma can also occur in non-UAT locations such as skin, soft tissue, gastrointestinal tract, bone marrow and with less frequency, lungs, central nervous system (CNS), spleen, testis, salivary glands and muscle [6,26,27].

1.4 Morphology

The distinctive morphology of ENKTCL is often composed of an ulcer with extended geographic necrosis secondary to a malignant diffuse lymphoid infiltrate with an angiocentric and angiodestructive growth pattern. The infiltrate may be accompanied by varying degrees of inflammation including granulocytes, lymphocytes, histiocytes and plasma cells. Sometimes, the malignant cells are small and bland looking simulating a purely reactive lymphocytic infiltrate, which can then be misdiagnosed as a benign inflammatory reaction [1,25,28]. Therefore, it is important to recognized the broad spectrum of morphologies of the neoplastic lymphocytes ranging from small, benign-looking cells or medium-sized cells to large pleomorphic cells [1]. The cells show a moderate amount of cytoplasm, irregularly folded nuclei, granular chromatin and inconspicuous nucleoli. The immunophenotype is characteristically CD56+, surface CD3-, cytoplasmic CD3+, CD2+ and express cytotoxic granules such as TIA-1+, granzyme B+ and perforin+. Other surface T-cell markers such as CD4, CD8, and CD5 are negative but CD7 is variably expressed. While the majority of these lymphomas show a NK cell immunophenotype, the expression of CD56 is not specific to this neoplasm and it can also be expressed in other T-cell lymphomas. In contrast, other NK receptors such as NKG2D and NKG2A are positive, whereas CD16 and CD57 are negative [29,30]. Between 15- 20% of all cases present a CD8+T-cell cytotoxic phenotype which is characterized by cytotoxic molecules, CD3+, CD5+, CD56- and TCRγδ+ or TCRαβ+. This subset of cases exhibits similar morphological and clinical characteristics to those cases with CD56 positivity [31,32]. Neoplastic cells express CD25+, FAS+ (CD95) and FASL+ CD95L or CD178 [33], whereas CD30 expression is not so common and only seen in 30-40% of the cases [32,34-36]. The megakaryocyte-associated tyrosine-kinase (MATK) is expressed but in low level compared to monomorphic epitheliotropic intestinal T-cell lymphomas (MEITL) and it can be used as an important tool in their differential diagnosis [37]. Other

markers, such as platelet-derived growth factor receptor alpha (PDGFRA) and programmed cell death ligand 1 (PD-L1), are frequently expressed (79% and 56% respectively). Their occurrence has been associated with a poor prognosis, indicating that these markers are somehow involved in immune escape mechanisms, becoming new targets for immunotherapy [38]. Moreover, survivin has also been considered as an important prognostic marker in ENKTCL, displaying a regulatory key in this lymphoma [39]. EBV infection should be suspected morphologically by the presence of geographical necrosis and should be confirmed using *in situ* hybridization for EBV encoded small RNA (EBER). In cases where the immunophenotype is characteristic of ENKTCL but the EBER is negative, the diagnosis needs to be reconsidered, as it is likely to be another type of peripheral T-cell lymphoma.

1.5 Pathogenesis

The etiology of ENKTCL is still unclear; however, the geographical prevalence of this disorder and the common association with EBV denotes a genetic background related to an EBV-induced mechanism of lymphomagenesis [40]. EBV is a ubiquitous lymphotropic DNA gammaherpesvirus (human herpesvirus 4), which as other members of the herpes virus family have a latency and lytic phase, allowing it to evade immune surveillance, maintaining a lifelong infection that is usually harmless [41]. Primary EBV infection in humans occurs in infants and is usually asymptomatic [42]. But, it can also occur in adolescence and in young adults, leading to infectious mononucleosis or so-called "kissing disease," an infection characterized by pharyngitis, lymphadenopathy and malaise, and may be associated with mild hematologic complications in 25% to 50% [43].

EBV enters the host through the nasopharyngeal tract, where it infects epithelial cells, replicates, and is shed [44]. Consequently, it is recognized by naïve and memory B lymphocytes circulating in the blood via the B lymphocyte surface receptor CD21 [45]. During productive replication of the virus, the EBV lytic viral genes are expressed, encoding viral transcription factors such as *BZLF1, BRLF1,* a viral DNA polymerase (*BALF5*), the viral IL-10 *(BCRF1)*, viral glycoproteins (e.g. gp350/220 and gp110) and structural proteins (capsid and tegument proteins) among others [46]. Following lytic infection, EBV establishes a latent infection

in B cells, epithelial cells and natural killer/T cells [47]. To evade the cytotoxic T-cell immune response, EBV shuts down its replication equipment (more than 100 viral genes) and expresses only around 10 latency genes in B cells. EBV persists as a circular episome in infected memory B-cells or integrates into the host genome [42]. During latency status, the main EBV "latent genes" expressed include 6 Epstein-Barr nuclear antigens (*EBNA1, EBNA2, EBNA3A, EBNA3B, EBNA3C* and leader protein), 3 latent membrane proteins (LMP1, 2A, 2B), 2 EBV-encoded noncoding RNAs (EBER 1 and 2) and many miRNAs from two regions of the EBV's genome: *BART* and *BHRF*, the so-called *BHRF1-* and *BART*-miR [47] (Table 1).

Table 1. EBV genes of latency

ORF	Gene product	Function
BKRF1	EBNA 1	Transactivator of latent and host genes; essential for the replication of the episomal EBV genome, also associated in p53 degradation
BKRF1	EBNA 2	Activates viral and cellular gene transcription crucial for EBV mediated B cell transformation, upregulates the expression of B-cell antigens.
BLRF3/BERF1	EBNA 3A	Participates in combination with EBNA-2 activating chemokines and latency genes to induce G1 arrest. Stimulate cell proliferation and B-cell transformation
BERF2a/b	EBNA 3B (EBNA 4)	
BERF3/4	EBNA 3C (EBNA 6)	
BamHI-W	EBNA-LP (EBNA 5)	Cooperates with EBNA-2-dependent viral and cellular gene transcription.
BNLF1	LMP1	Mimics the constitutively active form of CD40; activates NF-κB, JNK and p38 pathways; essential for EBV-mediated B-cell transformation.
Fused TRs	LMP2A/B	Mimics an antigen that activates the ERK/MAPK signaling pathway, blocking the antigen-dependent BCR signaling. Contributes to the B-cell EBV mediated oncogenesis.
BARTs	A73, RPMS1	BART and miRNAs interfere mainly in apoptosis
EBER1/2	miRNAs	

BART, *Bam*HI-A region rightward transcript; BCR B-cell receptor; EBER, EBV-encoded nuclear antigen; EBV, ERK, extracellular signal-regulated kinase; JNK, c-Jun N-terminal kinase; LMP, latent membrane protein; MAPK, mitogen-activated protein kinase; NF-κB, nuclear factor-κB; LP, leader protein. Adapted from **[46]**.

According to the expression of the EBV latency genes, four distinct latency programs are identified: latency 0, I, II or III [42,44,48]. The stage type III or "growth program" usually follows the primary infection in which all EBV latent genes are represented in naive B cells, defined by the expression of all viral proteins, EBNA (1, 2, 3A-C) and membrane latent proteins 1, 2A and 2B. This pattern is typically

seen in acute infections or severe immunosuppression states and in infectious mononucleosis. Latency II or “default program”, the most frequent, is highlighted by the absence of EBNA-2 expression but the presence of other oncogenic proteins related to EBV lymphomagenesis, such as *EBNA-1, LMP-1-2, BamH*i-a rightward transcripts (*BARTs*), *BHRF1 miRs, BZLF1, EBER*-1, -2. Type 0 / I, also called “latency program”, is found in memory B-cells and Burkitt’s lymphoma. This pattern is restricted to *EBNA-1* expression with the lack of any other viral genes [41,49,50] (Figure and Table 2).

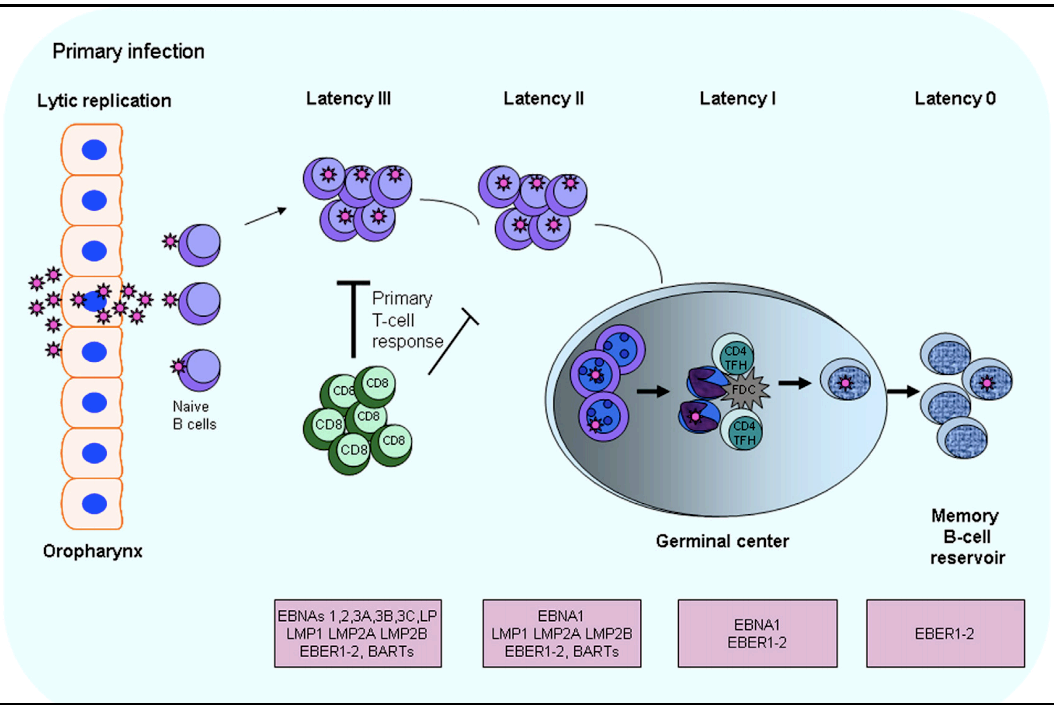

Figure 2. EBV life cycle and latency programms.
Epstein–Barr virus (EBV) enters the body through the oropharynx, where it replicates (lytic infection). The virus penetrates the mucosal epithelium and spread to lymphoid tissues. Here it targets circulating naïve and memory B cells, through the binding of the major envelope glycoprotein gp350/220 to the CD21 receptor. The virus remains in infected B cells; these cells will pass through the germinal center of the lymph node, where they multiply and mature and leave the germinal center into the circulation or persist as memory B cells. Occasionally, mature plasma cells may shed newly assembled free virions into saliva (lytic reactivation). The different viral latency stages and associated characteristic protein expression patterns are indicated [51]. Abbreviations: BART, BamH1-A rightward transcript EBER, EBV-encoded RNA; EBNA1, Epstein Barr nuclear antigen 1 2 3A; LMP1, latent membrane protein 1, 2 2A and 2B.

Table 2. EBV types of latency

Pattern of latency	Type I	Type II	Type III
EBNA-1	+	+	+
EBNA-2	-	-	+
EBNA-3	-	-	+
LMP-1	-	+	+
LMP-2	-	+	+
EBER	+	+	+
	Burkitt´s Lymphoma	Nasopharyngeal carcinoma, classic Hodgkin lymphoma Peripheral T-cell lymphoma	LPD, Infectious mononucleosis

* (+) plus sign indicates that the gene is expressed and minus (-) sign that is not expressed. Adapted from [42].

The memory EBV-infected B cells will then go into a latency stage where the virus integrates its DNA into the host cell DNA and may remain so for the rest of its life [42,52]. In the lifetime of this chronic infection, inflammatory lesions, immune disorders or various external factors may induce the infected B cells to enter their lytic cycle, which will lead to their activation and result in the transmission of the virus to the activated T-cells or NK cells, triggering a wide spectrum of lymphoproliferative disorders (LPD) [42,53], including carcinomas, B-cell and T-cell lymphomas, post-transplant lymphoproliferations, as well as classic Hodgkin lymphoma (CHL) [54-57].

1.5.1 EBV strains and their geographical distribution

In ENKTCL, EBV is found in an episomal form in the tumor cells displaying a latency pattern II, recognized by the positivity of LMP1 and EBER. Based on *EBNA* (*EBNA2* and *EBNA-3A*, *-3B* and *-3C*) genetic polymorphisms, two different strains are worldwide recognized: type A (type 1, B95-8 strain) and Type B (type 2, AG876 strain) [58,59]. Likewise, polymorphism sequence analyses have continued to identify a single amino acid change (S442D) in EBV type A as a key determinant of its strain. The occurrence of this amino acid substitution in strain A drifts toward an increased capacity to trigger the oncogenic protein LMP1 and other essential proteins in EBV oncopathogenesis [59]. Furthermore, in *in vitro* studies, type B strain reported less efficacy than the type A strain to convert B

cells into lymphoblastoid cell lines (LCL), highlighting a major role in neoplastic transformation [60].

EBV strains additionally display distinct geographical distribution worldwide, whereas EBV type A strain is more prevalent in Europe, Asia and North and Latino America, type B is frequently seen in Alaska, Papua New Guinea and Central Africa [59]. EBV strains A and B distribution has been partially investigated worldwide (Table 3).

Table 3. Geographical distribution of EBV strains in T-cell non-Hodgkin lymphoma

Country	Entity	n	EBV strain		Reference
			Type A	Type B	
China	ENKTCL	31 cases	29 (93.5%)	2 (6.5%)	[61]
Korea	T-cell NHL	15 cases	14 (93.3%)	1 (6.7%)	[62]
China	ENKTCL	16 cases	16 (100%)	0	[63]
Mexico	ENKTCL	23 cases	21 (91%)	2 (9%)	[5]
China/ Taiwan	Nasal and extranasal PTCL	19 cases	19 (100%)	1 (5.3%)	[64]
Malaysia	PTCL	9 cases	9 (100%)	0	[65]
Denmark	PTCL	18 cases	15 (83.3%)	3 (16.7%)	[65]

Adapted from [66].

Generally, EBV type B has a relatively higher frequency in Mexico in comparison to other western countries in B-cell lymphoproliferative disorders [67,68]. In two independents Mexican cohorts of diffuse large B cell lymphoma and CHL, EBV type B showed a frequency of 38% (10/26) and 50% (4/8), respectively [67,68]. Intriguingly, EBV type B was also identified in 53% of reactive lymphoid tissues (10/19), indicating that this strain is endemic in Mexico. Notwithstanding, effective B cell neoplastic transformation by EBV type B is found in the setting of immunodeficiency, mainly in HIV+ patients [69-72]. Despite this, some authors support the concept that EBV strain is not related with the immunodeficiency status of the host [73].

In parallel to EBV strain typing, seven phylogenetically different strains of LMP1 have also been described, whose differences lead to distinct virulence and role in the pathogenesis of EBV during B-cell transformation. These LMP1 strains are

distinguished by specific base pairs modifications: the presence or absence of a 30 bp deletion, the number of 33 bp repeats and an insertion of 15 bp within one of the repeats. LMP1 plays a main role in B-cell transformation [74]. LMP1 is codified by *BNLF,* a gene that contains three exons which are located within the *BamHI-N* region of the virus genome [75]. The product of this gene is an integral membrane protein which acts as a constitutive active receptor that induces B cell transformation, through its binding to a tumor necrosis factor receptor-associated factor (TRAF) and a tumor necrosis factor receptor-associated death domain (TRADD) protein [76,77]. LMP1 protein consists of 386 amino acids including a short cytoplasmic amino terminus, six transmembrane alpha-helical of hydrophobic nature, and a long cytoplasmic domain at the carboxyl terminus [76,78]. LMP1 has revealed various polymorphisms in its genome, among which a 30bp deletion *LMP-1* gene is prominent. This deletion occurs at the 3′ end of cytoplasmic C-terminal tail and close to the functional domain CTAR2. The outcome of the deletion is the loss of 10 amino acids from the carboxyl terminus, leading to lower immunogenic response and increase of the tumorigenic potential in comparison with *LMP1* wild-type [79,80]. This feature deletion has been identified in the Japanese population [81], but also in different cancers including Burkitt's lymphoma [82], gastric carcinoma [83], nasopharyngeal carcinoma [84], CHL [68], ENKTCL and peripheral T-cell lymphomas [85] (Table 4).

Table 4. Geographical distribution of LMP1 variants in T-cell non-Hodgkin lymphoma

Country	Entity	n	LMP1 variant		Reference
			30 bp del	**WT**	
China	ENKTCL	13 cases	10 (76.9%)	3 (23,1%)	[86]
China	ENKTCL	23 cases	21 (91,3%)	2 (8,7%)	[63]
Mexico	ENKTCL	23 cases	6 (26%)	17 (73,9%)	[5]
Malaysia	PTCL	9 cases	9 (100%)	0	[65]
Denmark	PTCL	18 cases	11 (61,1%)	7 (38,9%)	[65]

Adapted from [66]. Abbreviations: 30 bp del: 30 bp deletion, WT: wild-type.

So far, *LMP1* deletion variant has not been correlated with the EBV strain in the different EBV positive lymphoproliferations. Nevertheless, there is a low

incidence of the *LMP1* deletion variant in reactive lymphoproliferations in contrast to aggressive non-Hodgkin lymphomas (NHL), suggesting a correlation of immunodeficiency status with the *LMP1* polymorphism. Interestingly, in HIV patients with EBV infection, EBV type B strain is constantly associated with LMP1 deletion variant, suggesting that the oncogenic role of this strain is linked to the presence of the *LMP1* deletion [68,69,87]. Moreover, in some EBV infected individuals, infection with multiple strains and types of EBV can also occur, showing infection with both types of EBV associated *LMP1* polymorphisms [88]. EBV type of strain related to *LMP1* polymorphisms has also been studied in ENKTCL. From 23 Mexican ENKTCL cases, type A was present in most of the cases, about 91% (21/23 cases). Interestingly, *LMP1* deletion was detected in the 2 cases with EBV type B strain infection, demonstrating that in cases of immunocompetent status, EBV type B is constantly associated with *LMP1* 30 bp deletion [5].

1.5.2 Molecular features

Until recently, the mutational status of ENKTCL in Asian countries has been relatively well studied using different sequencing technologies. Despite the high frequency of this lymphoma in Latin America, there are no studies revealing the mutational landscape of this entity in this region. In the last decade, 6 independents Asian ENKTCL cohorts have been published with a limited number of patients. The limited number of samples is mainly explained by the low quality of the tissues, due to large amounts of necrosis with low purity of tumor cell content as a result of the high number of inflammatory cells. [89]. The most frequent mutated genes reported are members of the Janus kinase-signal transducer and activator of transcription (JAK-STAT) signalling pathway mainly *STAT3* (*JAK3, STAT5B*), the RNA helicase gene *DDX3X*, the tumour suppressor genes (*TP53, BCOR, MGA, PRDM1, FOXO3, HACE1*), genes involved in the RAS-MAPK signalling pathway (*NOTCH3, EPHA1, PTPRQ, PTPRK, GNAQ),* the epigenetic modifiers (*KMT2D, MLL2, ARID1A, ASXL1, BCOR, EP300*) and genes involved in the cell cycle regulation and apoptosis (*CDKN2A, CDKN2B, CDKN1A, FAS*) [61,90-96] (Table 5).

Table 5. Mutational landscape in ENKTCL

Genetic alteration			Reference
Recurrent mutations	JAK-STAT signaling pathway	*STAT3, STAT5b, JAK3,*	91,95,97
	RNA helicase family	*DDX3X*	92
	Tumor suppressors	*TP53, MGA*	16,92,93
	RAS-MAPK signaling pathway	*NOTCH3, EPHA1, PTPRQ, PTPRK, GNAQ*	61,96
	Apoptosis	*FAS*	98,99
	Epigenetic modifiers	*ARID1A, ASXL1, BCOR, KMT2D, MLL2, EP300*	93,100,101

Adapted from [66].

In the Chinese population, the frequencies of the most common mutated genes differ between the three independent studies, and this can be explained by the different sensitivities of the sequencing technologies applied (WES, panel sequencing and MassARRAY platform sequencing). *DDX3X* and *TP53* were the most common alterations followed by *STAT3* mutation in the Chinese population. *DDX3X* and *TP53* mutations were strongly correlated with poor prognosis independently of the variant allele frequencies [91,92,94]. In the two other studies performed in Korea and Japan, *STAT3* and *BCOR* were the most frequent mutated genes, respectively [90-94]. The only study performed in Latin-America, so far, showed *TP53* as the most frequent alteration, which associated with poor prognosis as in the Chinese cohort [16].

Chromosomal aberrations are also involved in ENKTCL pathogenesis promoting, directly or indirectly, the activation of oncogenes or the inactivation of tumor suppressor genes. Using genome-wide array analysis, the deletion of 6q21 was reported as the most common alteration in about 20 to 43% of the cases leading to the loss of genes involved in tumour suppression including *POPDC3, PREP, PRDM1, ATG5, AIM1* and *HACE1* [102,103]. Other recurrent typical genetic alterations observed are losses in chromosomes 1p4, 5p13, 12q3, 14q21, 15q24, 17p4 and 19q13, and gains in 2q5, 3q26, 7q34, 8q24, 13q4 and 10q3. Interestingly, 8q24.3 was related to significantly poorer survival [104,105]. More

recently, alterations differing from those displayed in ANKL were described including the gain of 2q and loss of 6q16-q27, 11q22-q23, 5p14-p14, 5q34-q35, 1p36-p36, 2p16, 4q12, and 4q31-q32 [106,107]. Other molecular clusters distinguished are also the loss of 14q11 found in the TCR alfa locus and gain of 1q32-q32 and loss of Xp22.33 [108].

1.5.1.2 Mutations in the JAK-STAT *signaling pathway*

The signaling pathway of the Janus kinase transcription transducers and activators (JAK-STAT) stimulates cell proliferation, differentiation, migration and apoptosis in T-cells. The JAK family includes four different kinases: *JAK1, JAK2, JAK3* and *TYK2*, which once they are activated, phosphorylate the C-terminal of their targets: the signal transducers and activators of transcription (STATs). There are seven known *STAT* family members (1, 2, 3, 4, 5a, 5b and 6), which show six functional domains including the N-terminal, DNA binding, Src homology 2 and 3 (SH2, SH3), transactivation and C-terminal domains. These transcription factors remain in the cytoplasm as monomers until they are activated by their phosphorylation, allowing STATs dimerization through a reciprocal interaction between the conserved SH2 domain and the phosphotyrosine residues. After their activation, these proteins enter the nucleus using importin α/β and RanGDP complexes to activate or repress their target genes [109]. Commonly, activating mutations in this pathway favors lymphomagenesis but, fortunately, this can be therapeutically reverted by JAK-1/2 inhibitors. Mutations in this signaling pathway are mostly present in widely malignant lymphoproliferations: *JAK1* G781E in uterine leiomyosarcomas, *JAK1* S703I in inflammatory adenoma and leukemia, *JAK2* V617F-T875N-V625F in myeloproliferative neoplasms, *JAK2* K539L in polycythemia vera, *JAK3* A572V-V722I-P132T in acute megakaryoblastic myeloid leukemia, *JAK3* M511I in prolymphocytic leukemia, *STAT3* Y640F-D661Y-D661V-N647I in large granular lymphocytic leukemia, *STAT5B* N642H in T-cell acute lymphoblastic leukemia and *STAT6* P419D/G in follicular lymphoma [110].

Genetic aberrations in *STAT3* are commonly reported in the Chinese and Korean population and are even more frequent compared to those in *JAK3* [101], representing the most frequent mutation in ENKTCL described to date, stated from 10.4 to 26.4% respectively. In other Asian countries, such as Japan, the frequency is

lower, reported in 8% in a cohort of 25 patients [90-92,95]. The *STAT3* mutations are predominantly found in the SH2 domain, which favors its activation by employing an independent cytokine signaling pathway [91,95]. This gene in normal T-cells is essential for T-cell expansion and its mutations are key players in T-cell lymphomagenesis in many sorts of mature T-cell lymphomas. In T-LGL, the frequency of *STAT3* mutations is higher than in ENKTCL (around 40%), and all main hotspots encountered (Y640F, D661V, D661Y and N647I) are located in the SH2 domain, as expected. Interestingly, regardless of the type of mutation (missense or insertion), all of them result in the activation of *STAT3,* which is proven by the detection of p-STAT3 by IHC or Western blot [111,112]. In other T-cell lymphomas, such as ALK-negative anaplastic large cell lymphoma (ALCL), *STAT3* alterations are also present in around 20% of the patients. Cell lines derived from these patients demonstrated an increase of p-STAT3 and the cell proliferation, which was efficiently targeted by the treatment with JAK1/2 inhibitors. Other target therapies have shown selective efficacy in ENKTCL: Static, a STAT inhibitor has been used successfully to treat cells harboring the hot Y640F and D661Y mutations of *STAT3*; however, the therapy was ineffective when cells with other *STAT3* mutations were treated. [97]. In these cases, the use of a selective JAK1/2 inhibitor (AZD1480) may be beneficial, as it has been shown to be beneficial in cell lines with wild-type *STAT3* mutations. [91]. Nevertheless, targeted therapy against *STAT3* can fail due to different regulatory factors that lead to the raise of *STAT3* in an independent way such as the regulatory subunit of phosphoinositide-3-kinase 3 *(PIK3R3)* and the adaptive protein *SH2B3 (SH2B3).* In ENKTCL patients *PIK3R3* is overexpressed, whereas *SH2B3* a negative regulator of STAT3 is lost in acute lymphoblastic leukaemia [90,113]. Moreover, EBV can also extrinsically activate the JAK-STAT signaling pathway using the LMP1 or EBNA-2, acting as a coactivator for the transcriptional enhancer of *STAT3* [114,115].

So far, the association of *STAT3* mutation with clinical outcome remains uncertain and no correlation with poor clinical outcome in ENKTCL has been detected, although in some other B-cell lymphomas high expression of p-STAT3 has been associated with a poor prognosis [116]. More recently, *STAT3* mutations have been correlated to the expression of the programed death ligand 1 (PD-L1).

It has been proposed a robust binding of the p-STAT3 to the *PD-L1* gene promoter contributing to tumor immune evasion. Therefore, the combination of PD-1/PD-L1 antibodies and *STAT3* inhibitors might become a new promising therapeutic approach for this lymphoma [95].

JAK3 mutations have a relatively low frequency in ENKTCL, and studies show a difference among frequencies, which can be explained by the sensitivity of the sequencing methods employed or the differences in ethnicity of the population studied. Using whole exome sequencing (WES) in ENKTCL patients, two somatic-activating mutations (A572V and A573V) were identified in the JH2 pseudokinase showing a frequency of 35.4% in 61 cases [95,117]. Nevertheless, in the Japanese and the Chinese population the frequency of these mutations is relatively low, stated from 0-7% [91,92].

1.5.1.2 Mutations altering the NOTCH signaling pathway

BCOR is an epigenetic modifier which interacts with the zinc finger protein domain *of BCL-6* and serves as a its co-repressor*,* leading to *BCL-6* target silencing. *BCOR* and *BCL-6* have a key role in germinal center formation and apoptosis [118]. More recent data support that *BCL-6/BCOR* interactions also leads to inhibition of NOTCH signaling pathway [119].

Mutations in *BCOR* have been reported in different B-cell lymphomas, myeloid disorders such as myeloid leukemia, myelodysplastic syndromes and ENKTCL, but not other mature T-cell lymphomas [120,121]. Surprisingly, the frequency of *BCOR* mutations in the Japanese population is relatively high (32%) [93] in contrast with other Asian populations [93]. Mutations described in *BCOR* are mostly missense and sometimes stop codon mutations, and are heterogeneously located along the gene, generally resulting in loss of the function. It is important to note that EBV infection is associated with *BCOR* mutations and loss of function, not only in ENKTCL but also in gastric cancer [90]. This leads to the hypothesis that EBV and *BCOR* may interact through an epigenetic mechanism in EBV carcinogenesis.

1.5.2.3 Mutations disrupting the cell cycle

TP53

Somatic mutations in the *TP53* gene occur in almost every type of cancer at rates from 38-50% in ovarian, esophageal, colorectal, head and neck, larynx, and lung cancers, to about 5% in primary leukemia, sarcoma, testicular cancer, malignant melanoma, and cervical cancer [122]. *TP53* acts as a tumor suppressor gene encoding a protein (p53), which induces G1 cell cycle arrest in DNA damaged cells promoting the expression of genes involved in apoptosis, namely PUMA (p53 upregulated modulator of apoptosis), Bax, Fas, PIG3 and Killer/DR5 [123,124]. Other well-known examples of *TP53* target genes, resulting in the regulation of cell cycle, senescence and apoptosis, are *MDM2* and p21 [125,126].

Mutations in the oncogene *TP53* were the first genetic alterations reported in the Mexican population, in 24% of the ENKTCL cases (5/21) [16]. Subsequently, a high rate of *TP53* mutations were also described in the Asian population: 63% in Indonesia (17/23 cases) [127], 40% in China (8/20 cases) [89] and 62% in Japan (36/58 cases) [128]. However, the incidence of these mutations is lower in more recent studies. A cohort of ENKTCL in the Chinese population describes 13.3% of *TP53* mutations in 105 cases. [91]

According to previous studies in different solid tumors, 86% of *TP53* mutations are mostly missense mutations located in the DNA binding domain, leading to the loss of antiproliferation signals [122]. Some other studies have also shown that mutant p53 proteins not only lose their antiapoptotic activity but also gain an oncogenic function, a phenomenon named “the gain of function of mutant p53” [129]. Mutations in *TP53* result in stabilization and nuclear accumulation of p53 protein in neoplastic cells [130]. This phenomenon is useful since p53 overexpression can be predicted in tissue using IHC as a surrogate to predict *TP53* gene status in cancer [131], except in EBV disorders since in these conditions p53 can be accumulated due to EBV induction rather than by the mutational status [16,132].

TP21 is also a regulator of the cell cycle with strong interaction with *TP53*. The p53-mediated apoptosis is preceded by elevation in the levels of the p21 protein [133]. Therefore, p53 mutations were assumed to be related to the absence of p21; however, in some cases of ENKTCL, TP21 overexpression has been found to be

present irrespective of *TP53* mutation [16]. This mechanism is not well understood, but one of the hypotheses is the role of EBV in the regulation of p53 and p21 through NF-kB activity enhanced by EBNA2 and LMP1, a feature previously described in B-cell lymphoproliferative disorders. but one of the hypotheses raised EBV for associated B-cell lymphoproliferative disorders is the upregulation of p53 and p21 by EBV through NF-kB activity enhanced by EBNA2 and LMP1 [16,134]. p53 overexpression may also be enhanced by binding to the ZEBRA viral protein or EBNA-5 [135,136].

DDX3X

DDX3X is a member of the family of RNA helicases known as “DEAD-box”, which refers to the conserved Asp-Glu-Ala-Asp sequence motif “helicase motif” that contains the catalytic base for ATP hydrolysis. Recent studies described recurrent mutations within the *DDX3X* gene in different cancers, including T-cell acute lymphoblastic leukemia [137], chronic lymphocytic leukemia [138], lung carcinomas [139], head and neck squamous cell carcinomas [140], carcinomas of the breast [141], medulloblastomas [142] and ENKTCL [92]. In cancer, *DDX3X* participates as a tumor suppressor through regulation of RNA translation initiation and assembly in the ribosome and spliceosome [143]. Besides, it also has been associated to the signal transduction impairment in WNT/β-catenin signaling pathway [143,144], the loss of cell cycle suppression and the transcriptional activation of the NF-κB and MAPK pathways [92]. Furthermore, synergistic *DDX3X* and *TP53* transcriptional suppression of CDKN1A expression has been documented in non-small cell lung carcinoma [145]. So far, *DDX3X* is listed as the most frequently mutated gene in ENKTCL cases from the Chinese population (20% of 105 cases), although it is mutated in only 12% of cases (3/25 cases) in a cohort from Japan. *DDX3X* mutations also occur in aggressive natural killer leukemia (29%, 4/14 cases), being all mutations restricted to the C-terminal helicase domain. It is interesting to note that although *DDX3X* mutations in ENKTCL happen randomly within the gene, most variations affect the function of its protein. Also, concurrent mutations of *DDX3X* and *TP53* are correlated with advanced stage of disease

and poor prognosis, suggesting that these two genes interact and enhance similar biological processes in tumor suppression.

1.5.2.4 Other affected signaling pathways

MGA

MGA is a transcription factor with double specificity that holds a DNA binding motif of the T-domain. Its main function is to inhibit the *MYC* proto-oncogene, which promotes oncogenesis via cell growth and proliferation. Moreover, *MGA* achieves the inactivation of *MYC* by heterodimerization with *MAX,* a known activator of *MYC* [146]. Recent reports of somatic mutations in *MGA* that lead to loss of *MYC* function have been reported in small cell lung cancer [147] and colorectal cancer [148]. Most interestingly, chronic lymphocytic leukemia (CLL) and ENKTCL also show *MGA* mutations, but with low frequency [149]. For CLL, the frequency is about 5.4%, while for ENKTCL it is 8% of the cases reported in Japanese and Chinese cohorts [92,93].

MSN

Moesin (MSN), a spike protein that organizes membrane extension, is expressed in membrane protrusions and participates in maintaining cytoskeleton and cell movement [150]. *MSN* is a member of the ezrin radixin-moesin (ERM) family that act as crosslinkers between the cellular actin filaments and the plasma membrane, which in turn interacts with different proteins and adhesion molecules and acts as a molecular signal transducer within the cells. Moreover, *MSN* shows strong expression in hematopoietic tissues and endothelial cells suggesting participation in the invasion of neoplastic cells [151-153]. Although recurrent *MSN* mutations are reported in ENKTCL, their biological significance is still unclear.

1.6 Therapy and Prognosis

The 5-year progression-free survival (PFS) and overall survival (OS) rates in ENKTCL range from 60 to 85% and 64 to 89% respectively, showing a relatively poor prognosis in comparison to other localized non-Hodgkin lymphomas. ENKTCL in the nasal region is regularly diagnosed in stages I-II of the disease and requires simultaneous or sequential chemotherapy and/or local radiotherapy.

This approach presents an overall response of 80 to 90%. In contrast, extranasal lymphomas are often diagnosed in stages III-IV of the disease and require systemic chemotherapy, habitually based on L-asparaginase containing regimens [154-159]. The recent development of new treatment approaches avoiding anthracyclines and favoring the use of combined therapy containing platinum or l-asparaginase has contributed to improved prognosis. However, almost half of the patients experience disease progression and the reported 5-year survival rate is still low (40-60%), especially for extranasal cases [6,160-162]. Therefore, new treatments are needed for the group of patients with poor prognosis and can also be beneficial as a first line of therapy for the prevention of relapses to improve the prognosis of these patients.

As stated in this introduction, there is little knowledge about the mutation landscape of ENKTCL in Latin American populations and the pathways associated with it. The main objective of this study is to examine the landscape of mutations in a series of ENKTCL cases collected in three Latin American countries (Mexico, Peru and Argentina) and compare it with the information available from the Asian cohorts. A secondary goal of this research is to learn more about the role of EBV strain and *LMP1* gene status in the pathogenesis of ENKTCL by analyzing its distribution and its clinical correlation.

2. Material and methods

2.1 Material

2.1.1 Patients, clinical data

As a cooperation from the Latin American society of Hematopathology, 135 cases previously diagnosed as ENKTCL were retrospectively collected from six national cancer reference centers, including Instituto Nacional de Cancerologia (Mexico City, Mexico), Instituto Nacional de Enfermedades Neoplasicas (Lima, Peru), Department of Pathology, Hospital Ángel C. Padilla (San Miguel Tucumán, Argentina), Instituto de Oncología Ángel H. Roffo (Buenos Aires, Argentina), Hospital Italiano de Buenos Aires (Buenos Aires, Argentina), and Instituto de Investigaciones Hematologicas (Buenos Aires, Argentina). The clinical data were retrieved by a certified hematologist from each reference center. Variables were analyzed at the time of the diagnosis including age, sex, previous medical history, presentation, disease extent, staging, B symptoms, International Prognostic Index (IPI) score, Eastern Cooperative Oncology Group (ECOG) performance status, treatment, and follow-up. The OS was evaluated from the date of diagnosis to 1-year or 5-year, or the last follow up. This work was carried out under the Declaration of Helsinki guidelines and was approved by the local Ethical Review Committee of the contributing institutions and Tubingen Ethical Committee (780/2016B02) [163].

2.1.2 Biopsies

Diagnostic ENKTCL biopsies from the last 15 years were collected at the reference institutes and sent to the Institute of Pathology and Neuropathology of the University of Tübingen. To confirm the previous diagnoses, all biopsies were reviewed by two pathologists (Ivonne Aidee Montes-Mojarro and Bo-Jung Chen) and a reference hematopathologist (Prof. Leticia Quintanilla-Martinez) following the criteria of the 2017 World Health Organization (WHO) Classification of Tumours of Hematopoietic and Lymphoid Tissues. Morphological criteria, IHC

stains (CD3 and CD56) and *in situ hybridization* using oligonucleotides complementary to EBER were assessed in formalin-fixed, paraffin-embedded (FFPE) tissue (Table 8) [163].

2.1.3 Equipment

Table 6. Equipment

Equipment	Company
Automated Immunostainer	Ventana Medical Systems
Axiostar Plus Microscope	Zeiss
Centrifuge/Vortex Combi-Spin FVL2400	Peqlab
Vortexer	Biozym
GeneAmp PCR System 9700	Applied Biosystems
Gel chamber	Peqlab
Gel documentation system CN-300-WL/LC	Peqlab
Ion OneTouch ES	Thermofisher scientific
Ion Torrent PGM	Thermofisher scientific
LightCycler 480	Roche
Magnetplatte Agencourt SPRIPlate 96R ring	Beckman Coulter
Maxwell 16 MDx Research Instrument	Promega
Microtom	Microm International GmbH
Pipetten	Gilson, Eppendorf
Qubit® Fluorometer 3.0	Thermofisher scientific
Thermo Cycler	Applied Biosystems

2.1.4 Kits

Table 7. Kits

Kits	Manufacturer
DNA isolation and quantification	
Maxwell 16 LEV Cartrigde Rack	Promega
Maxwell 16 FFPE Plus LEV DNA Purification Kit:	Promega
Qubit® dsDNA HS Assay Kit	Thermofisher scientific
Sequencing	
Ion AmpliSeq Library Kit 2.0	Thermofisher scientific
Ion Xpress Barcode Adapters Kit	Thermofisher scientific
Ion Library Quantitation Kit	Thermofisher scientific
Ion PGM Template Kit	Thermofisher scientific
Ion PGM Sequencing Kit	Thermofisher scientific
Ion Sphere Quality Control Kit	Thermofisher scientific
Ion 318 Chip Kit V2	Thermofisher scientific

ISH	
iVIEW Blue Detection Kit	Ventana

2.1.5 Antibodies

Table 8. Antibodies

Antibody	Clone	Company
CD3	2FGV6	Roche
CD30	Ber-H2	Dako
CD56	MRQ-42	Menarini
P53	DO-7	Novocastra
P-STAT3	Y705	Cell signaling
Probe ISH		
EBV-ISH	INFORM EBER # 800-2842	

2.1.6 Reagents

Table 9. Reagents

Reagent	Company
Electrophoresis	
GelRed Nucleic Acid Stain	Biotium
LE-Agarose	Lonza
6x Loading Buffer	Thermofisher scientific
TBE Buffer (Tris, Oric acid, EDTA)	Sigma-Aldrich /Merck /AppliChem
Gene ruler 50 bp	Thermofisher scientific
Gene ruler 100 bp	Thermofisher scientific
EBV-ISH	
ISH counterstain II	Ventana
ISH Protease 1	Ventana
PCR	
dNTPs	Fermentas
AmpliTaq Gold DNA Polymerase	Thermofisher scientific
Dnase/Rnase Free	Gibco

2.1.7 Primers

Table 10. Primers

ID	5 to 3”
Primers to determine the amplifiable DNA length [164]	
AF4/X3U	GGAGCAGCATTCCATCCAGC
AF4/X3L	CATCCATGGGCCGGACATAA
AF4/X11U	CCGCAGCAAGCAACGAACC
AF4/X11L	GCTTTCCTCTGGCGGCTCC
PLZF/X1U	TGCGATGTGGTCATCATGGTG
PLZF/X1L	CGTGTCATTGTCGTCTGAGGC
RAG1/X2U	TGTTGACTCGATCCACCCCA
RAG1/X2L	TGAGCTGCAAGTTTGGCTGAA
Primers to characterize EBV strain [165]	
*EBNA2*_forward	AGGCTGCCCACCCTGAGGAT
*EBNA2*_reverse	GCCACCTGGCAGCCCTAAAG
*LMP1*_forward	CGGAGGAGGTGGAAAACAA
*LMP1*_reverse	GTGGGGGTCGTCATCATCTC

Sequencing primers to perform the variant validation using fusion method

Primers design was performed using Primer 3 free available online software (v. 0.4.0). Oligonucleotides were subsequently synthetized by Sigma-Aldrich with the following specifications: desalt purification and 0.025 µmol concentrations. Subsequent dilution with distilled water was performed to reach a final stock concentration of 100µM.

*DDX3X*_G36E_A_BC96_F	CCATCTCATCCCTGCGTGTCTCCGACTCAGTTAAGCGGTCGATCAGAAATTTAAATGGGAAGGTTTTT
*DDX3X*_G36E_A_BC96_R	CCATCTCATCCCTGCGTGTCTCCGACTCAGTTAAGCGGTCGATCGGTTCCTTAAATGAGGAGGA
*DDX3X*_G36E_TRP1_F	CCTCTCTATGGGCAGTCGGTGATCAGAAATTTAAATGGGAAGGTTTTT
*DDX3X*_G36E_TRP1_R	CCTCTCTATGGGCAGTCGGTGATCGGTTCCTTAAATGAGGAGGA
*MSN*_E395K_A_BC95_F	CCATCTCATCCCTGCGTGTCTCCGACTCAGCGGACAGATCGATTGGAAGAACAGACCCGTAGG
*MSN*_E395K_A_BC95_R	CCATCTCATCCCTGCGTGTCTCCGACTCAGCGGACAGATCGATTCAGCTTCTTGACGCTCCTT
*MSN*_E395K_TRP1_F	CCTCTCTATGGGCAGTCGGTGATTGGAAGAACAGACCCGTAGG
*MSN*_E395K_TRP1_R	CCTCTCTATGGGCAGTCGGTGATTCAGCTTCTTGACGCTCCTT

*STAT5B*_G719E_A_BC94_F	CCATCTCATCCCTGCGTGTCTCCGACTCAGTCCGACAAGCGATGCTCTGTTCTCTTCCTTCTGC
*STAT5B*_G719E_A_BC94_R	CCATCTCATCCCTGCGTGTCTCCGACTCAGTCCGACAAGCGATCCCACAAGAATGCCACCTAC
*STAT5B*_G719E_TRP1_F	CCTCTCTATGGGCAGTCGGTGATGCTCTGTTCTCTTCCTTCTGC
*STAT5B*_G719E_TRP1_R	CCTCTCTATGGGCAGTCGGTGATCCCACAAGAATGCCACCTAC
*BCOR*_A1521T_A_BC93_F	CCATCTCATCCCTGCGTGTCTCCGACTCAGCTTGTCCAATCGATTGCATGAAGCTTGTGCTAGG
*BCOR*_A1521T_A_BC93_R	CCATCTCATCCCTGCGTGTCTCCGACTCAGCTTGTCCAATCGATCCATCCTGGGCACTACAGTT
*BCOR*_A1521T_TRP1_F	CCTCTCTATGGGCAGTCGGTGATTGCATGAAGCTTGTGCTAGG
*BCOR*_A1521T_TRP1_R	CCTCTCTATGGGCAGTCGGTGATCCATCCTGGGCACTACAGTT
*BCOR*_K922*_A_BC92_F	CCATCTCATCCCTGCGTGTCTCCGACTCAGCTAGGAACCGCGATTGTTCTGGCAGGTACCAACA
*BCOR*_K922*_A_BC92_R	CCATCTCATCCCTGCGTGTCTCCGACTCAGCTAGGAACCGCGATTTTTGGTATAGGTGGGGGTCA
*BCOR*_K922*_TRP1_F	CCTCTCTATGGGCAGTCGGTGATTGTTCTGGCAGGTACCAACA
*BCOR*_K922*_TRP1_R	CCTCTCTATGGGCAGTCGGTGATTTTGGTATAGGTGGGGGTCA
*BCOR*_E481K_A_BC91_F	CCATCTCATCCCTGCGTGTCTCCGACTCAGCGGAAGGATGCGATAGGGCTGGAAGTGGCTTAGT
*BCOR*_E481K_A_BC91_R	CCATCTCATCCCTGCGTGTCTCCGACTCAGCGGAAGGATGCGATTTTTTCAGCGACATGCTTTTG
*BCOR*_E481K_TRP1_F	CCTCTCTATGGGCAGTCGGTGATAGGGCTGGAAGTGGCTTAGT
*BCOR*_E481K_TRP1_R	CCTCTCTATGGGCAGTCGGTGATTTTTCAGCGACATGCTTTTG
*BCOR*_G723D_A_BC90_F	CCATCTCATCCCTGCGTGTCTCCGACTCAGCTAACCACGGCGATCCGTCCAGAGTTTGTGACCT
*BCOR*_G723D_A_BC90_R	CCATCTCATCCCTGCGTGTCTCCGACTCAGCTAACCACGGCGATAATCTCGGAAAACCGATTCC
*BCOR*_G723D_TRP1_F	CCTCTCTATGGGCAGTCGGTGATCCGTCCAGAGTTTGTGACCT
*BCOR*_G723D_TRP1_R	CCTCTCTATGGGCAGTCGGTGATAATCTCGGAAAACCGATTCC
*BCOR*_H281Y_A_BC89_F	CCATCTCATCCCTGCGTGTCTCCGACTCAGTCCTGAATCTCGATTTCTCCAGTCTGCACCAATG
*BCOR*_H281Y_A_BC89_R	CCATCTCATCCCTGCGTGTCTCCGACTCAGTCCTGAATCTCGATATCTTCCACGGGAGGCTTT
*BCOR*_H281Y_TRP1_F	CCTCTCTATGGGCAGTCGGTGATTTCTCCAGTCTGCACCAATG
*BCOR*_H281Y_TRP1_R	CCTCTCTATGGGCAGTCGGTGATATCTTCCACGGGAGGCTTT
*DDX3X*_A170T_A_BC88_F	CCATCTCATCCCTGCGTGTCTCCGACTCAGCCGAACACTTCGATTGGAGGCAACACTGGGTT
*DDX3X*_A170T_A_BC88_R	CCATCTCATCCCTGCGTGTCTCCGACTCAGCCGAACACTTCGATATGTGGAGGACAGTTGTTGC
*DDX3X*_A170T_TRP1_F	CCTCTCTATGGGCAGTCGGTGATTGGAGGCAACACTGGGATTA
*DDX3X*_A170T_TRP1_R	CCTCTCTATGGGCAGTCGGTGATATGTGGAGGACAGTTGTTGC
*MGA*_S1706F_A_BC87_F	CCATCTCATCCCTGCGTGTCTCCGACTCAGTTGGCTGGACGATTGGCTTCAGTTGCTTTTCCT
*MGA*_S1706F_A_BC87_R	CCATCTCATCCCTGCGTGTCTCCGACTCAGTTGGCTGGACGATCTCACTGGTGGACTCCCATT
*MGA*_S1706F_TRP1_F	CCTCTCTATGGGCAGTCGGTGATTGGCTTCAGTTGCTTTTCCT
MGA_S1706F_TRP1_R	CCTCTCTATGGGCAGTCGGTGATCTCACTGGTGGACTCCCATT
STAT5B_D727N_A_BC86_F	CCATCTCATCCCTGCGTGTCTCCGACTCAGCTTGGTTATTCGATCTTCTGCAGGTTTGTGAACG

STAT5B_D727N_A_BC86_R	CCATCTCATCCCTGCGTGTCTCCGACTCAGCTTGGTTATTCGATCCCACAAGAATGCCACCTAC
STAT5B_D727N_TRP1_F	CCTCTCTATGGGCAGTCGGTGATCTTCTGCAGGTTTGTGAACG
STAT5B_D727N_TRP1_R	CCTCTCTATGGGCAGTCGGTGATCCCACAAGAATGCCACCTAC
STAT3_E696K_A_BC85_F	CCATCTCATCCCTGCGTGTCTCCGACTCAGCCAGCCTCAACGATCTGACATTCCCAAGGAGGAG
STAT3_E696K_A_BC85_R	CCATCTCATCCCTGCGTGTCTCCGACTCAGCCAGCCTCAACGATGCCAGGAACATGGAAAATCA
STAT3_E696K_TRP1_F	CCTCTCTATGGGCAGTCGGTGATCTGACATTCCCAAGGAGGAG
STAT3_E696K_TRP1_R	CCTCTCTATGGGCAGTCGGTGATGCCAGGAACATGGAAAATCA
MGA_E525K_A_BC84_F	CCATCTCATCCCTGCGTGTCTCCGACTCAGCTTCCATAACGATCCAATGAGACTGCCTTCTGC
MGA_E525K_A_BC84_R	CCATCTCATCCCTGCGTGTCTCCGACTCAGCTTCCATAACGATTTTCCACTGAGGCTCTTTCAG
MGA_E525K_TRP1_F	CCTCTCTATGGGCAGTCGGTGATCCAATGAGACTGCCTTCTGC
MGA_E525K_TRP1_R	CCTCTCTATGGGCAGTCGGTGATTTTCCACTGAGGCTCTTTCAG

2.1.8 Softwares

Table 11. Software and online tools

Equipment	Company
Primer3web (Version 4.1.0)	Whitehead Institute for Biomedical Research
Ion AmpliSeq™ Designer (Version 7.4.3)	Thermofisher scientific
Torrent Suite™ Software (Version 5.1)	Thermofisher scientific
Integrative Genomics Viewer (Version 2.3)	Broad Institute
Ensembl	WTSI / EBI
Exome Variant Server	NHLBI GO ESP
COSMIC (Catalogue of somatic mutations in cancer)	Welcome Trust Sanger Institute
Universal Protein Resource (UniProt)	European Bioinformatics Institute (EMBL-EBI), the SIB Swiss Institute of Bioinformatics and the Protein Information Resource (PIR)
Microsoft Office	Microsoft
EndNote X9	Thomson Reuters

2.2 Methods

2.2.1 Workflow of the study.

ENKTCL cases were reviewed under the microscope (Axiostar Plus Microscope, Zeiss) and tumor cell content was assessed taking in account EBER and CD56 immunostaining. The integrity and quantity of extracted DNA was analyzed and then NGS was performed using a customized AmpliSeq panel designed to sequence the most frequently mutated genes in Asian ENKTCL (Figure 3).

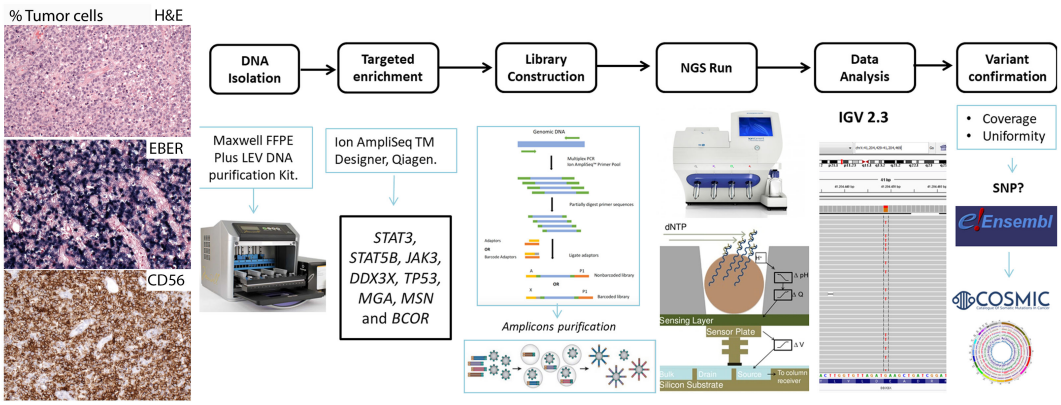

Figure 3. Overview of the main steps in the targeted Next Generation Sequencing workflow performed in this study.
H&E: Hematoxylin and eosin stain; CD56: NKT-cell marker immunohistochemistry; EBER: *in situ* hybridization for Epstein-Barr virus.

2.2.2 Immunohistochemistry and ISH

On a rotating microtome (Microm International GmbH) the FFPE tissue sections were cut to a thickness of 2.5 µm. The IHC was performed on a Ventana Benchmark Ultra according to the protocol specified by the manufacturer (Roche Tissue Diagnostics). The following antibodies were used in order to corroborate the diagnosis CD3 (2FGV6, Roche), CD56 (MRQ-42, Menarini), CD30 (Ber-H2, Dako). Additional antibodies were used to confirm gene mutational status p-STAT3 (Y705 Cell signalling) and TP53 (DO-7, Novocastra) (Table 5).

EBV- *in situ* hybridization (EBV-ISH) was done using the iVIEW Blue Detection Kit, the INFORM EBER probe and the ISH counterstain (Red Counterstain II) according to manufacturer's protocol, after ISH-protease I treatment.

2.2.3 Quantitative and qualitative DNA analysis

Tumor DNA was extracted using the Maxwell 16 FFPE plus LEV DNA Purification Kit according to the manufacturer's instructions. 10 sections of 5 µm thickness where cut from the FFPE tissue and the DNA was digested using proteinase K (20mg/ml) overnight at 70°C. Clean up of DNA was done using the Maxwell 16 platform and the "DNA isolation from FFPE tissue" program. DNA quantification was assessed on all samples by Qubit fluorescence plate reader using HS Assay Kit (Thermofisher) according to the manufacturer´s protocol.

2.2.4 Qualitative DNA analysis

Processing of FFPE tissue leads to DNA fragmentation and degradation. Therefore, qualitative PCR was performed to evaluate the length of the DNA fragments and determine if they remained sufficiently in length to be sequenced with the intended panel (Table 12). DNA quality was assessed by quality Polymerase Chain Reaction (PCR) using the modified protocol from Van Dongen *et al* [164] to estimate their amplifiable DNA length fragments.

Table 12. PCR reagents of the qualitative-PCR

Reagent	**Final concentration**	**Volume (µl)**
ddH2O		to 25
10x Buffer without MgCl2	1x	2,5
25 mM $MgCl_2$	2mM	2
5 µM dNTPs	0,2 µM	0,5
Primer mix (forward and reverse)		2
AmpliTaq Gold	0,04 U/ µl	0,3
DNA (50 ng/µl)	100 ng/ µl	2
Total volume		25
Primer mix	**Final concentration**	
AF4/X3U und AF4/X3L	2.5 pmol	
AF4/X11U und AF4/X11L	1.25 pmol	
PLZF/X1U und PLZF/X1L	1.25 pmol	
RAG1/X2U und RAG1/X2L	1.25 pmol	
TBXAS1/X9U und *TBXAS1/X9L*	1.25 pmol	

PCR was performed in a thermocycler (Table 13). Electrophoresis was carried out with 10 µl of the PCR product accompanied by 100 bp DNA ladder in 2% Agarose gel (ME Agarose, TBE Buffer 1x) at 140 Volts for 40 minutes. DNA was visible by gel-red staining. Gel documentation was performed using UV-Light to visualize the DNA (CN-300-WL/LC, Peqlab). Cases were considered for future analysis if at least 200 bp were amplifiable.

Table 13. Thermocycler parameters of the qualitative-PCR

Program Thermocycler		
95°C		7’
	35 cycles	
95°C		45’’
60°C		45 ‘’
72°C		1’
72°C		4´
4°C		hold

2.2.5 Next generation sequencing

NGS analysis using targeted sequencing was performed on the Ion Torrent PGM (Thermo Fisher Scientific, South San Francisco, CA, USA). From 135 cases collected only 71 ENKTCL cases were sequenced, since 64 cases had maximum amplifiable DNA fragments below 200 bp or low amount of tumour DNA with extensive necrosis. Therefore these 64 cases were not sequenced to avoid sequencing artefacts. Targeted sequencing was performed using a designed Ion AmpliSeq™ custom panel of 27.43 kb (Table 14) designed with the Ion AmpliSeq Designer software from Thermo Fisher Scientific (version 3.4). This panel covered eight of the most frequently mutated genes found in the previous Asian cohorts in patients diagnosed with ENKTCL [90,92,117].

Table 14. Overview of the designed Ion AmpliSeq Custom Panel (27.43 kb)

Gene symbol	Position	Exon (s)	Amplicons
STAT3	chr17: 40475270 - 40475375	19	1 (105 bp)
	chr17: 40475020 - 40475165	20	2 (145 bp)
	chr17 :40474280 - 40474520	21	3 (240 bp)
	chr17:40469195 - 40469245	22	1 (50 bp)
STAT5B	chr17:40362415 - 40362520	14	2 (105 bp)
	chr17:40362185 - 40362320	15	2 (135 bp)

	chr17:40359570 - 40359750	16	3 (180 bp)
	chr17:40354770 - 40354830	17	1 (60 bp)
	chr17:40354430 - 40354470	18	1 (40 bp)
JAK3	chr19 :17948000 - 17948015	13	1 (15 bp)
	chr19 :17945690 - 17945700	16	1 (10 bp)
DDX3X	chrX:41196655 - 41196723	2	1 (68 bp)
	chrX:41206887 - 41206977	17	2 (90 bp)
	chrX:41202984 - 41203080	8	2 (96 bp)
	chrX:41201984 - 41202094	6	2 (110 bp)
	chrX:41206106 - 41206270	15	2 (164 bp)
	chrX:41205752 - 41205880	14	2 (128 bp)
	chrX:41204651 - 41204806	12	2 (155 bp)
	chrX:41206559 - 41206709	16	2 (150 bp)
	chrX:41205476 - 41205668	13	3 (192 bp)
	chrX:41202463 - 41202609	7	2 (146 bp)
	chrX:41201742 - 41201911	5	3(169 bp)
	chrX:41203277 - 41203386	9	2 (109 bp)
	chrX:41193500- 41193555	1	1 (55 bp)
	chrX:41198283- 41198341	3	2 (58 bp)
	chrX:41203486 - 41203657	10	3 (171 bp)
	chrX:41204427 - 41204582	11	3 (155 bp)
	chrX:41206562 - 41206709	16	2 (147 bp)
	chrX:41200731- 41200874	4	3 (143 bp)
*TP53**	chr17:7577013 - 7577160	8	3 (147 bp)
	chr17:7573921 - 7574038	10	2 (117 bp)
	chr17:7576619- 7576662	10	1 (43 bp)
	chr17:7576531 - 7576589	10	1 (58 bp)
	chr17:7579694- 7579726	3	0 (32 bp)
	chr17:7572921- 7573013	11	2 (92 bp)
	chr17:7579306- 7579574	4	3 (268 bp)
	chr17:7579306- 7579595	4	4 (289 bp)
	chr17:7578365- 7578559	5	2 (194 bp)
	chr17:7578365- 7578457	5	2 (92 bp)
	chr17:7576847- 7576931	9	1 (84 bp)
	chr17:7579833- 7579917	2	2 (84 bp)
	chr17:7578171- 7578294	6	2 (123 bp)
	chr17:7577493- 7577613	7	2 (120 bp)
	chr17:7578365- 7578538	5	2 (173 bp)
*MGA**	chr15:41961087 - 41962161	2	11 (1074 bp)
	chr15:41999920 - 42000062	6	3 (142 bp)
	chr15:42057078 - 42057265	23	2 (187 bp)
	chr15:42019372 - 42019609	10	3 (237 bp)
	chr15:42054321 - 42054565	22	3 (244 bp)
	chr15:42026714 - 42026797	12	2 (83 bp)
	chr15:42005343 - 42005699	9	4 (356 bp)
	chr15:42032245 - 42032406	14	2 (161 bp)
	chr15:42021356 - 42021552	11	3 (196 bp)
	chr15:42028373 - 42028901	13	6 (528 bp)
	chr15:41991256 - 41991362	5	2 (106 bp)
	chr15:42058196 - 42059483	24	13 (1287 bp)
	chr15:42002883 - 42003552	8	7 (669 bp)
	chr15:42041303 - 42042818	17	15 (1515 bp)
	chr15:41991055 - 41991144	4	2 (89 bp)
	chr15:42000296 - 42000411	7	2 (115 bp)
	chr15:42049980 - 42050042	19	2 (62 bp)
	chr15:42046629 - 42046770	18	2 (141 bp)
	chr15:42040829 - 42041130	16	3 (301 bp)
	chr15:42053931 - 42054053	21	2 (122 bp)

	chr15:41988267 - 41989226	3	11 (959 bp)
	chr15:42034738 - 42035375	15	7 (637 bp)
	chr15:42052515 - 42052732	20	3 (217 bp)
*MSN**	chrX:64958826 - 64959061	12	4 (235 bp)
	chrX:64936674 - 64936768	2	1 (94 bp)
	chrX:64951694 - 64951851	6	2 (157 bp)
	chrX:64887703 - 64887725	1	1 (22 bp)
	chrX:64953040 - 64953147	7	1 (107 bp)
	chrX:64949294 - 64949579	4	3 (285 bp)
	chrX:64950963 - 64951057	5	1 (94 bp)
	chrX:64958381 - 64958484	11	2 (103 bp)
	chrX:64955123 - 64955297	8	2 (174 bp)
	chrX:64956651 - 64956792	9	2 (141 bp)
	chrX:64959585 - 64959760	13	2 (175 bp)
	chrX:64947670 - 64947776	3	2 (106 bp)
	chrX:64957034 - 64957205	10	2 (171 bp)
BCOR	chrX:39922855- 39923108	8	3 (253 bp)
	chrX:39914615- 39914771	12	2 (156 bp)
	chrX:39930220- 39930417	6	3 (197 bp)
	chrX:39923583- 39923857	7	3 (274 bp)
	chrX:39935701- 39935790	3	1 (89 bp)
	chrX:39921993 - 39922329	9	5 (336 bp)
	chrX:39911356- 39911658	15	3 (302 bp)
	chrX:39922855- 39923210	8	4 (355 bp)
	chrX:39921386- 39921651	10	3 (265 bp)
	chrX:39913133 -39913300	14	2 (167 bp)
	chrX:39937091- 39937187	2	2 (96 bp)
	chrX:39931596- 39934438	4	30 (2842 bp)
	chrX:39930884- 39930948	5	2 (64 bp)
	chrX:39913503- 39913591	13	1 (88 bp)
	chrX:39916402- 39916579	11	3 (177 bp)

* All complete sequence by primer design is covered except 575 base pairs due to sequence specific incompatibility [163]

Targeted sequencing was performed according to the manufacturer's protocol. Genes of interest were amplified with the designed AmpliSeq Custom Panel primers. Libraries were constructed using the Ion AmpliSeq Library Kit (V2.0). and quantified by real-time qPCR using the Library Quantitation Kit on the LightCycler 480. Amplicons were diluted to a 5 pm concentration and pooled for the sequencing. Clonal amplification took place on the Ion OneTouch instrument using Ion Sphere particles that were subsequently enriched on the Ion OneTouch ES and loaded on a semiconductor chip for sequencing on the Ion Torrent PGM. The sequencing data generated in every run was routinely uploaded to the Ion Torrent™ server which converts raw data into base calls to analyse the genetic information with a specific algorithm. The Ion Torrent Suite software (V 5.12.0) outputs the data in FASTQ, VCF and BAM formats for downstream further analysis.

Variant calling was performed using the Ion Reporter software (Thermo Fisher Scientific). Each obtained variant was analysed in the program Integrative Genomics Viewer (IGV, Broad Institute), to exclude panel specific or sequencing artefacts and confirm the veracity of the mutations. Nucleotide variants were filtered according to variant effect, variant allele frequency (VAF) and coverage. Only missense, frameshift, nonsense, insertions or deletions variants with a VAF above 5% were taken in account for further analysis. Single nucleotide variants (SNVs) were verified to rule out single nucleotide polymorphisms (SNPs) in accordance with known SNPs database such as Exome Variant Server, Clinically Associated Human Variations of the National Center for Biotechnology Information (NCBI) VarSome and Ensembl. To assess and confirm our presumed mutations, we compared our results with the updated literature using freely available databases such as NCBI and the Catalogue of Somatic Mutations in Cancer (COSMIC) and Varsome. Frameshift mutations, nonsense mutations and insertions or deletions were considered as pathogenic variants. Missense alterations were evaluated using the prediction tools “sorting intolerant from tolerant” (SIFT) and “polymorphism phenotyping” (PolyPhen2). Alterations were considered as pathogenic when predicted by at least one of these tools.

VAFs below 10% and not reported previously in the literature were validated on the Ion Torrent using a targeted resequencing approach with the Ion Amplicon Library Preparation kit (Fusion Method) (Life Technologies). This method allows the amplification of short amplicons (<150 bp) by PCR, using two fusion primers to attach the amplicons to the adapters, Ion A and truncated P1 (trP1). Design of the primers to confirm specific mutations was carried out with the freely available online program Primer3web (version 4.0.0). Amplicons were also diluted to 5 pM and pooled for the sequencing. The subsequent workflow is like the workflow described above for the Ion Torrent PGM.

2.2.6 Correlation of the protein status with the mutational status.

In order to investigate the impact of the mutation at protein level, correlation of the mutational status with IHC was performed. Cases with p-STAT3 mutation and wild-type controls (three cases) were stained using phosphorylated STAT3 antibody (Y705, Cell Signalling). On the other hand, cases with TP53 mutations and

three representative wild-type controls were stained using TP53 (DO-7, Novocastra). The intensity and percentage of overexpression of p53 by IHQ was correlated with *TP53* mutational status, which is expected to be strong and homogenous in mutated cases. The VAF correlated with the percentage and intensity of the immunostainings.

2.2.6 Analysis of EBV strain and the 30 bp LMP1 deletion using PCR.

To study the EBV strain carried in these cases, PCR analysis for EBV A and B strain typing was performed, as previously reported by Kingma et al. 1996 [69]. Primers flanking a region of the *EBNA2* gene differing between type A and EBV type B were used. In addition, to identify the 30 bp *LMP1* gene deletion PCR reactions were carried out using primers flanking the characteristic 30 bp deletion. All reactions were performed in duplicates using 20 *n*g DNA, accompanied by a positive and negative control (Table 15).

Table 15. PCR reagents for the EBV strain and LMP1 variant analysis

Reagent	Final concentration	
Reagent	**Final concentration**	**Volume (µl)**
ddH2O		37
10x Buffer with MgCl2	1x/1,5mM	5
dNTPs	0,2 mM	1
Primer Table 10 (Forward)	10 µM	1
Primer Table 10 (Reverse)	10 µM	1
Ampli Taq Gold	5U/µL	1
DNA (5ng/µl)	20 ng	4
Final volume		50

PCR was performed in a thermocycler (Table 16). Electrophoresis was carried out with 20 µl of the PCR product accompanied by 50 bp DNA ladder in 3% Agarose gel (ME Agarose, TBE Buffer 1x) at 80 Volts during 2 and 3 hours, according to the size of the product.

Table 16. Thermocycler parameters for the EBV strain analysis

Program Thermocycler	
94°C	5’
42 cycles (EBV), 45 cycles (LMP1)	
94°C	1’
56°C	30 ‘’
72°C	30 ‘’
72°C	7´
94°C	5’
4°C	hold

DNA was visualized by gel-red staining. Photos were taken in the gel documentation system (CN-300-WL/LC, Peqlab). Cases with expected fragments of 168 bp were interpreted as EBV strain A and fragments with 184 bp product length were interpreted as EBV strain B. On the other hand, cases rendering a 161 bp product for wild-type *LMP1* and 131 bp for the deletion variant.

2.2.7 Statistical analysis

Descriptive analysis was performed; categorical variables were described using absolute and relative frequency. Numerical variables were described as means and standard deviation or, medians and interquartile ranges (IQR) according to the distribution of their data. Normality of the distribution was assessed by investigating kurtosis, skewness as well as QQ graphs, box plots and histograms. When comparing patient groups, categorical variables were compared using X^2 tests of Fisher exact test. Continuous variables were compared using independent samples t-test for normally distributed data or Mann Whitney test for non-normally distribute data.

Bivariate analysis to check differences between groups was performed. X^2 test of Fisher´s exact test for categorical variables was used. Independent samples t-test were used to compare quantitative variables that were normally distributed, whereas Mann-Whitney test were used to evaluated skewed variables.

The effect of the different clinicopathological variants including mutational status and EBV strain on OS was evaluated using the Kaplan Meier curve and compared using the statistic Log-rank test. The association of covariates with the results time to disease-related death was estimated by the Cox proportional hazard (PH) models. In this model, the exp^{Coef} gives the estimated Hazard Ratio for the effect of each variable. The method of estimation used to obtain the coefficient for each model was the maximum likelihood estimation (ML). Crude Hazard ratios and 95% confidence intervals (CI) and p-values were calculated. Patients for whom the event had not occurred (patients that survived along the follow up) were treated as censored observations. All statistical tests were 2 tailed and the significance level was set at $p<0.05$. All statistical analysis was performed using IBM SPSS software, version 24 (Armonik, NY: IBM Corp)

3. Results

In total, 71 ENKTCL cases, recollected from three different centers in Latin America (42 from Mexico, 27 from Peru and 12 from Argentina), were studied. All cases were evaluated by three qualified pathologists and met the diagnostic criteria for ENKTCL according to the WHO classification 2017. The DNA integrity was above 200 bp and DNA quantity was at least 200 ng in order to perform all subsequent sequencing and EBV characterization analysis.

3.1 Clinical features of ENKTL in Latin America

Most of the NKTCL cases collected in this cohort (58/71 cases, 89%) showed nasal involvement, as it is typical of this lymphoma, while only few cases (7/71 cases, 11%) presented extranasal involvement including the stomach (1 case), small intestine (2 cases), vulva (1 case), lungs (1 case), submandibular soft tissue (1 case) and lymph nodes associated with extranodal systemic spread (1 case). Males were more commonly affected, the male-to-female ratio was 1.8 and the median age of the patients at the time of diagnosis was 40 years (range, 14-83 years). Although the most common symptoms in this lymphoma are related to nasal obstruction, in this series more common symptoms reported were night sweats, fever and weight loss. Indeed, two-thirds (34/71, 67%) of the cases presented B symptoms and elevated LDH. The performance status of the ECOG was 0-1 in 31/71 (61%) of cases, which in most cases correlated with a low International Prognostic Index (IPI 0-2) indicating an early stage of the disease. Treatment was variable in each case; half of the cases (26/50, 52%) received chemotherapy with concomitant local radiotherapy, whereas the other half (20/50, 28%) received chemotherapy or radiotherapy alone. Four patients did not receive any treatment due to low family income or advanced stage of the disease. To evaluate the prognosis of the patients and correlate it with the clinical and mutation analysis, follow-up after 1 and 5 years were investigated; however, this was only available for 51 patients. At 5 year follow up, 25/51 (49%) patients were dead of disease (DOD), 18/51 (33%) patients were alive but with disease (AWD) and 8/51

(16%) patients were alive with no evidence of disease (NED). The median survival time was 29.47 months (range, 0-60 months). The 1-year and 5-year survival rates were 57% and 51%, respectively All clinical data are summarized in table 17 [163].

Table 17. Clinical data and outcome of extranodal NK/T-cell lymphoma patients in Latin America

	Total (n = 71)
Median age (range)	40 (14-83)
Gender (n = 62)	
Male	40 (65%)
Female	22 (35%)
M:F ratio	2:1
Site of involvement (n = 65)	
Nasal	58 (89%)
Extranasal	7 (11%)
B symptoms (n = 51)	34 (67%)
LDH elevation (n = 51)	34 (67%)
ECOG (n = 51)	
0-1	31 (61%)
2-5	20 (39%)
IPI score (n = 49)	
0-2	37 (76%)
3-5	12 (24%)
Therapy (n = 50)	
Combined chemoradiotherapy	26 (52%)
Chemotherapy alone	10 (20%)
Radiotherapy alone	10 (20%)
No therapy	4 (8%)
Outcome (n = 51)	
DOD	25 (49%)
NED	18 (33%)
AWD	8 (16%)
Median survival in months	61.6
Overall survival rate	
1-year	57%
5-year	51%

AWD, alive with disease; DOD, dead of disease; ECOG, Eastern Cooperative Oncology Group; IPI, International Prognostic Index; LDH, lactate dehydrogenase; NED, no evidence of disease [163].
* Only information from 50/51 patients was retrieved for follow-up evaluation.

3.2 Histopathological patterns in ENKTCL in Latin America.

To evaluate the histological features of this lymphoma, all cases were histologically assessed. In the evaluation, variable degrees of inflammatory background, tumor necrosis, angiocentricity and angiodestruction were distinguished in all

cases, which made the identification of tumor cells challenging in some cases. However, since all tumor cells stained positive for CD56, CD3ε and EBER, the diagnosis of ENKTCL was relatively straightforward.

ENKTCL with nasal involvement demonstrated three different patterns of appearance. The first pattern showed small-sized neoplastic cells with bland cytological features, mimicking a reactive infiltrate (Figure 4A) (Figure 4D). The second pattern was mainly composed of a dense tumoral population of intermediate-sized cells and pale cytoplasm, surrounding the glands with few or no necrosis (Figure 4B). In the third pattern the neoplastic cells show markedly atypia, the cells were large-sized with large nuclei, hyperchromasia and pale to clear cytoplasm (Figure 4C). In all three patterns, all neoplastic cells were positive for EBER (Figure 4D, E And F) [163,166].

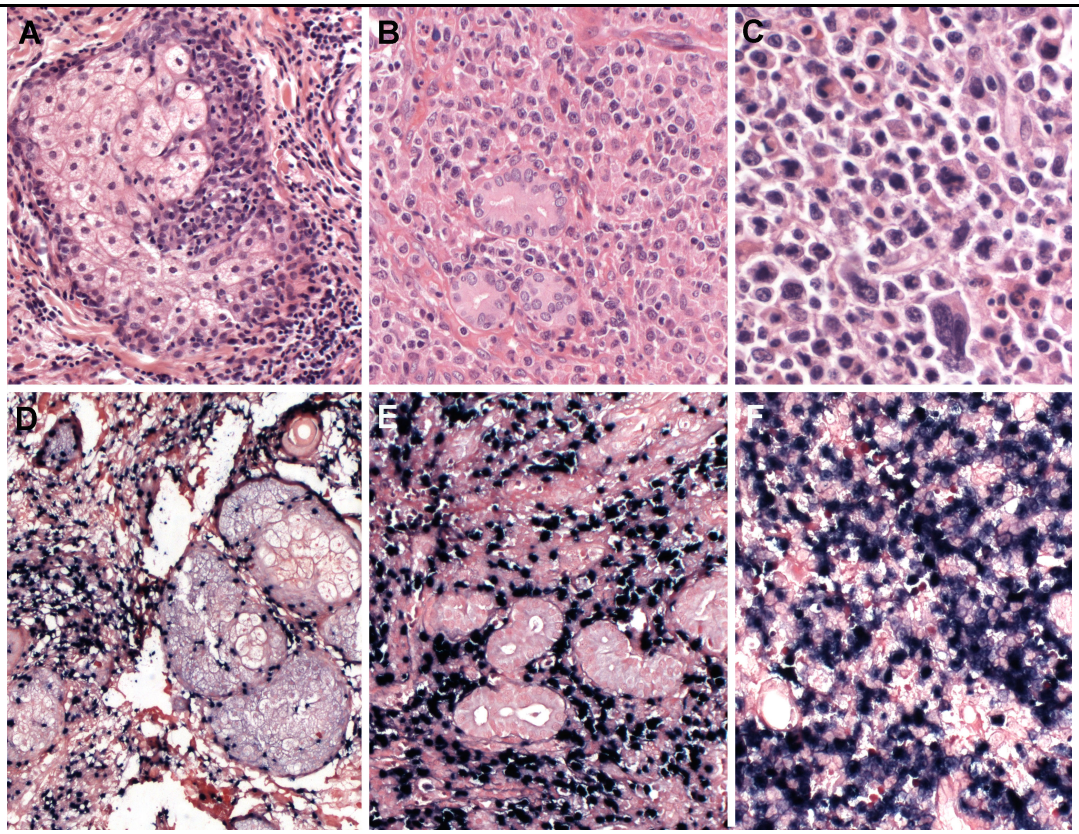

Figure 4. **Different cytological appearances of ENKTCL in the nasal region.**

Pattern 1 (A) Diffuse infiltrate of small lymphoid cells with bland cytology around the sebaceous glands (H&E, 400×). Pattern 2 (C) Medium-sized cell infiltrate with nuclear irregularity and pale cytoplasm. (H&E, 400×). Pattern 3 (E) Large cell, pleomorphic infiltrate with abundant pale to clear cytoplasm (H&E, 400×). (B, D and F) EBER is positive in the neoplastic cells (EBER-ISH, 400×) [166,167].

Abbreviations: H&E: Hematoxylin.

ENKTCL with extranasal involvement displayed varied histological features. Skin involvement in some cases simulate a reactive reaction as it was previously shown in pattern 1 (Figure 4A and C) but tumor histology showed a dense infiltrate of neoplastic cells forming a mass and involving the entire dermis but without epidermotropism (Figure 4A). Cytologically, the tumor cells vary in size. In the case shown below, the cells were intermediate-sized with homogeneous and strong CD3 membranous staining (CD3ε) (Figure 5B). All neoplastic cells were infected by EBV, as confirmed by EBER positivity (Figure 5C) [167].

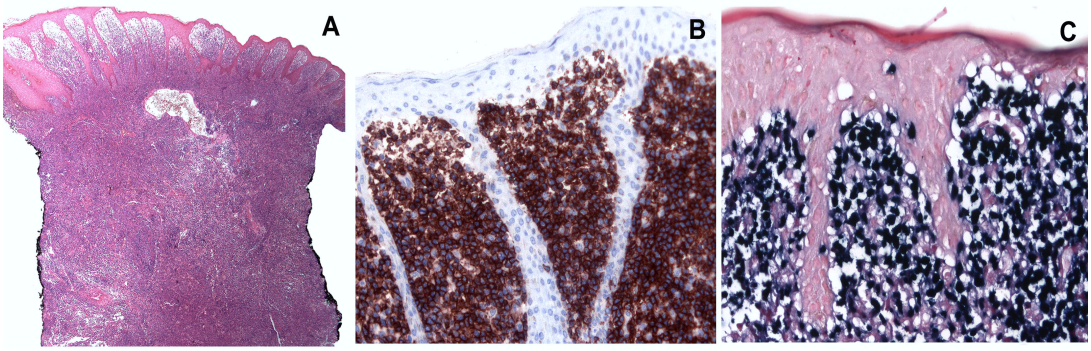

Figure 5. **Extranodal NK/T-cell lymphoma, nasal type in the skin.**

(A) Skin biopsy showing a dense infiltration by ENKTCL in the dermis without epidermotropism. (H&E, x12.5). (B) Tumor cells show strong CD3 cytoplasmic (CD3ε) stainning (IHC, x100) and EBER positive (EBER-ISH x200) [167].
Abbreviations: H&E: Hematoxylin.

Three ENKTCL cases (3/71 cases) showed gastrointestinal tract involvement (3/71 cases), especially in large and small intestine (Figure 6). The clinical presentation of these cases was related to a mass, and the symptoms were associated with partial or complete intestinal obstruction. In those cases, the tumor was composed of a dense infiltrate of neoplastic cells invading completely the intestinal wall. Tumoral cells were large, pleomorphic and tend to invade the blood vessels, a feature frequently seen in ENKTCL (Figure 6A and B). IHC confirmed the ENKTCL immunophenotype: cells were partially positivity for CD56 (Figure 6C) and EBER (Figure 6D). The majority of the neoplastic cells showed a CD3ε (Figure 6E). Interestingly, CD30 was positive in a minority of tumor cells

showing a membrane and dot-like paranuclear staining of the Golgi apparatus (Figure 6F) [167].

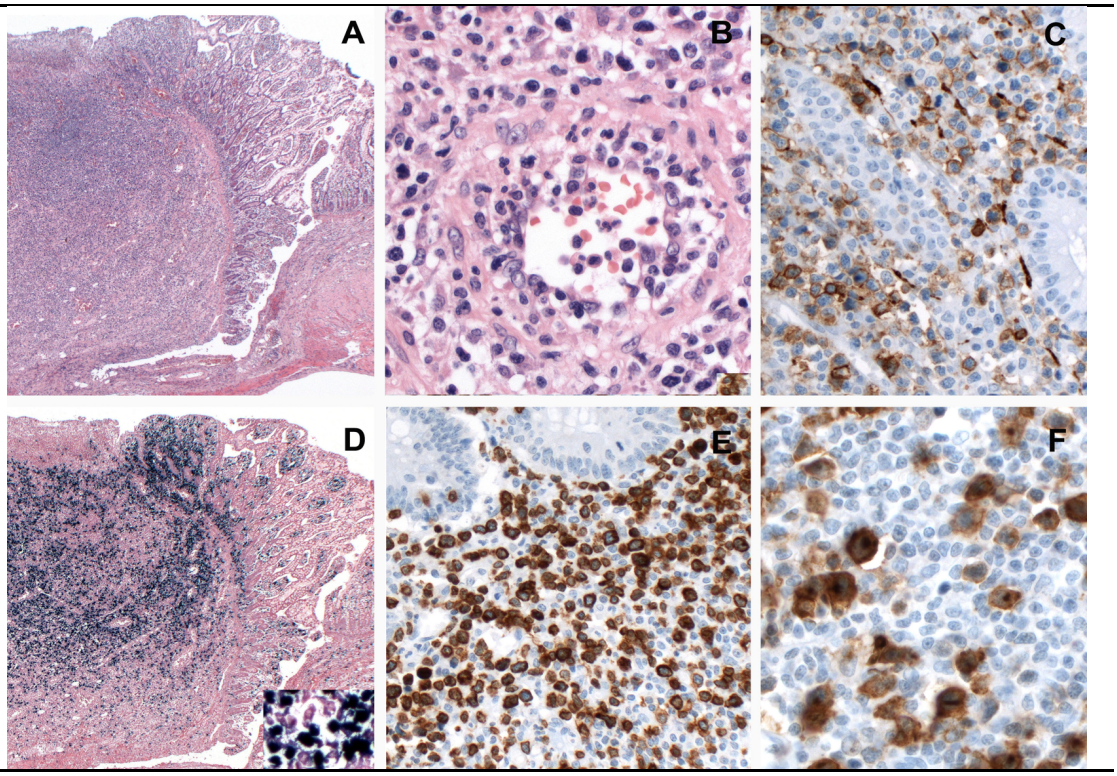

Figure 6. **Extranodal NK/T-cell lymphoma, nasal type in the small intestine.**

(A) H&E stain of intestinal resection with a dense neoplastic lymphoid infiltration (H&E, x12.5). (B) Tumor cells are large, pleomorphic with irregular nuclei and pale or clear cytoplasm, with evident angiodestruction (H&E, x400) (C) CD56 is positive in the majority of the neoplastic cells. (D) EBER positive cells within the intestinal wall (*EBER-ISH*, x12.5). (E) CD3 is positive (CD3ε) within the tumor infiltrate (CD3 IHC, x200). (E) Scattered large neoplastic cells are CD30 positive with a membranous and Golgi zone pattern (CD30 IHC, x400) [167].
Abbreviations: H&E: Hematoxylin.

The histological evaluation of all cases allowed the differential diagnosis with other T-cell lymphomas, including peripheral T-cell not otherwise specified (NOS) lymphomas, aggressive NK-cell leukemia, and other EBV-positive T-cell and NK-cell lymphoproliferative disorders.

3.3 ENKTCL mutational profile in Latin America

Targeted sequencing analysis was performed revealing 53 mutations in the 71 cases investigated. Mean average of read depth sequencing was 4063.4 (range, 413.3-6334). The majority of the mutations were missense point mutations (42/53, 79%), only 8 nonsense mutations (8/53, 15%) and 3 frameshift insertions (3/53, 6%). Somatic mutation load per case varied remarkably in all samples, showing VAFs that ranged from 5% to 77% (mean 33%). From all cases studied, 42 cases (59%) carried at least one mutation and 29 cases (41%) demonstrated the wild-type sequence in the investigated gene regions (Figure 7). Single-hit mutations were observed in 34/42 cases (81%) and concurrent mutation were presented in 8/42 (19%, 6 cases two mutations, 1 case three mutations, 1 case four mutations). Missense mutations were highly frequent in the eight genes studied. Nonsense mutations were only found in *MSN, BCOR, MGA* and *DDX3X* genes, whereas frameshift insertions were exclusively of *MSN* and *MGA* genes. Interestingly, all *STAT3* and *TP53* alterations in this study represented missense mutations. Among all missense mutations, the most frequent substitutions were G>A, G>T and A>T, found in 23%, 21% and 21% of cases, respectively. Analysis by SIFT and/or Polyphen2 predicted a damaging effect of the variant at protein level in all missense mutations described in this cohort (Table 15). Mutations frequently involved the JAK-STAT signaling pathway, more frequently affecting the *STAT3* gene, which was mutated in 16 cases (16/71, 23%), followed by *MSN* mutations in 10 cases (10/71, 14%), *BCOR* mutations in 9 cases (9/71, 13%), *DDX3X* mutations in 6 cases (6/71, 8%), *TP53* mutations in 6 cases (6/71, 8%) and *MGA* mutations in 3 cases (3/71,4%). Interestingly, other members of the JAK-STAT signaling pathway were rarely mutated: *JAK3* (2/71, 3%) and *STAT5B* (1/71, 1%). Mutations in *STAT3 and DDX3X* were almost mutually exclusive, but the mutations in *BCOR*, *MSN, TP53* and *MGA* co-occurred with other mutations. All mutations detected in this study are enlisted in table 18 [163].

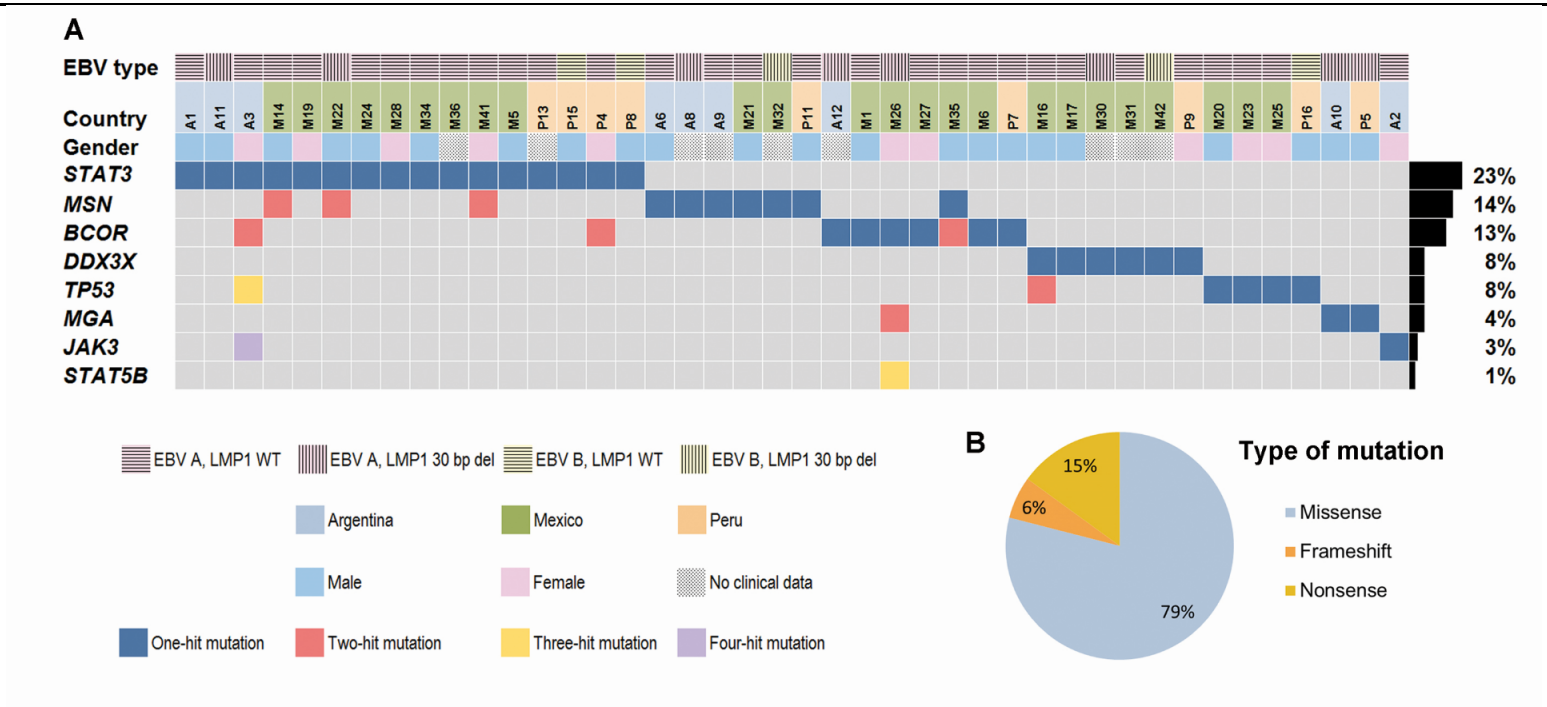

Figure 7. **Overview of mutational profile, country distribution and EBV strain of ENKTL in Latin America.**
(A) Each column of the heat map represents one ENKTL case and each line one specific analysis/gene. On the right side of the figure, the frequency of the particular result of the analysis is shown. Gene mutations were identified in 42 of 71 cases (59%). (B) Type of mutations identified [163].

Table 18. Mutations detected in ENKTL cases in Latin America

ID	Gene	Variant protein level	Variant cDNA Level	VAF	Coverage	PolyPhen-2	SIFT
M1	*BCOR*	p.R1678H	c.5033G>A	5%	174	Damaging	Damaging
M5	*STAT3*	p.G618R	c.1852G>C	16%	6780	Damaging	Damaging
M6	*BCOR*	p.S1704C	c.5110A>T	45%	1829	Damaging	Damaging
M14	*STAT3*	p.N647I	c.1940A>T	16%	5972	Benign	Damaging
	MSN	p.A500fs	c.1496_1497insG	40%	2202	Damaging	Damaging
M16	*TP53*	p.R248W	c.742C>T	12%	10887	Damaging	Damaging
	DDX3X	p.E348*	c.1042G>T	36%	3108	Damaging	Damaging
M17	*DDX3X*	p.L235Q	c.704T>A	22%	670	Damaging	Damaging
M19	*STAT3*	p.D661Y	c.1981G>T	54%	1996	Damaging	Damaging
M20	*TP53*	p.G266R	c.796G>A	56%	4374	Damaging	Damaging
M21	*MSN*	p.E575A	c.1724A>C	25%	1817	Damaging	Damaging
M22	*STAT3*	p.E638V	c.1913A>T	21%	1998	Damaging	Damaging
	MSN	p.E573*	c.1717G>T	69%	1462	Damaging	Damaging
M23	*TP53*	p.Y163H	c.487T>C	12%	1997	Damaging	Damaging
M24	*STAT3*	p.Y640F	c.1919A>T	14%	12498	Damaging	Tolerated
M25	*TP53*	p.P152Q	c.455C>A	63%	1192	Damaging	Damaging
M26	*MGA*	p.H533fs	c.1596_1597insC	32%	1344	Damaging	Damaging
	STAT5B	p.N642H	c.1924A>C	30%	4589	Damaging	Tolerated
	BCOR	p.K922*	c.2764A>T	22%	3385	Damaging	Damaging
M27	*BCOR*	p.Y204C	c.611A>G	15%	9895	Damaging	Damaging
M28	*STAT3*	p.G618R	c.1852G>C	25%	6988	Damaging	Damaging
M30	*DDX3X*	p.V168L	c.502G>C	51%	228	Benign	Damaging
M31	*DDX3X*	p.L431P	c.1292T>C	49%	489	Damaging	Damaging
M32	*MSN*	p.E573*	c.1717G>T	52%	285	Damaging	Damaging
M34	*STAT3*	p.Q643K	c.1927C>A	9%	6220	Damaging	Tolerated
M35	*BCOR*	p.A61T	c.181G>A	5%	1795	Damaging	Damaging
	MSN	p.A271T	c.811G>A	6%	1807	Benign	Damaging
M36	*STAT3*	p.Y640F	c.1919A>T	15%	9185	Damaging	Tolerated
M41	*STAT3*	p.N647I	c.1940A>T	19%	11665	Benign	Damaging
	MSN	p.E575D	c.1725G>C	42%	1483	Damaging	Damaging
M42	*DDX3X*	p.G406R	c.1216G>C	38%	1997	Damaging	Damaging
P4	*STAT3*	p.Y640F	c.1919A>T	8%	1917	Damaging	Tolerated
	BCOR	p.E1355K	c.4063G>A	51%	2699	Damaging	Damaging
P5	*MGA*	p.I1984M	c.5952A>G	10%	913	Benign	Damaging
P7	*BCOR*	p.Q224*	c.670C>T	28%	3476	Damaging	Damaging
P8	*STAT3*	p.D661Y	c.1981G>T	39%	1997	Damaging	Damaging
P9	*DDX3X*	p.V513L	c.1537G>C	42%	1958	Damaging	Damaging
P11	*MSN*	p.E575D	c.1725G>C	17%	1649	Damaging	Damaging

P13	*STAT3*	p.E616K	c.1846G>A	40%	1865	Benign	Damaging
P15	*STAT3*	p.N647I	c.1940A>T	7%	1999	Benign	Damaging
P16	*TP53*	p.G244S	c.730G>A	6%	2000	Damaging	Damaging
A1	*STAT3*	p.D661Y	c.1981G>T	69%	64718	Damaging	Damaging
A2	*JAK3*	p.A573V	c.1718C>T	77%	6093	Damaging	Damaging
A3	*TP53*	p.S240R	c.720T>A	72%	13469	Damaging	Damaging
	STAT3	p.E616G	c.1847A>G	25%	6069	Damaging	Damaging
	JAK3	p.V722I	c.2164G>A	46%	9547	Benign	Damaging
	BCOR	p.R1375W	c.4123C>T	42%	20171	Damaging	Damaging
A6	*MSN*	p.Q410*	c.1228C>T	36%	684	Damaging	Damaging
A8	*MSN*	p.N566D	c.1696A>G	46%	1159	Damaging	Damaging
A9	*MSN*	p.K327fs	c.976_977insA	47%	1182	Damaging	Damaging
A10	*MGA*	p.E1315*	c.3943G>T	23%	6380	Damaging	Damaging
A11	*STAT3*	p.D661Y	c.1981G>T	24%	18553	Damaging	Damaging
A12	*BCOR*	p.E867*	c.2599G>T	60%	3316	Damaging	Damaging

A, Argentinian case; fs, frameshift; M, Mexican case; P, Peruvian case; PolyPhen-2, Polymorphism Phenotyping v2; SIFT, sorting intolerant from tolerant; *stop codon amino acid [163].

3.3.1 ENKTCL mutational profile among the Latin American countries analyzed.

The distribution of the recurrent somatic mutations among the three different Latin American countries show no differences in their frequencies. *STAT3* was the most common mutated gene in all countries (Table 19). However, *JAK3*, another member of the JAK-STAT signaling pathway was only mutated in the Argentinian population (Fisher Test p=0.02). When compared to other Asian series, Latin American mutational distribution presented a comparable pattern of frequency to the Korean population, highlighting the JAK-*STAT as* the most common affected pathway. *DDX3X, TP53, BCOR* and *MGA* were relatively less frequent. Interestingly, *MSN* mutations were mostly absent in other Asian series when compared to the frequency of this cohort. The different studies comparing the ENKTCL Latin American mutational profile with the Asian profile are described in Table 20

Table 19. Recurrent mutation of extranodal NK/T-cell lymphoma in Latin America

	Total (n=71)	Mexico (n=42)	Peru (n=17)	Argentina (n=12)	*p*-value*
Genetic mutation					
STAT3 mutation	16 (23%)	9 (21.4%)	4 (23.5%)	3 (25%)	1.00
MSN mutation	10 (14%)	6 (14.3%)	1 (5.9%)	3 (25%)	0.40
BCOR mutation	9 (13%)	5 (11.9%)	2 (11.8%)	2 (16.7%)	0.88
DDX3X mutation	6 (8%)	5 (11.9%)	1 (5.9%)	0	0.60
TP53 mutation	6 (8%)	4 (9.5%)	1 (5.9%)	1 (8.3%)	1.0
MGA mutation	3 (4%)	1 (2.4%)	1 (5.9%)	1 (8.3%)	0.36
JAK3 mutation	2 (3%)	0	0	2 (16.7%)	0.02
STAT5B mutation	1 (1%)	1 (2%)	0	0	
No mutation detected	29 (41%)	18 (42.9%)	8 (47.1%)	3 (25%)	0.44

**p*-value using Chi-square test or Fisher´s exact test with bivariate analysis. bp, base pair [163].

Table 20. Most common mutations in ENKTCL described in the different Asian cohorts

	Latin America	**China**	**Japan**	**China**	**China**	**Korea**	**Singapur / China**
No. of cases	71	88	25	105	51	30	109
Technology	Targeted sequencing	WES (5), Sequenom MassARRAY platform (85), Targeted sequencing	Targeted sequencing	WES (25), Targeted sequencing (80)	WES (1), RNA-seq (15), Sanger sequencing (35)	WES (9), •RNA-seq (3) Targeted sequencing (21),	Targeted sequencing
STAT3	23%	3.4%	16%	10.5%	6% (3/51)	20%	21.1%
MSN	14%	NA	NA	8.6%	0%	0%	NA
BCOR	13%	5.7%	32%	0%	20%	16.7%	NA
TP53	8%	10.2%	16%	13.3%	13%	10%	11.9%
DDX3X	8%	8%	12%	20%	7%	0%	NA
MGA	4%	NA	8%	8.6%	0%	0%	NA
JAK3	3%	NA	8%	0%	0%	6.7%	6.4%
STAT5B	1%	3.4%	0%	1.9%	6% (3/51)	0%	NA
Reference		94	93	92	91	90	95

Table updated from [163].

3.3.2 Recurrent somatic mutations involving the JAK-STAT *signaling pathway*

Somatic mutations in the JAK-STAT signaling pathway were the most frequent recurrent mutations in this cohort, including mutations in *JAK3, STAT3*, and/or *STAT5B*, found in 19/71 cases (27%). *STAT3* was the most frequently mutated gene of this signaling pathway, found in 23% of the cases. VAF ranged from 7 to 69%. All missense *STAT3* mutations were found in the Src homology (SH2) domain with hotspots in D661Y, N647I, or Y640F, G618R and E616G (Figure 8A).

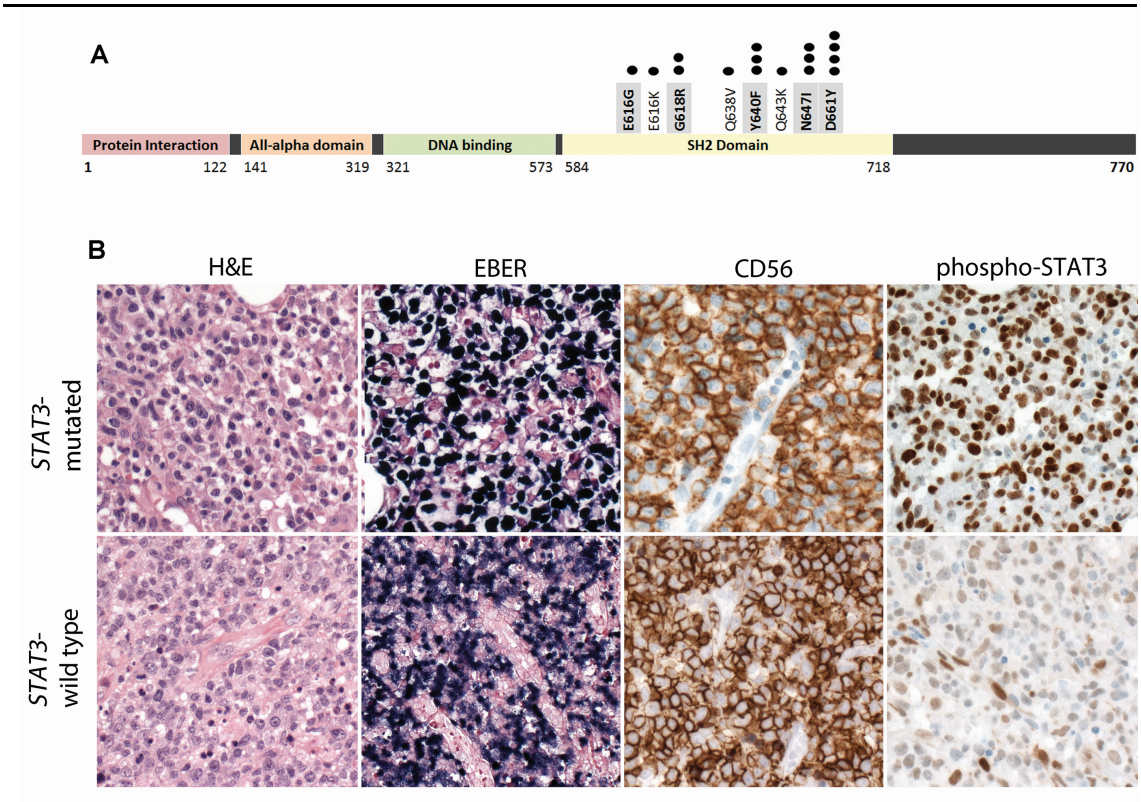

Figure 8. Distribution of *STAT3* mutations among the protein and its correlation with its expression.
(A) Exact positions of all *STAT3* mutations are depicted in the protein within its different domains (www.uniprot.org; UniProtK P40763). The distribution of mutations is illustrated.
(B) Mutated case (upper picture) shows intermediate-sized cell morphology (H&E, x400) with high content of tumoral cells positive for EBER, > 90% of cells (EBER-ISH, x400), CD56 (CD56 IHC, x400) and show homogeneous and strong staining for phospho-STAT3, >90% of tumoral cells. *STAT3*-wild-type case (lower picture) showing a similar morphology (H&E, x400) with high content of tumoral cells positive for EBER and CD56 IHC (> 90% of cells, EBER-ISH, x400, CD56 IHC, x400) but reveals heterogeneous and weaker staining of phospho-STAT3 (>30% of tumoral cells) with stronger staining of endothelial cells as internal control [163]. Abbreviations: H&E: Hematoxylin

STAT3 mutations were predicted to lead to a constitutive activation of STAT3 protein confirmed by its phosphorylation. Therefore, in the *STAT3* mutated cases IHC for the p-STAT3 protein was performed, showing a strong and homogenous staining (in more than 90% of the cells), in contrast to wild-type cases, where the staining was weak and heterogeneous (in approximately 30% of tumoral cells). Two representative cases corroborating this hypothesis are illustrated in Figure 8. [163].

3.3.3 Recurrent somatic mutations altering the NOTCH signaling pathway

The *BCOR* mutations detected in this cohort are illustrated in Figure 9. The majority of these were missense mutations (6/9 cases), while the remaining ones were nonsense mutations leading to a stop codon (3/9 cases.) VAF ranged from 5 to 59.5%. The hotspot mutations Q224*, S1016L, E1355K found in these series lead to an inactivation of *BCOR*. All *BCOR* mutations were located heterogeneously among the gene domains and no mutation was detected in the Ankyrin repeat-containing domain. Interestingly, only 2 cases (A3 and P4) demonstrated concurrent *STAT3* and *BCOR* alterations. The case A3 from Argentina revealed also two additional alterations in *TP53* and *JAK3*, indicating a complex genetic instability. On the other hand, the case M35 from Mexico displayed concurrent *MSN* mutation in addition to the *BCOR* alteration.

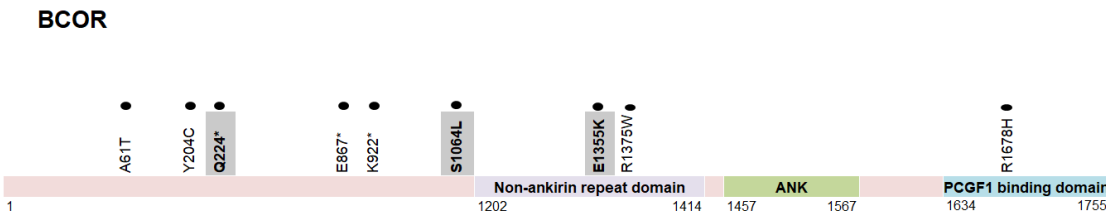

Figure 9. Distribution of *BCOR* mutations among the protein.

Exact positions of all mutation are depicted in the BCOR protein within its different domains (www.uniprot.org; UniProtK Q6W2J9).

3.3.4 Mutations disrupting the cell cycle

3.3.4.1 TP53

Six different mutations leading to p53 inactivation were identified (Figure 10). All variants identified represented missense mutations with VAF between 6 and 72%. Specific locations of the mutations among the gene domains are illustrated in Figure 10A. Interestingly, all these mutations were located in the DNA binding domain. In order to correlate the inactivation of the protein and loss of function of *TP53* which leads to p53 overexpression, p53 IHC was performed. TP53 positivity by IHC was compared between three cases of *TP53* wild-type (controls) and six cases with *TP53* mutation.

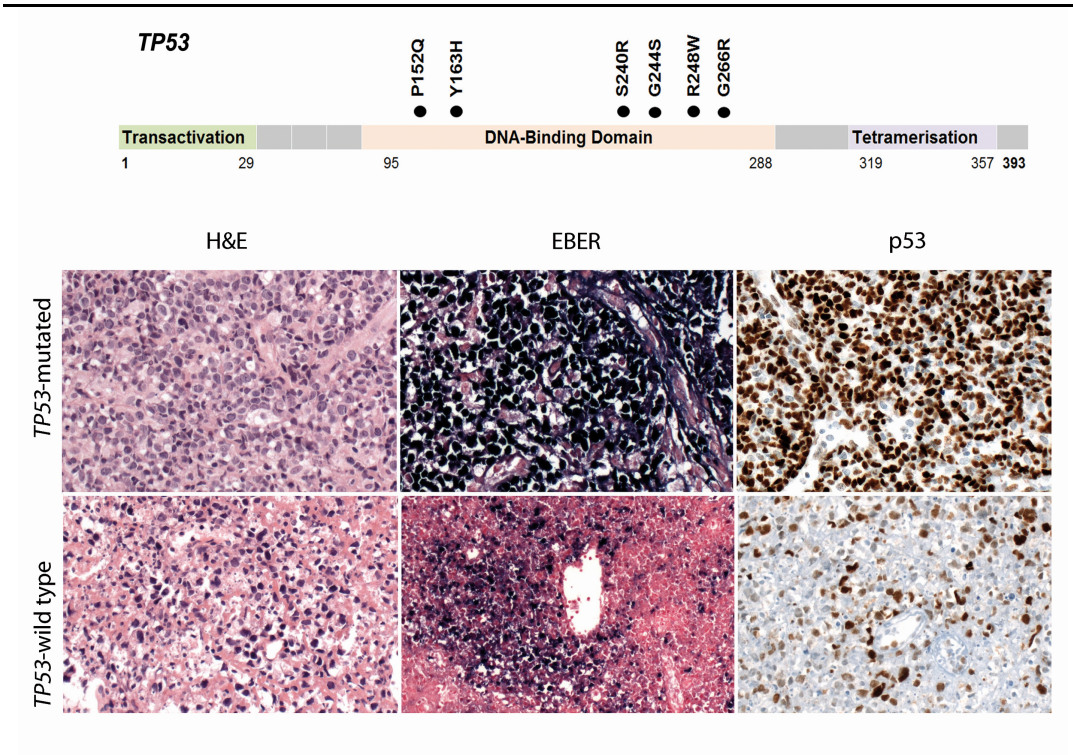

Figure 10. ***TP53*** **mutation and protein expression.**

Upper panel : All mutations of *TP53* are missense mutations located in the DNA-binding domain, specific mutations are depicted. (B) Upper picture: *TP53*-mutated case with large cell morphology (H&E, x400). All neoplastic cells are EBV positive (EBER-ISH, x400) and reveal homogeneous and strong staining of p53 (p53 IHC, x400). Lower picture: *TP53*-wild-type case with large cell morphology accompanied by tumoral necrosis (H&E, x400), tumoral cells are exposed by EBER positivity (EBER-ISH, x400) and some of these cells (10% approximately) show p53 heterogeneous positivity (p53 IHC, x400)
A: source from InterPro (UniProtK Q6W2J9) [163].
Abbreviations: H&E: Hematoxylin

p53 staining was strong and homogenous in cases with large cell morphology carrying a *TP53* mutation with high VAF. In contrast, the *TP53* wild-type cases showed heterogeneous positivity in a small percentage of cells. In general, only cases with homogenous and strong p53 positive in more than 80% of the cells by IHC had a good correlation with its mutational status. Figure 10B illustrates *TP53* mutated case with strong and homogenous p53 staining in comparison to a wild-type case [163]. In order to get to know the role of *TP53* mutations and its interaction with p21, a protein that also has an important role in cell cycle and apoptosis, the positivity for p21 was investigated by IHC. The staining was performed in six representative cases. The detailed information is summarized in table 21.

Table 21. p53 and p21 Immunohistochemistry in *TP53*-mutated and wild-type cases

ID	*TP53* gene status	Amino acid	VAF	p53 IHC	p21 IHC	Cyto-morphology
M20	Mutated	p.G266R	56%	Homogeneous and strong	<5% of tumor cells	Large cells
M25	Mutated	p.P152Q	63%	Homogeneous and strong	<5% of tumor cells	Large cells
P16	Mutated	p.G244S	6%	Heterogeneous and moderate to strong (40% of tumor cells)	5-10% of tumor cells	Large cells
M15	Wild-type			Heterogeneous and moderate to strong (40% of tumor cells)	5-10% of tumor cells	Large cells
M38	Wild-type			Heterogeneous and weak to moderate (10-20% of tumor cells)	10% of tumor cells	Intermediate-sized cells
M39	Wild-type			Heterogeneous and moderate to strong (60% of tumor cells)	<5% of tumor cells	Intermediate-sized cells

IHC, immunohistochemistry; VAF, variant allele frequency

In *TP53* mutated cases (n=3), p53 immunostaining was homogeneous and strong positive in 2 cases, but heterogeneous in 1 case; whereas the positivity for p21 immunostaining was <5% in tumor cells (loss of p21) of all mutated cases. In contrast, p53 immunostaining was weak and heterogeneous in 10 to 20% of the neoplastic population of *TP53* wild-type cases, also demonstrating loss of p21.

3.3.4.2 DDX3X

All *DDX3X* mutations analyzed in this cohort are depicted in Figure 11. Most of the cases (5/6) presented missense mutations, whereas only one case displayed a nonsense mutation. VAF among mutations ranged from 22 to 51%. Interestingly, all *DDX3X* mutations were heterogeneously distributed amongst the protein domains and non-hotspot were found (Figure 11). Concurrent mutations of *DDX3X* and *TP53* were only found in a case, in which a nonsense mutation of *DDX3X* was revealed.

In order to get to interpret the possible origin of the genetic alterations, tumor contents were calculated. In a Mexican case (M16), tumor content and VAF of *DDX3X* were around 30% likely representing a homozygous mutation, whereas other mutations found in *TP53 show* VAF around 12%, probably a concurrent heterozygous mutation. These variations in the VAF could also exemplify different genetic events, such as a loss of heterozygosity event as well as copy number variation.

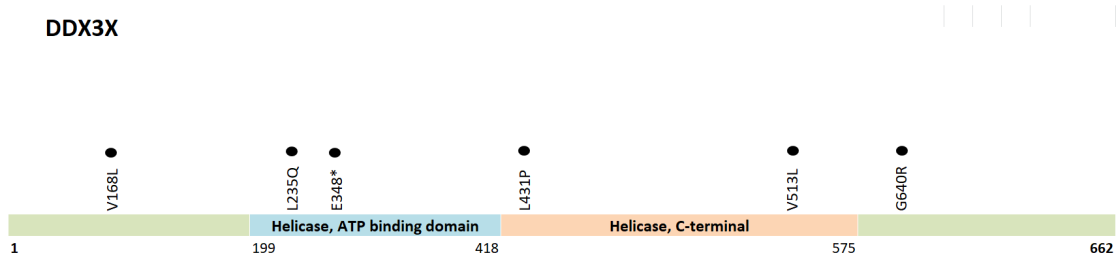

Figure 11. Distribution of DDX3X mutations along the protein.

Exact positions of all mutations detected are illustrated in the DDX3X protein within its different domains (www.uniprot.org; UniProtK O00571).

3.3.5 Mutations in other signaling pathways

MSN

In contrast to other studies, *MSN* mutations were relative frequent (10/53 mutations, 14%). Missense mutations were the most common alterations (5/10), followed by nonsense mutations (3/10) and frameshift mutations (2/10). VAF ranged from 6 to 69%. Interestingly, regardless of the type of mutation, most of the alterations were located in the helicase C-terminal domain. Moreover, concurrent *MSN* and *STAT3* mutation were recognized in cases M14, M22 and M41.

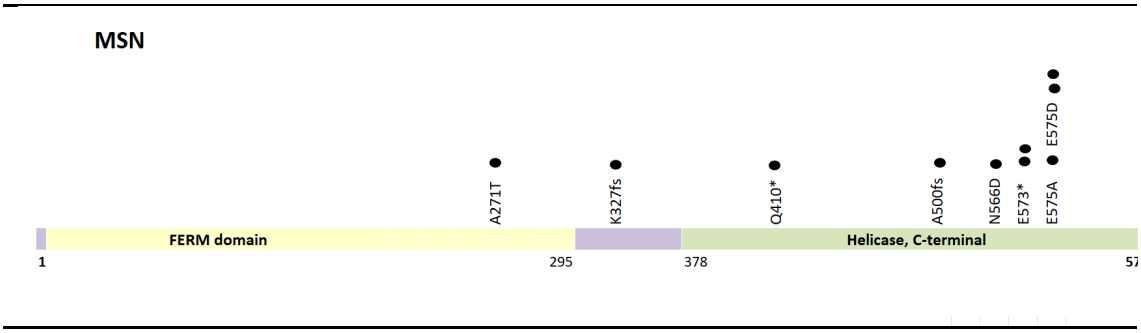

Figure 12. Distribution of MSN mutations within its protein domains.

Exact positions of all mutations detected are illustrated in the MSN protein within its different domains (www.uniprot.org; P26038).

MGA

In this study, only three recurrent somatic mutations in *MGA* were identified (cases M25, P5 and A10). Three type of mutations were detected: 1 nonsense mutation in case A10, 1 frame shift mutation in case M25 and one missense mutation in case P5, and VAF ranged from 10 to 32%. Concurrent mutation of *MGA* was only recognized in the case M25 with *TP53*. In this case, *MGA* seems to show a secondary role, since this mutation was concurrent with other genetic alterations, specifically with *TP53* mutation. In addition, the lower VAF (32%) in comparison with the higher tumor content of this case (70%), probably reflects heterozygous mutation whereas the mutations found in *TP53* mutation show higher VAF (63%).

3.4 PCR analysis of EBV strain and LMP1 gene deletion

All cases were analyzed for the characterization of EBV strain and *LMP1* deletion; data are presented in Table 19 and Figure 13. From the 71 cases, only 6 cases were EBV type B (6/71, 8%) but 65 cases (65/71, 92%) were recognized as EBV type A, showing that the latest was the most frequent strain detected among the three different Latin American countries studied. In EB type A as well as in type B cases, *LMP1* wild-type was the most frequent variant. However, in cases with EBV type B, 30bp *LMP1* deletion variant was more common. In Mexico EBV type A was commonly associated with *LMP1* wild-type, whereas EBV type B was frequently related to the 30 bp *LMP1* deletion variant. Peruvian ENKTCL cases showed EBV type A as the most common strain, and surprisingly none of the cases showed the 30 bp *LMP1* deletion variant. Examples of the PCR products electrophoresis showing the EBV strain and *LMP1* deletion distribution among the different countries are illustrated in Figure13. EBV type A was the most common strain in Argentina and was relatively commonly related with the 30 bp *LMP1* deletion variant. Comparison of the EBV strain among the countries revealed no significant difference (Table 22) [163].

Table 22. EBV strain distribution of extranodal NK/T-cell lymphoma in Latin America

	Total (n=71)	**Mexico (n=42)**	**Peru (n=17)**	**Argentina (n=12)**	***P*-value***
EBV strain					
EBV type A	65 (92%)	39 (93%)	15 (88%)	11 (92%)	
***LMP1* wild-type**	53 (75%)	32 (76%)	15 (88%)	6 (50%)	<0.05
***LMP1* 30-bp deletion**	12 (17%)	7 (17%)	0	5 (42%)	
EBV type B	6 (8%)	3 (7%)	2 (12%)	1 (8%)	
***LMP1* wild-type**	3 (4%)	0	2 (12%)	1 (8%)	1.0
***LMP1* 30-bp deletion**	3 (4%)	3 (7%)	0	0	

**p*-value using Fisher´s exact test with bivariate analysis. bp, base pair [163].

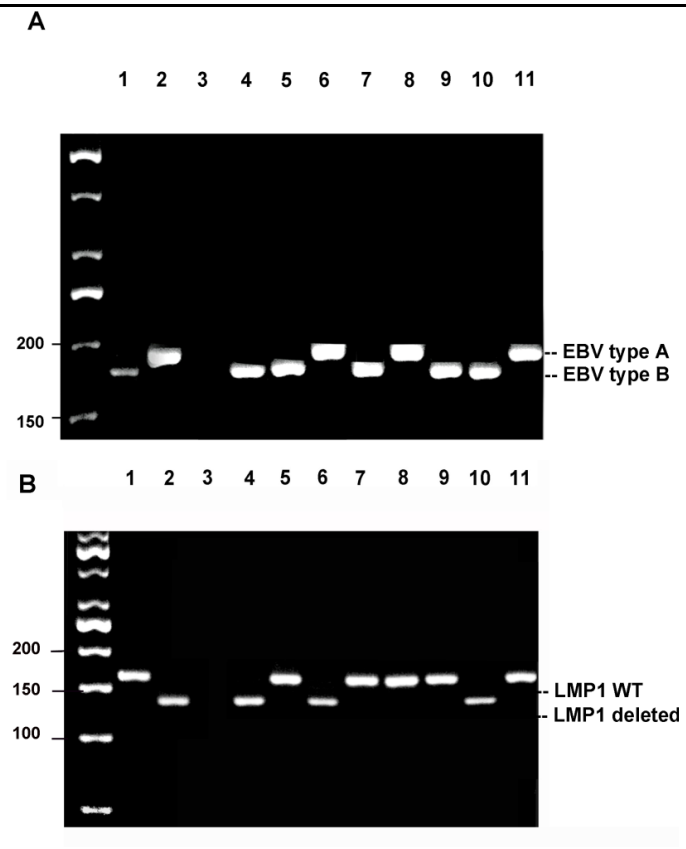

Figure 13. **Characterization of EBV strain and LMP1 gene.**

Electrophoresis from PCR products of the EBV type and *LMP1* gene deletion.
(A) Upper gel illustrates EBV type A and B analysis. The lanes 1 and 2 exemplify EBV type A (168 bp fragments) and B (184 bp fragments) according to the left 50bp ladder. The line 3 is the negative control. Cases from the three different countries are represented in lanes 4-6, Peruvian cases in lanes 7-8 and Argentina cases in lanes 9-11. EBV type B is displayed in lanes 6 (Mexican case), 8 (Peruvian case) and 11 (Argentinian case).
(B) Lower gel exhibit *LMP1* gene status. The lanes 1 and 2 show *LMP1* **wild-type** (161 bp fragment) and 30 bp *LMP1* **deletion** (131 bp fragment) in lanes 1 and 2 respectively, according to the left 50bp ladder. The negative control is in the lane 3. Cases carrying type A or B EBV strain with 30-bp deletion of *LMP1* gene are exposed in lane 4, 6, and 10, whereas cases with *LMP1* gene wild-type are displayed in lanes 5, 7, 8, 9 and 11. [163].

3.5 Correlation of clinicopathological factors and overall survival

OS rate was calculated at 1 and 2 year and assessed for all variants. As expected, low OS to 1 and 2 years was correlated with LDH elevation, >1 ECOG performance, >1 IPI score and therapy employed. According to the Cox proportional hazard model, >1 IPI score (HR 7.25, p=<0.001) and to receive chemotherapy alone (HR 4.76, p=0.014) were the highest risk factors for poorer survival. Although male gender has a higher risk of poor prognosis, this was not statistically significant (HR 2.42 p=0.07). The statistical analysis of the different clinicpathological factors on OS is described in table 23.

Age, site of involvement, clinical symptoms, mutational status as well as EBV strain type were not related to poor prognosis. However, the 30 bp *LMP1* deletion revealed a propensity to inferior OS in comparison to *LMP1* wild-type cases, which was independent of the EBV strain type.

Table 23. Analysis of the clinicopathological factors and overall survival in 51 patients with follow-up

	1-year OS rate	2-year OS rate	Hazard ratio	95% CI	*p*-value
Country					0.123
Mexico	49.4%	46.3%	2.50	0.74-8.40	
Peru	84.6%	84.6%	Reference		
Median age					0.524
<=66	61.0%	54.1%	Reference		
>66	29.6%	29.6%	1.38	0.51-3.75	
Gender					0.070
Male	45.9%	41.3%	2.42	0.90-6.49	
Female	76%	68.4%	Reference		
Site of involvement					0.356
Nasal	58.2%	55.3%	Reference		
Extranasal	40.0%	40.0%	1.76	0.52-5.93	
B symptoms					0.124
Yes	48.1%	44.9%	2.13	0.79 -5.71	
No	76.0%	76.0%	Reference		
LDH elevation					0.008*
Yes	43.0%	38.7%	3.90	1.32-11.55	
No	81.9%	73.7%	Reference		
ECOG > 1	38.2%	32.7%	2.75	1.21-6.23	0.011*
ECOG 0-1	68.9%	68.9%	Reference		
IPI score > 1	28.6%	23.8%	7.25	2.43-21.66	<0.001*
IPI score 0-1	86.3%	79.7%	Reference		
Therapy					0.014*
Combined chemoradiotherapy	59.6%	54.2%	2.02	0.45-9.08	

Chemotherapy alone	40.0%	40.0%	4.76	0.95-23.8	
Radiotherapy alone	80.0%	80.0%	Reference		
No therapy	0%	0%	9.012	1.49-55.57	
***STAT3* mutation**	63.6%	53.0%	0.947	0.35-2.54	0.913
***STAT3* wild-type**	53.8%	53.8%	Reference		
***MSN* mutation**	53.6%	53.6%	0.922	0.27-3.12	0.895
***MSN* wild-type**	57.0%	54.0%	Reference		
***BCOR* mutation**	66.7%	66.7%	1.198	0.41-3.54	0.743
***BCOR* wild-type**	54.9%	54.0%	Reference		
***DDX3X* mutation**	33.3%	33.3%	2.097	0.49-8.99	0.307
***DDX3X* wild-type**	58.1%	55.3%	Reference		
***TP53* mutation**	60.0%	60.0%	0.836	0.20-3.57	0.808
***TP53* wild-type**	56.6%	53.8%	Reference		
Number of mutation					0.946
0	49.6%	49.6%	Reference		
1	62.3%	56.1%	1.06	0.45-2.49	
>1	57.1%	57.1%	0.85	0.23-3.11	
JAK-STAT pathway*					0.913
Mutated	63.6%	53%	0.95	0.35-2.54	
Wide type	53.8%	50%	Reference		
EBV strain					0.932
Type A	56.8%	54.1%	Reference		
Type B	53.3%	53.3%	1.07	0.25-4.57	
LMP1					0.09
Wild-type	63.5%	60.3%	Reference		
30-bp deletion	25%	25%	2.21	0.87-5.62	

*JAK-STAT pathway includes mutation of *JAK3, STAT3* or *STAT5B* genes. **p*-value <0.05. bp, base pair; CI, confidence interval; ECOG, Eastern Cooperative Oncology Group; IPI, International Prognostic Index; LDH, lactate dehydrogenase; NA, not available; OS, overall survival [163].

4. Discussion

This study represents the largest cohort of ENKTCL patients collected in Latin America so far, identifying the JAK-STAT signaling pathway as the main disrupted pathogenic pathway in this entity (27% of the cases). Other genes involved in the NOTCH or cell cycle signaling pathways, such as *BCOR* and *DDX3X* were also mutated, but with a lower frequency. Moreover, mutations in *STAT3, DDX3X* and *BCOR* were nearly mutually exclusive, demonstrating the central role of these pathways in the lymphomagenesis of ENKTCL and highlighting them as potential therapeutic targets. EBV infection was confirmed in all cases, being EBV type A carrying *LMP1* wild-type the most frequent EBV strain reported in these patients (75%). The OS of these patients was low and it was not related to sequencing and EBV infection variables such as mutational status or EBV strains. The clinical variants high IPI score, >ECOG performance status, elevated serum LDH level and chemotherapy alone were associated with an inferior OS.

ENKTCL is an aggressive lymphoma, quite common in Asia and in the indigenous population of Latin America, with a relatively low survival rate (55%) [1]. In recent years, the emergence of new modalities of therapy and the use of combination therapy containing platinum or l-asparaginase has contributed to improve the prognosis of this disease. However, relapses and refractory cases are still frequent; therefore, it is crucial to develop specific individualized therapies based on genomic analysis [154]. In previous years, the mutational landscape has been further investigated in Asian populations (China, Japan, Korea and Singapore), revealing recurrent mutations in the JAK-STAT signaling pathway, the RNA helicase family, the RAS and NOTCH signaling pathways, as well as in some known tumor suppressors (*TP53* and *MGA*) and in epigenetic modifiers such as *ARID1A* among others [61,90-96]. Unfortunately, the mutational landscape of these studies only shows little overlapping and differ in the most mutated genes and their frequencies. These discrepancies are probably due to the different genetic

background among these populations, case selection or because the different sequencing methodologies applied which carry diverse sensitivities (whole-exome sequencing, targeted sequencing, Sequenom MassARRAY platform) [61,90-96]. In our study, *STAT3* represented the most commonly mutated gene, featured as a single mutation in 69% of *STAT3* mutated cases, comparable to the mutational profile from the Korean and China-Singapore cohorts [90,95]. However, lower mutational frequencies of this gene have been reported in the Chinese [92] and Japanese cohorts [93]. The lower detection of these mutations might be a result of the geographical and ethnic variations of the population surveyed, the status of the disease or merely related to the lymphoma cell of origin (NK or T-cell origin). In a recent study, Song *et al.* also distinguished *STAT3* as the most frequently mutated gene in ENKTCL, in comparison to the lower mutation frequency detected in other peripheral T-cell lymphomas such as angioimmunoblastic T-cell lymphoma (AILT) or ALCL [95], highlighting it as one of the main oncogenic events in the pathogenies of ENKTCL [168,169]. In contrast, other gamma-delta T-cell lymphomas, such as hepatosplenic T-cell lymphoma, primary cutaneous gamma-delta T-cell lymphoma and MEITL, also display activating mutations in the JAK-STAT signaling pathway, but interestingly predominantly in *STAT5B* and not in other members of these pathways such as *STAT3* and *JAK1/2/3* [91]. This led us to think that the lower frequency of *STAT5B* abnormalities in ENKTCL is correlated to the gamma-delta T-cell of origin, since most of ENKTCL cases display NK-cell origin (80%) and only less than 20% show a gamma-delta T-cell phenotype [91].

STAT proteins are essential regulators of T-cell proliferation, differentiation and survival. *STAT3* and *STAT5B* are two members of this family involved in angiogenesis and oncogenesis enhancement [170]. Despite the fact that these proteins have four to five different functional domains, [171] all of the pathogenic mutations in this series were located in the SH2 domain, a domain which favors its activation by reciprocal SH2 phosphotyrosine interaction [91,95]. Other studies have also recognized additional mutations in the DNA binding domain and the coiled-coil domain of *STAT3,* stressing other activation pathways. Thus, the constitutive activation of *STAT3* may be triggered by different mechanisms, including somatic

mutations along the different domains of the protein which lead to its activation, increased upstream stimulation of kinases, positive feedback loops or absence of negative regulation [172]. From all mutations, D661Y and Y640F represent the main hotspots of *STAT3* described in ENKTCL; nonetheless, they are also found in other T-cell lymphomas suggesting its role as T cell oncogenic drivers [112]. Interestingly, regardless of the type of mutation, all *STAT3* variations in this analysis resulted in its activation. Different studies have affirmed the use of the IHC p-STAT3 as a surrogate to study its mutational state and detect its activation. In this study, p-STAT3 staining was correlated with its mutational state and also showed an association of the tumor content with the percentage of VAF [111,112]. Although nearly all *STAT3* mutations in this series were mutually exclusive (69%), concurrent mutations with *MSN, BCOR* and *TP53* were present, emphasizing the primary role of *STAT3* and the secondary role of other mutations. [93]. Concurrent *STAT3* and *MSN* mutations was the most frequent concurrent event, probably linked to an enhanced tumoral activity since *MSN* seems to trigger invasion of tumoral cells [151-153]. On the other hand, concurrent *TP53* mutations and JAK-STAT signaling pathway abnormalities were not common and only reported in a genetically complex case (A3) presenting different mutations in *JAK3* and *STAT3* accompanied by *BCOR* and *TP53* mutations. The presence of *TP53* mutation in this case seemed to be related to poor prognosis, as it was previously reported in other cancers and related to transformation of myeloproliferative neoplasms into leukemia [173,174].

Activating mutations in the gene *JAK3,* an additional member of the JAK-STAT signaling pathway, were also reported in various hematological malignancies such as myeloproliferative diseases and acute lymphoblastic leukemia. In our study, the frequency of *JAK3* alterations in ENKTCL was relatively low (3%) in comparison with the cohort from Singapore, in which 35.4% of 65 samples harbored a *JAK3* mutation [117]. However, the frequency of *JAK3* mutations of our study resembled the results in the other Asian cohorts, where frequencies are reported from 0 to 8% [90-96].

JAK3 mutations (A573V and V722I) have also been reported and validated in IL-3 dependent pro-B-cells (Ba/F3) as transforming activating mutations [175].

Intriguingly, only the *JAK3* A573V mutation was located within the JH2 pseudo-kinase domain, a known regulator of the JAK kinase activity. Mutations located in the JH2 domain were studied *in vitro* and associated with independent IL-2 lymphoproliferation, resulting in activation of the JAK-STAT signaling pathway, which can be efficiently targeted in vitro by the JAK inhibitor CP-690550 [117], highlighting the use of JAK inhibitors as an alternative therapeutic modality in ENKTCL. Strikingly, EBV Infection likewise play a role in JAK-STAT pathway switch through its latent proteins. Two control mechanisms have been described: interaction of the cytoplasmic carboxyl-terminal of LMP1 with JAK, resulting in increased phosphorylation of JAK3 tyrosine, or activation of NF-κB due to the similarity of LMP1 with the CD40 receptor [176-178].

Surprisingly, 14% of the NKCTL cases of this study presented recurrent *MSN* mutations whereas in the Asian cohorts the frequency of this alterations is comparatively low (0-8 to 6%) [90-92]. 60% of these cases revealed this mutation as a single alteration and nearly half of these patients had a concurrent *STAT3* mutation, suggesting that these alterations do not represent main driver in the pathogenesis of ENKTCL. *MSN* function has been closely related to cell-cell recognition, cell movement, cell signaling [179,180] and related to carcinogenesis and survival in epithelial oral cancers [181]. However, little is known of its biological role in malignant lymphoproliferations. Hemizygous mutations involving *MSN* gene are identified in X-linked primary immunodeficiency (R171W, R533X) leading to premature stop codons. In this setting, it is believed, that *MSN* mutations leads to impaired T cell proliferation, poor chemokine expression and disturbances in the migration and adhesion of T cells [182]. In other T-cell lymphomas, such as (ALK)-positive ALCL, genomic alterations in *MSN* are also related to oncogenesis, specifically associated with the enhancement of ALK function. [183]. In ENKTCL, recurrent *MSN* mutations (stop codon, missense and frameshift) seem to lead to loss of function of *MSN*, but their biological implication until date is still unclear. It is needed to perform more studies in order to understand the role of *MSN* and its relationship with other signaling pathways in the pathogenesis of ENKTCL.

In addition to the JAK-STAT signaling pathway, the NOTCH signaling pathway is also impaired through recurrent alterations in *BCOR* [93], a *BCL-6* co-repressor [118] which acts as a epigenetic regulator involved in cell differentiation, body structure development and histone modification [184]. Epigenetic alterations are relatively frequent in ENKTCL and are not exclusive to *BCOR*, also involving other genes such as *ARID1A, ASXL1, BCOR, KMT2D, MLL2, EP300* [93,100,101]. However, *BCOR* is the most frequent epigenetic alteration investigated in recent cohorts [90-95], specifically in the Japanese population where the frequency of the mutation is reported around 32%. In comparison, Chinese and Korean population report lower frequencies comparable to the Latin-American population [90,91,93]. The recurrent *BCOR* abnormalities are reported in T-cell lymphomas, but also displayed in other hematopoietic disorders including myelodysplastic syndromes [185], B-cell lymphomas including splenic marginal zone lymphoma [186] and splenic diffuse small B-cell lymphoma [187]. In chronic myeloid leukemia and acute myeloid leukemia, *BCOR* alterations result in truncated proteins with loss of function [121]. In this study, only 3 of 9 *BCOR* mutations led to a truncated protein but all alterations were predicted as damaging mutations by the different software algorithms, irrespectively of the location within the gene. The loss of function of the tumor suppressor *BCOR* is also associated to the loss of negative regulation of the *NOTCH* signaling pathway [188], epigenetic dysregulation, underlining additional oncogenic mechanisms in the pathogenesis of ENKTCL. Furthermore, the upregulation of this pathway represents a main therapeutic target in cases of refractory ENKTCL [189]. In other disorders, such as MDS, frameshift *BCOR* mutations represent also prognostic factors closely related to the OS [185]. Unfortunately, given the limited number of *BCOR* mutations in this cohort, it was not feasible to establish an association between *BCOR* alterations and survival.

Another recurrent mutation previously associated with poor prognosis is the RNA Helicase *DDX3X*, which participates as a key player in the regulation of cell cycle, probably acting as a tumor suppressor gene in ENKTCL [92]. *DDX3X* mutations are common in T- and B-cell lymphomas [137,]. In ENKTCL frequencies in Asian cohorts range from 4 to 20%, whereas in this study the frequency average was

under 10% (8.5%) [91-93]. The function of *DDX3X* is not completely understood, but preliminary functional studies supports *DDX3X* as a candidate component of the pathogenic WNT/β-catenin signaling in medulloblastoma [190]. In ENKTCL, inactivating *DDX3X* mutations are related in cell cycle progression and transcriptional activation of the NF-κB pathway [92]. In this series, 5 out of the 6 *DDX3X* mutations reported were seen as single mutations affecting the helicase C-terminal domain, highlighting the functional part of the protein. Concurrent *DDX3X* and *TP53* alterations are frequent genetic events described in ENKTL [92] and CLL [191]. However, there is only one case reported in this study. It is known, that *TP53* and *DDX3X* interact and regulate intrinsic and extrinsic apoptotic pathways after DNA damage, which suggest that *DDX3X* positively regulates the camptothecin-induced apoptotic signaling by p53 accumulation (intrinsic pathway) and/or interacts with p53 mutated protein and inhibits caspase activation (extrinsic pathway) [192]. Interestingly, *DDX3X* and *TP53* mutations seem to enhance their activity in ENKTCL, with a poor prognosis in cases carrying both mutations [92]. In this study, probably due to the low mutational rate (8.5%) of *DDX3X,* similar to the one reported for *BCOR*, associations to survival render no statistically significant correlations.

TP53 is a well-known tumor suppressor with inactivating mutations described in a wide range of malignant disorders. In ENKTCL, *TP53* mutations were earlier frequently reported in the Asian population (40-62%) [89,127,128] and in a Mexican cohort (24%) [16]. However, in later studies of similar cohorts, a lower frequency was reported, 13.3% and 8.5% respectively [92]. The reasons for the frequency disparity could be related merely to the cohort sampling and the earlier diagnosis of these cases. TP53 are not exclusive of ENKTCL and are also reported in aggressive B- and T- cell lymphomas, such as intestinal T-cell lymphoma and peripheral T-cell lymphoma, NOS, displaying a similar frequency as reported in ENKTCL, 22.2% of and 21.7%, respectively [193].

Interestingly, all *TP53* mutations reported in our study were missense mutations predicted to promote damage of the protein and loss of function. In accordance to our study, 90% of *TP53* mutations were located in the DNA binding domain, indicating the role of the mutation in the protein disruption and the alteration of its

ability to bind to DNA [194,195]. *TP53* mutational status can be evaluated by p53 IHC and it has been previously used as a surrogate; however, in our study only strong and homogeneous p53 staining in more than 80% of tumoral cells was associated with the *TP53* mutation [131]. The absent correlation with weaker staining can be attributable to the disturbance of other signaling pathways not studied in this cohort, which can also lead to the accumulation of p53 in the nuclei of neoplastic cells. Other genetic mechanisms related to p53 disruption includes loss of 17p and *TP53* downregulation targeted by EBV proteins such as EBNA-1 and miR-BART20-5p [196]. *TP53* mutations in ENKTCL are clinically related with extranasal or lymph node involvement, advanced stage of the disease and high IPI score [16,92,193]. However, in our study, the low frequency of *TP53* mutations did not show any correlations with clinical variables related to poor clinical outcome. Since *TP53* overexpression leads to further tumor suppressor mechanisms such as cell cycle arrest, other proteins related to *TP53* cell cycle function, including *TP21*, have been investigated in ENKTCL [197]. The positivity of p21 staining was previously assessed in ENKTCL by using IHC and correlating it with *TP53* mutational status and/or protein expression [16]. However, in the wild-type and *TP53*-mutated cases evaluated, there was no overexpression of p21, suggesting that other signaling pathways must be involved in TP21 down-regulation or that other EBV-related mechanisms may also be implicated. However, in this cohort only a limited number of cases were investigated [16] and further investigations to elucidate the role of *TP21* in ENKTCL are required.

Other rather frequently mutated gene in ENKTCL with unclear function is *MGA. MGA* mutations in ENKTCL of Asian cohorts are reported up to 8% of the cases, but in the current study, the NGS panel only detected 3 loss of function mutations (4%). The function of *MGA* is not fully understood, but it appears to be involved in the regulation of cell proliferation by inhibiting the proto-oncogene *MYC. MYC* was originally identified as the target of t(8;14)(q24;q32) chromosome translocation in Burkitt lymphoma, but in later days *MYC* up-regulation was also recognized in other mature B-cell neoplasms and associated with aggressive clinical behavior [198]. Interestingly, in T-cell lymphomas the upregulation of *MYC*, by activating

mutations in *NOTCH1,* is also acknowledged [199]. Until now, WES sequencing has not recognized any *MYC* pathogenic variations in ENKTCL, but gene expression profile studies have displayed that *MYC* is overexpressed in ENKTCL [200]. However, the presence of inactivating mutations in *MGA* could lead us to the question of whether this phenomenon represents an indirect or secondary mechanism for the regulation of this oncogene. Intriguingly, as *MYC* is a transcriptional target of *EBNA2* and *LMP1*, EBV can also be responsible of *MYC* upregulation in ENKTCL [200]. These oncogenic mechanisms point out *MYC* as a therapeutic target that needs to be investigated in ENKTCL.

The advent of high throughput NGS in the last years has accelerated the knowledge and new findings about the genomic landscape in many different diseases such as ENKTCL [61]. Recently, a new broad genetic analysis in ENKTCL have suggested a new molecular classification differentiating 3 different subgroups, which correlate with the biology and cell of origin as well as the clinical behavior, revealing the distinctive therapeutic targets to be investigated in this lymphoma. The first group named Tumor Suppressors and Immune Modulators (TSIM) comprises the cases with recurrent JAK-STAT signaling pathway activation, presence of *TP53* mutations, del6q21 and other mechanisms involved in the immune surveillance, such as PD-L1 overexpression. In the Latin-American cohort from this study most of the cases fall into this category, pointing to JAK-STAT inhibitors and immune modulators as a potential therapy for these cases. The second subgroup involves *MGA* mutations and loss of heterozygosity of the Brodomain Testis Associated (*BRD*) locus and is designated as MB subgroup. This second subgroup is less frequent in our cohort, since only 4 cases presented *MGA* alterations. The third subgroup HEA is named after the genomic alterations in the epigenetic modifiers: *HDAC1, EP300* and *ARID1*. This subgroup shows one of the limitations of our study since the mutational status of these epigenetic modifiers were not investigated in our cohort. However, 13% of the cases displayed *BCOR* alterations related with epigenetic alterations and the NOTCH signaling disturbance, suggesting that these belong to the MB and HEA group. On the other hand, cases with *DDX3X* mutations may represent cases

heterogeneously distributed among the TSIM and the HEA subgroups, in which asparaginase based therapy regimens can be beneficial.

In addition to the various mechanisms of oncogenesis, such as immune response and epigenetic alterations related to the mutational status of ENKTCL, described above, other features related to EBV infection could also play an important role in the lymphomagenesis of this lymphoma. EBV is a known human pathogen with tropism for B-cells, but with an important role in the oncogenesis of a broad spectrum of NK and T-cell malignant neoplasias. Although the association of EBV and ENKTCL is well recognized, the exact role of EBV in ENKTCL oncogenesis remains unclear [40]. However, EBV malignant transformation has been related to induction of several "latent genes", including *EBNA1, EBNA2, EBNA3A, EBNA3B, EBNA3C* and *LMP1, 2A, 2B* [47]. According to *EBNA2* genetic alterations, EBV was further classified as described earlier, into type A and type B, leading to the recognition of the worldwide distribution of EBV types and their association with different EBV-related benign or malignant disorders [58,59]. EBV type A infection is widely more common and it was found in the majority of the ENKTCL cases, in comparison to EBV type B. Interestingly, the majority of ENKTCL cases with EBV type A infection correlated with LMP1 wild-type protein, highlighting the oncogenic potential of this strain despite the *LMP1* status [59]. In contrast, EBV type B shows low transformation capacity in lymphoblastoid cells [60], which can be enhanced by the presence of the *LMP1* deletion [201]. Interestingly, all Mexican cases carrying EBV type B were associated with *LMP1* deletion, whereas the Argentinian and Peruvian cases show EBV type B in absence of *LMP1* deletion, which is generally described in cases with immunodeficiency [69-72]. The distribution of the EBV strain among the different Latin American countries in this study may be related to their geographical differences, but also is influence by the different immunodeficiency status of the hosts.

Recently, the genome and transcriptome studies of the EBV in human tissues has led to the recognition of new distinct EBV strains and sequence variants, providing new hits for understanding the EBV classification and pathogenesis [59,202]. Some of these novel studies analyzed the complete sequence of LMP1 and

EBNA resulting in six different strains, which show an uncertain correlation with the different clinical settings [203,204] and therefore, the widely used classification into type 1 and 2 remain valid to date. However, it is important to emphasize that there may be errors in this classification, explained by recombination events of EBV related genes (*EBNA2 and EBNA 3s*) [205,206]. In our study, the correlation of EBV strain type and *LMP1* status with the different clinicopathological variables as well as with the NKTCL mutational status and clinical outcome did not show any association. However, although the 30 bp deletion in *LMP1* gene tends to predict lower OS in comparison to *LMP1* wild-type cases, this statement can be influenced by the host immune status; therefore, a prospective larger study is required to further investigate and validate this hypothesis.

In general, ENKTCL patients show variable outcome, but poorer than expected for a localized non-Hodgkin lymphoma, which is often associated with invasion of the bone or the skin, high circulating of EBV DNA levels, EBV positive cells in the bone marrow and Ki-67 proliferation index [1]. However, in the current analysis, clinical outcome was fatal in half of the cases, although these cases were diagnosed at an early stage of the disease, confirmed by low of IPI score (<1). OS to 1 and 2 years seems to be poorest in the Mexican patients (HR 2.5, p=0.123). In the statistical OS analysis of this cohort, the only factors that correlated with poor prognosis were elevated DHL, >1 IPI score and > ECOG performance status. In recent studies, the molecular factors associated with poor prognostic factors are the overexpression of PDGFRA, PD-L1 and Ki-67 [207]. Interestingly, *STAT3* activation promotes PD-L1 overexpression in ENKTCL [95]; however, activating *STAT3* mutations were not associated with poorer OS or as a poor prognostic factor in comparison to wild-type cases.

Overall, the mutation status of all genes examined in this cohort was not associated with OS. In order to further evaluate this association, it is necessary to expand our mutation panel and to include in the statistical analysis other mutation characteristics such as location, type and clonal hierarchy, which may influence the prognostic implications of genomic abnormalities.

4.1 Conclusions and perspectives

ENKTCL mutational landscape in the Latin American population exhibits recurrent somatic mutations in the JAK-STAT (*JAK, STAT5B, STAT3*) and NOTCH (*BCOR*) signaling pathway, in cell cycle regulators (*DDX3X, TP53*) among other genes with less known functions such as *MSN* and *MGA*. Activating *STAT3* mutations were the most frequent in this study (27% of the cases), highlighting its main role in the pathogenesis of ENKTCL and encouraging the use of JAK inhibitors as a targeted therapy in these patients. In comparison to Asian populations, *MSN, BCOR, DDX3X* and *TP53* mutations were also found but with different frequencies. EBV type A with *LMP1* wild-type was the most frequent EBV strain in this cohort, independently of the stage of disease and mutational status. In addition, only elevated LDH, therapy and IPI score as well as ECOG performance status were correlated with OS. Finally, ENKTCL mutational status as well as EBV strain appeared to have no role in OS.

5. Summary

Extranodal NK/T-cell lymphoma (ENKTCL) nasal type, is an aggressive lymphoma associated with EBV infection, highly prevalent in Asian and Latin American populations with characteristic clinicopathological features. Several studies in Asian ENKTCL cohorts have identified the most common recurrent somatic mutations in *STAT3, STAT5B, JAK3, DDX3X, TP53, MGA, MSN* and *BCOR*; however, the genomic landscape in the ENKTCL is still incomplete and the mutation status in cases from Latin America remains to be investigated. The main objective of this study was to investigate the mutation landscape in a cohort of ENKTCL cases from Latin America (Mexico, Peru and Argentina), to compare it with Asian cohorts and to investigate EBV strain type and *LMP1* gene status. We analyzed 71 cases of ENKTCL from 3 different centers in Latin America. Hematoxylin staining (H&E), CD56 and EBER *in situ* hybridization were performed to confirm the diagnosis and calculate the tumor content in all cases. Sequencing of the most frequently mutated genes was performed using NGS workflow based on a custom AmpliSeq panel. In addition, EBV strain type classification and LMP1 deletion at 30 bp was carried out by PCR. Mutations affecting the JAK-STAT pathway were the most frequent mutation anomaly followed by *MSN* (10 cases, 14%). *STAT3* was the most frequently mutated gene (16 cases, 22%), while other members of the JAK-STAT pathway, *STAT5B* (one case) and *JAK3* (2 cases), were rarely identified. All *STAT3* mutations were activating mutations, located within the SH2 domain, leading to expression of pSTAT3 evidenced by immunohistochemistry. Inactivating mutations in *BCOR* and *DDX3X* were found in 9 (13%) and 6 (8.5%) cases, respectively. *TP53* mutations were identified in only 6 cases (8.5%). Interestingly, mutations in *STAT3, BCOR* and *DDX3X* were mutually exclusive, indicating the key role of JAK-STAT, NOTCH and cell cycle signaling pathways. EBV type A with the wild-type LMP1 gene (53/71; 75%) was the most common genotype in all cases, while EBV type B with *LMP1* deletion was detected only in 3 Mexican cases. The ENKTCL mutation status in Latin America showed frequent *STAT3*-activating mutations. Furthermore, EBV type A with

LMP1 wild-type was the most common strain found in this cohort. However, none of these variables affected overall survival. Finally, the ENKTCL mutation landscape of Latin America was comparable to that of Asian cohorts.

German summary

Das extranodale natürliche Killer/T-Zell-Lymphom (NK/T) vom nasalen Typ (ENKTCL) ist ein hoch aggressives Lymphom, das mit einer EBV-Infektion einhergeht und in der asiatischen und lateinamerikanischen Bevölkerung sehr häufig vorkommt und charakteristische klinisch-pathologische Merkmale aufweist. Mehrere Studien in asiatischen HNO-Kohorten haben die häufigsten rekurrenten somatischen Mutationen in *STAT3, STAT5B, JAK3, DDX3X, TP53, MGA, MSN* und *BCOR* identifiziert. Allerdings ist das Spektrum genetischer Veränderungen bei ENKTCL unvollständig beschrieben und der Mutationsstatus von ENKTCL Patienten in Lateinamerika noch nicht untersucht worden. Das Hauptziel dieser Studie war es, das Spektrum an Mutationen in einer Kohorte von ENKTCL-Fällen aus Lateinamerika (Mexiko, Peru und Argentinien) zu untersuchen, sie mit einer asiatischen Kohorte zu vergleichen und sowohl den EBV-Typ als auch den *LMP1*-Genstatus zu untersuchen. Dafür wurden 71 Fälle von ENKTCL aus 3 verschiedenen Zentren in Lateinamerika analysiert. HE-Färbung, CD56 und EBER-in-situ-Hybridisierung wurden durchgeführt, um die Diagnose zu bestätigen und den Tumorgehalt zu bestimmen. Die Sequenzierung der in asiatischen ENKTCL am häufigsten mutierten Gene wurde mittels NGS mit Hilfe eines selbst zusammengestellten AmpliSeq-Panels durchgeführt. Darüber hinaus wurden der EBV-Typ und die LMP1-Deletion von 30 bp mittels PCR untersucht. Am häufigsten fanden sich Mutationen, die den JAK-STAT-Signalweg beeinflussen, gefolgt von *MSN* (10 Fälle, 14%). *STAT3* war das am häufigsten mutierte Gen (16 Fälle, 22%), während andere Mitglieder des JAK-STAT-Signalwegs, *STAT5B* (ein Fall) und *JAK3* (2 Fälle), selten identifiziert wurden. Alle *STAT3*-Mutationen waren aktivierende Mutationen, die sich innerhalb der SH2-Domäne befinden und zur pSTAT3-Expression führten. Inaktivierende Mutationen in *BCOR* und *DDX3X* wurden ebenfalls in 9 (13%) bzw. 6 (8,5%) Fällen gefunden. *TP53*-Mutationen wurden nur in 6 Fällen (8,5%) identifiziert. Interessanterweise schlossen sich Mutationen in *STAT3*, *BCOR* und *DDX3X* gegenseitig aus, was auf eine Schlüsselrolle der JAK-STAT, NOTCH und Zellzyklus-Signalwege hinweist. Typ-A-EBV mit dem Wildtyp-*LMP1*-Gen (53/71; 75%) war der häufigste Genotyp, während EBV

Typ-B mit *LMP1*-Deletion nur in 3 mexikanischen Fällen nachgewiesen wurde. ENKTCL in Lateinamerika weisen häufig STAT3-aktivierende Mutationen auf. Darüber hinaus war das EBV vom Typ A mit *LMP1*-Wildtyp der häufigste Stamm, der in dieser Kohorte gefunden wurde. Keine dieser Variablen beeinflusste jedoch das Gesamtüberleben. Außerdem war das ENKTCL-Mutationsspektrum Lateinamerikas mit der asiatischen Kohorte vergleichbar.

6. References

1. Chan JK, Quintanilla-Martinez L, A. FJ. Extranodal NK/T-cell lymphoma, nasal type. In: H. SS, ed. *WHO classification of tumours of haematopoietic and lymphoid tissues*. Revised 4th. ed. IARC; 2017:368-371. *World Health Organization classification of tumours*.
2. Jaffe ES, Harris NL, Stein H, Isaacson PG. Classification of lymphoid neoplasms: the microscope as a tool for disease discovery. *Blood*. Dec 1 2008;112(12):4384-99. doi:10.1182/blood-2008-07-077982
3. Jaffe ES, Krenacs L, Raffeld M. Classification of cytotoxic T-cell and natural killer cell lymphomas. *Seminars in hematology*. Jul 2003;40(3):175-84.
4. Lee J, Kim WS, Park YH, et al. Nasal-type NK/T cell lymphoma: clinical features and treatment outcome. *British journal of cancer*. Apr 11 2005;92(7):1226-30. doi:10.1038/sj.bjc.6602502
5. Elenitoba-Johnson KS, Zarate-Osorno A, Meneses A, et al. Cytotoxic granular protein expression, Epstein-Barr virus strain type, and latent membrane protein-1 oncogene deletions in nasal T-lymphocyte/natural killer cell lymphomas from Mexico. *Modern pathology : an official journal of the United States and Canadian Academy of Pathology, Inc*. Aug 1998;11(8):754-61.
6. Au WY, Weisenburger DD, Intragumtornchai T, et al. Clinical differences between nasal and extranasal natural killer/T-cell lymphoma: a study of 136 cases from the International Peripheral T-Cell Lymphoma Project. *Blood*. Apr 23 2009;113(17):3931-7. doi:10.1182/blood-2008-10-185256
7. Barrionuevo C, Zaharia M, Martinez MT, et al. Extranodal NK/T-cell Lymphoma, Nasal Type: Study of Clinicopathologic and Prognosis Factors in a Series of 78 Cases From Peru. *Applied Immunohistochemistry & Molecular Morphology*. 2007;15(1):38-44. doi:10.1097/01.pai.0000205062.27174.56
8. Quintanilla-Martinez L, Franklin JL, Guerrero I, et al. Histological and immunophenotypic profile of nasal NK/T cell lymphomas from Peru: High prevalence of p53 overexpression. *Human Pathology*. 1999/07/01/ 1999;30(7):849-855. doi:10.1016/S0046-8177(99)90147-8
9. Laurini JA, Perry AM, Boilesen E, et al. Classification of non-Hodgkin lymphoma in Central and South America: a review of 1028 cases. *Blood*. Dec 6 2012;120(24):4795-801. doi:10.1182/blood-2012-07-440073
10. Arber DA, Weiss LM, Albujar PF, Chen YY, Jaffe ES. Nasal lymphomas in Peru. High incidence of T-cell immunophenotype and Epstein-Barr virus infection. *The American journal of surgical pathology*. Apr 1993;17(4):392-9.
11. Barros MH, Vera-Lozada G, Soares FA, Niedobitek G, Hassan R. Tumor microenvironment composition in pediatric classical Hodgkin lymphoma is modulated by age and Epstein-Barr virus infection. *Int J Cancer*. Sep 1 2012;131(5):1142-52. doi:10.1002/ijc.27314

12. Altemani A, Barbosa AC, Kulka M, et al. Characteristics of nasal T/NK-cell lymphoma among Brazilians. *Neoplasma*. 2002;49(1):55-60.

13. Bellei M, Chiattone CS, Luminari S, et al. T-cell lymphomas in South america and europe. *Rev Bras Hematol Hemoter*. 2012;34(1):42-47. doi:10.5581/1516-8484.20120013

14. Schwartz EJ, Molina-Kirsch H, Zhao S, Marinelli RJ, Warnke RA, Natkunam Y. Immunohistochemical Characterization of Nasal-Type Extranodal NK/T-Cell Lymphoma Using a Tissue Microarray: An Analysis of 84 Cases. *American journal of clinical pathology*. 2008;130(3):343-351. doi:10.1309/v561qtm6854w4wav

15. Cabrera ME, Eizuru Y, Itoh T, et al. Nasal natural killer/T-cell lymphoma and its association with type "i"/XhoI loss strain Epstein-Barr virus in Chile. *Journal of clinical pathology*. Jun 2007;60(6):656-60. doi:10.1136/jcp.2005.034199

16. Quintanilla-Martinez L, Kremer M, Keller G, et al. p53 Mutations in nasal natural killer/T-cell lymphoma from Mexico: association with large cell morphology and advanced disease. *Am J Pathol*. Dec 2001;159(6):2095-105. doi:10.1016/S0002-9440(10)63061-1

17. Aviles A. Nasal NK/T-Cell Lymphoma. A Comparative Analysis of a Mexican Population with the Other Populations of Latin-America. *Mediterr J Hematol Infect Dis*. 2015;7(1):e2015052. doi:10.4084/MJHID.2015.052

18. McBride P. Photographs of a case of rapid destruction of the nose and face. 1897. *The Journal of laryngology and otology*. Dec 1991;105(12):1120.

19. Tse E, Kwong YL. Diagnosis and management of extranodal NK/T cell lymphoma nasal type. *Expert review of hematology*. Sep 2016;9(9):861-71. doi:10.1080/17474086.2016.1206465

20. Harris NL, Jaffe ES, Stein H, et al. A revised European-American classification of lymphoid neoplasms: a proposal from the International Lymphoma Study Group. *Blood*. Sep 1 1994;84(5):1361-92.

21. Kwong YL, Khong PL. Central palatal perforation in nasal natural killer cell lymphoma. *British journal of haematology*. Jan 2011;152(1):2.

22. Tse E, Kwong YL. The diagnosis and management of NK/T-cell lymphomas. *Journal of hematology & oncology*. Apr 14 2017;10(1):85. doi:10.1186/s13045-017-0452-9

23. Kwong YL, Chan AC, Liang R, et al. CD56+ NK lymphomas: clinicopathological features and prognosis. *British journal of haematology*. Jun 1997;97(4):821-9.

24. Cheung MM, Chan JK, Lau WH, et al. Primary non-Hodgkin's lymphoma of the nose and nasopharynx: clinical features, tumor immunophenotype, and treatment outcome in 113 patients. *Journal of clinical oncology : official journal of the American Society of Clinical Oncology*. Jan 1998;16(1):70-7. doi:10.1200/jco.1998.16.1.70

25. Hasserjian RP, Harris NL. NK-cell lymphomas and leukemias: a spectrum of tumors with variable manifestations and immunophenotype. *American journal of clinical pathology*. Jun 2007;127(6):860-8. doi:10.1309/2f39nx1al3l54wu8

26. Chim CS, Au WY, Poon C, Ooi GC, Lam CC, Kwong YL. Primary natural killer cell lymphoma of skeletal muscle. *Histopathology*. Oct 2002;41(4):371-4.

27. Oshimi K, Kawa K, Nakamura S, et al. NK-cell neoplasms in Japan. *Hematology (Amsterdam, Netherlands)*. Jun 2005;10(3):237-45. doi:10.1080/10245330400026162

28. Chan JK. Natural killer cell neoplasms. *Anatomic pathology (Chicago, Ill : annual)*. 1998;3:77-145.

29. Haedicke W, Ho FC, Chott A, et al. Expression of CD94/NKG2A and killer immunoglobulin-like receptors in NK cells and a subset of extranodal cytotoxic T-cell lymphomas. *Blood*. Jun 1 2000;95(11):3628-30.

30. Lin CW, Chen YH, Chuang YC, Liu TY, Hsu SM. CD94 transcripts imply a better prognosis in nasal-type extranodal NK/T-cell lymphoma. *Blood*. Oct 1 2003;102(7):2623-31. doi:10.1182/blood-2003-01-0295

31. Jhuang JY, Chang ST, Weng SF, et al. Extranodal natural killer/T-cell lymphoma, nasal type in Taiwan: a relatively higher frequency of T-cell lineage and poor survival for extranasal tumors. *Hum Pathol*. Feb 2015;46(2):313-21. doi:10.1016/j.humpath.2014.11.008

32. Kim WY, Nam SJ, Kim S, et al. Prognostic implications of CD30 expression in extranodal natural killer/T-cell lymphoma according to treatment modalities. *Leuk Lymphoma*. Jun 2015;56(6):1778-86. doi:10.3109/10428194.2014.974048

33. Ng CS, Lo ST, Chan JK. Peripheral T and putative natural killer cell lymphomas commonly coexpress CD95 and CD95 ligand. *Hum Pathol*. Jan 1999;30(1):48-53.

34. Li P, Jiang L, Zhang X, Liu J, Wang H. CD30 expression is a novel prognostic indicator in extranodal natural killer/T-cell lymphoma, nasal type. *BMC Cancer*. Nov 28 2014;14:890. doi:10.1186/1471-2407-14-890

35. Kuo TT, Shih LY, Tsang NM. Nasal NK/T cell lymphoma in Taiwan: a clinicopathologic study of 22 cases, with analysis of histologic subtypes, Epstein-Barr virus LMP-1 gene association, and treatment modalities. *Int J Surg Pathol*. Oct 2004;12(4):375-87. doi:10.1177/106689690401200410

36. Li S, Feng X, Li T, et al. Extranodal NK/T-cell lymphoma, nasal type: a report of 73 cases at MD Anderson Cancer Center. *The American journal of surgical pathology*. Jan 2013;37(1):14-23. doi:10.1097/PAS.0b013e31826731b5

37. Chen Y, Tan S-Y, Petersson BF, Khor YM, Gopalakrishnan SK, Tan D. Occult recurrence of monomorphic epitheliotropic intestinal T-cell lymphoma and the role of MATK gene expression in diagnosis. *Hematological Oncology*. 2017;35(4):852-855. doi:10.1002/hon.2288

38. Zeng L, Huang W, Cao Z, et al. The correlation of clinicopathological features and prognosis in extranodal natural killer/T cell lymphoma: a report of 42 cases

in the early stage. *Annals of Hematology*. 2019/06/01 2019;98(6):1467-1476. doi:10.1007/s00277-019-03643-9

39. Zhang L, Wei Y, Yan X, et al. Survivin is a prognostic marker and therapeutic target for extranodal, nasal-type natural killer/T cell lymphoma. *Ann Transl Med*. 2019;7(14):316-316. doi:10.21037/atm.2019.06.53
40. Kanavaros P, Briere J, Emile JF, Gaulard P. Epstein-Barr virus in T and natural killer (NK) cell non-Hodgkin's lymphomas. *Leukemia*. Jun 1996;10 Suppl 2:s84-7.
41. Cai Q, Chen K, Young KH. Epstein-Barr virus-positive T/NK-cell lymphoproliferative disorders. *Exp Mol Med*. Jan 23 2015;47:e133. doi:10.1038/emm.2014.105
42. Cohen JI. Epstein-Barr virus infection. *N Engl J Med*. Aug 17 2000;343(7):481-92. doi:10.1056/NEJM200008173430707
43. Luzuriaga K, Sullivan JL. Infectious Mononucleosis. *New England Journal of Medicine*. 2010;362(21):1993-2000. doi:10.1056/NEJMcp1001116
44. Di Pietro A. Epstein–Barr Virus Promotes B Cell Lymphomas by Manipulating the Host Epigenetic Machinery. *Cancers*. 2020;12(10):3037.
45. Roschewski M, Wilson WH. EBV-associated lymphomas in adults. *Best Pract Res Clin Haematol*. Mar 2012;25(1):75-89. doi:10.1016/j.beha.2012.01.005
46. Young LS, Arrand JR, Murray PG. EBV gene expression and regulation. In: Arvin A, Campadelli-Fiume G, Mocarski E, et al, eds. *Human Herpesviruses: Biology, Therapy, and Immunoprophylaxis*. Cambridge University Press 2007
47. Kang M-S, Kieff E. Epstein–Barr virus latent genes. *Experimental & Molecular Medicine*. 2015/01/01 2015;47(1):e131-e131. doi:10.1038/emm.2014.84
48. Dharnidharka VR, Webster AC, Martinez OM, Preiksaitis JK, Leblond V, Choquet S. Post-transplant lymphoproliferative disorders. *Nature Reviews Disease Primers*. 2016/01/28 2016;2(1):15088. doi:10.1038/nrdp.2015.88
49. Thorley-Lawson DA. Epstein-Barr virus: exploiting the immune system. Perspective. *Nature Reviews Immunology*. 10/01/online 2001;1:75. doi:10.1038/35095584
50. Coleman CB, Lang J, Sweet LA, et al. Epstein-Barr Virus Type 2 Infects T Cells and Induces B Cell Lymphomagenesis in Humanized Mice. *J Virol*. 2018;92(21):e00813-18. doi:10.1128/JVI.00813-18
51. Linke-Serinsöz E, Fend F, Quintanilla-Martinez L. Human immunodeficiency virus (HIV) and Epstein-Barr virus (EBV) related lymphomas, pathology view point. *Seminars in Diagnostic Pathology*. 2017/07/01/ 2017;34(4):352-363. doi:10.1053/j.semdp.2017.04.003
52. Ohshima K, Suzumiya J, Kanda M, Kato A, Kikuchi M. Integrated and episomal forms of Epstein-Barr virus (EBV) in EBV associated disease. *Cancer letters*. Jan 9 1998;122(1-2):43-50. doi:10.1016/s0304-3835(97)00368-6

53. Taylor GS, Long HM, Brooks JM, Rickinson AB, Hislop AD. The immunology of Epstein-Barr virus-induced disease. *Annual review of immunology*. 2015;33:787-821. doi:10.1146/annurev-immunol-032414-112326

54. Cai Q, Chen K, Young KH. Epstein-Barr virus-positive T/NK-cell lymphoproliferative disorders. *Experimental & molecular medicine*. Jan 23 2015;47(1):e133. doi:10.1038/emm.2014.105

55. Anagnostopoulos I, Hummel M, Kreschel C, Stein H. Morphology, immunophenotype, and distribution of latently and/or productively Epstein-Barr virus-infected cells in acute infectious mononucleosis: implications for the interindividual infection route of Epstein-Barr virus. *Blood*. Feb 1 1995;85(3):744-50.

56. Hudnall SD, Ge Y, Wei L, Yang NP, Wang HQ, Chen T. Distribution and phenotype of Epstein-Barr virus-infected cells in human pharyngeal tonsils. *Modern pathology : an official journal of the United States and Canadian Academy of Pathology, Inc*. Apr 2005;18(4):519-27. doi:10.1038/modpathol.3800369

57. Hatton OL, Harris-Arnold A, Schaffert S, Krams SM, Martinez OM. The interplay between Epstein-Barr virus and B lymphocytes: implications for infection, immunity, and disease. *Immunol Res*. May 2014;58(2-3):268-76. doi:10.1007/s12026-014-8496-1

58. Dambaugh T, Hennessy K, Chamnankit L, Kieff E. U2 region of Epstein-Barr virus DNA may encode Epstein-Barr nuclear antigen 2. *Proceedings of the National Academy of Sciences of the United States of America*. Dec 1984;81(23):7632-6. doi:10.1073/pnas.81.23.7632

59. Kanda T, Yajima M, Ikuta K. Epstein-Barr virus strain variation and cancer. *Cancer Sci*. 2019;110(4):1132-1139. doi:10.1111/cas.13954

60. Rickinson AB, Young LS, Rowe M. Influence of the Epstein-Barr virus nuclear antigen EBNA 2 on the growth phenotype of virus-transformed B cells. *J Virol*. May 1987;61(5):1310-7.

61. Xiong J, Cui BW, Wang N, et al. Genomic and Transcriptomic Characterization of Natural Killer T Cell Lymphoma. *Cancer Cell*. Mar 16 2020;37(3):403-419 e6. doi:10.1016/j.ccell.2020.02.005

62. Kim I, Park E-R, Park S-H, Lin Z, Kim Y-S. Characteristics of Epstein-Barr virus isolated from the malignant lymphomas in Korea. *Journal of Medical Virology*. 2002;67(1):59-66. doi:10.1002/jmv.2193

63. Chiang AK, Wong KY, Liang AC, Srivastava G. Comparative analysis of Epstein-Barr virus gene polymorphisms in nasal T/NK-cell lymphomas and normal nasal tissues: implications on virus strain selection in malignancy. *Int J Cancer*. Jan 29 1999;80(3):356-64. doi:10.1002/(sici)1097-0215(19990129)80:3<356::aid-ijc4>3.0.co;2-d

64. Wu S-J, Lay J-D, Chen C-L, Chen J-Y, Liu M-Y, Su I-J. Genomic analysis of Epstein-Barr virus in nasal and peripheral T-cell lymphoma: A comparison with nasopharyngeal carcinoma in an endemic area. *Journal of Medical Virology*.

1996;50(4):314-321. doi:10.1002/(sici)1096-9071(199612)50:4<314::Aid-jmv6>3.0.Co;2-b

65. Sandvej K, Peh S, Andresen B, Pallesen G. Identification of potential hot spots in the carboxy-terminal part of the Epstein-Barr virus (EBV) BNLF-1 gene in both malignant and benign EBV-associated diseases: high frequency of a 30-bp deletion in Malaysian and Danish peripheral T-cell lymphomas. *Blood*. 1994;84(12):4053-4060. doi:10.1182/blood.V84.12.4053.bloodjournal84124053

66. Montes-Mojarro IA, Fend F, Quintanilla-Martinez L. EBV and the Pathogenesis of NK/T Cell Lymphoma. *Cancers (Basel)*. Mar 19 2021;13(6)doi:10.3390/cancers13061414

67. Hofscheier A, Ponciano A, Bonzheim I, et al. Geographic variation in the prevalence of Epstein-Barr virus-positive diffuse large B-cell lymphoma of the elderly: a comparative analysis of a Mexican and a German population. *Modern pathology : an official journal of the United States and Canadian Academy of Pathology, Inc*. Aug 2011;24(8):1046-54. doi:10.1038/modpathol.2011.62

68. Dirnhofer S, Angeles-Angeles A, Ortiz-Hidalgo C, et al. High prevalence of a 30-base pair deletion in the Epstein-Barr virus (EBV) latent membrane protein 1 gene and of strain type B EBV in Mexican classical Hodgkin's disease and reactive lymphoid tissue. *Hum Pathol*. Jul 1999;30(7):781-7. doi:10.1016/s0046-8177(99)90138-7

69. Kingma DW, Weiss WB, Jaffe ES, Kumar S, Frekko K, Raffeld M. Epstein-Barr virus latent membrane protein-1 oncogene deletions: correlations with malignancy in Epstein-Barr virus--associated lymphoproliferative disorders and malignant lymphomas. *Blood*. Jul 1 1996;88(1):242-51.

70. Chang CM, Yu KJ, Mbulaiteye SM, Hildesheim A, Bhatia K. The extent of genetic diversity of Epstein-Barr virus and its geographic and disease patterns: a need for reappraisal. *Virus Res*. Aug 2009;143(2):209-21. doi:10.1016/j.virusres.2009.07.005

71. De Re V, Boiocchi M, De Vita S, et al. Subtypes of epstein-barr virus in HIV-1-associated and HIV-1-unrelated hodgkin's disease cases. *International Journal of Cancer*. 1993;54(6):895-898. doi:10.1002/ijc.2910540603

72. Kyaw MT, Hurren L, Evans L, et al. Expression of B-type Epstein-Barr virus in HIV-infected patients and cardiac transplant recipients. *AIDS research and human retroviruses*. Nov 1992;8(11):1869-74. doi:10.1089/aid.1992.8.1869

73. Fassone L, Cingolani A, Martini M, et al. Characterization of Epstein-Barr virus genotype in AIDS-related non-Hodgkin's lymphoma. *AIDS research and human retroviruses*. Jan 1 2002;18(1):19-26. doi:10.1089/088922202753394682

74. Kaye KM, Izumi KM, Kieff E. Epstein-Barr virus latent membrane protein 1 is essential for B-lymphocyte growth transformation. *Proceedings of the National Academy of Sciences of the United States of America*. Oct 1 1993;90(19):9150-4. doi:10.1073/pnas.90.19.9150

75. Fennewald S, van Santen V, Kieff E. Nucleotide sequence of an mRNA transcribed in latent growth-transforming virus infection indicates that it may encode a membrane protein. *J Virol*. Aug 1984;51(2):411-9.

76. Gires O, Zimber-Strobl U, Gonnella R, et al. Latent membrane protein 1 of Epstein-Barr virus mimics a constitutively active receptor molecule. *EMBO J*. Oct 15 1997;16(20):6131-40. doi:10.1093/emboj/16.20.6131

77. Martin J, Sugden B. The latent membrane protein oncoprotein resembles growth factor receptors in the properties of its turnover. *Cell Growth Differ*. Dec 1991;2(12):653-600.

78. Coffin WF, 3rd, Erickson KD, Hoedt-Miller M, Martin JM. The cytoplasmic amino-terminus of the Latent Membrane Protein-1 of Epstein-Barr Virus: relationship between transmembrane orientation and effector functions of the carboxy-terminus and transmembrane domain. *Oncogene*. Aug 30 2001;20(38):5313-30. doi:10.1038/sj.onc.1204689

79. Li SN, Chang YS, Liu ST. Effect of a 10-amino acid deletion on the oncogenic activity of latent membrane protein 1 of Epstein-Barr virus. *Oncogene*. May 16 1996;12(10):2129-35.

80. Knecht H, Bachmann E, Brousset P, et al. Deletions within the LMP1 oncogene of Epstein-Barr virus are clustered in Hodgkin's disease and identical to those observed in nasopharyngeal carcinoma. *Blood*. Nov 15 1993;82(10):2937-42.

81. Itakura O, Yamada S, Narita M, Kikuta H. High prevalence of a 30-base pair deletion and single-base mutations within the carboxy terminal end of the LMP-1 oncogene of Epstein-Barr virus in the Japanese population. *Oncogene*. Oct 3 1996;13(7):1549-53.

82. Chen WG, Chen YY, Bacchi MM, Bacchi CE, Alvarenga M, Weiss LM. Genotyping of Epstein-Barr virus in Brazilian Burkitt's lymphoma and reactive lymphoid tissue. Type A with a high prevalence of deletions within the latent membrane protein gene. *Am J Pathol*. Jan 1996;148(1):17-23.

83. Mori S, Itoh T, Tokunaga M, Eizuru Y. Deletions and single-base mutations within the carboxy-terminal region of the latent membrane protein 1 oncogene in Epstein-Barr virus-related gastric cancers of southern Japan. *J Med Virol*. Feb 1999;57(2):152-8. doi:10.1002/(sici)1096-9071(199902)57:2<152::aid-jmv11>3.0.co;2-k

84. da Costa VG, Marques-Silva AC, Moreli ML. The Epstein-Barr virus latent membrane protein-1 (LMP1) 30-bp deletion and XhoI-polymorphism in nasopharyngeal carcinoma: a meta-analysis of observational studies. *Syst Rev*. Apr 13 2015;4:46. doi:10.1186/s13643-015-0037-z

85. Sandvej K, Peh SC, Andresen BS, Pallesen G. Identification of potential hot spots in the carboxy-terminal part of the Epstein-Barr virus (EBV) BNLF-1 gene in both malignant and benign EBV-associated diseases: high frequency of a 30-bp deletion in Malaysian and Danish peripheral T-cell lymphomas. *Blood*. Dec 15 1994;84(12):4053-60.

86. Huang Y-H, Wu Q-L, Zong Y-S, Feng Y-F, Hou J-H. Nasopharyngeal Extranodal NK/T-Cell Lymphoma, Nasal Type: Retrospective Study of 18 Consecutive Cases in Guangzhou, China. *International Journal of Surgical Pathology*. 2011;19(1):51-61. doi:10.1177/1066896910388806

87. Dolcetti R, Zancai P, De Re V, et al. Epstein-Barr virus strains with latent membrane protein-1 deletions: prevalence in the Italian population and high association with human immunodeficiency virus-related Hodgkin's disease. *Blood*. Mar 1 1997;89(5):1723-31.

88. Srivastava G, Wong KY, Chiang AK, Lam KY, Tao Q. Coinfection of multiple strains of Epstein-Barr virus in immunocompetent normal individuals: reassessment of the viral carrier state. *Blood*. Apr 1 2000;95(7):2443-5.

89. Hoshida Y, Hongyo T, Jia X, et al. Analysis of p53, K-ras, c-kit, and beta-catenin gene mutations in sinonasal NK/T cell lymphoma in northeast district of China. *Cancer Sci*. Mar 2003;94(3):297-301.

90. Lee S, Park HY, Kang SY, et al. Genetic alterations of JAK/STAT cascade and histone modification in extranodal NK/T-cell lymphoma nasal type. *Oncotarget*. Jul 10 2015;6(19):17764-76. doi:10.18632/oncotarget.3776

91. Kucuk C, Jiang B, Hu X, et al. Activating mutations of STAT5B and STAT3 in lymphomas derived from gammadelta-T or NK cells. *Nat Commun*. Jan 14 2015;6:6025. doi:10.1038/ncomms7025

92. Jiang L, Gu ZH, Yan ZX, et al. Exome sequencing identifies somatic mutations of DDX3X in natural killer/T-cell lymphoma. *Nat Genet*. Sep 2015;47(9):1061-6. doi:10.1038/ng.3358

93. Dobashi A, Tsuyama N, Asaka R, et al. Frequent BCOR aberrations in extranodal NK/T-Cell lymphoma, nasal type. *Genes Chromosomes Cancer*. May 2016;55(5):460-71. doi:10.1002/gcc.22348

94. Wen H, Ma H, Cai Q, et al. Recurrent ECSIT mutation encoding V140A triggers hyperinflammation and promotes hemophagocytic syndrome in extranodal NK/T cell lymphoma. *Nature medicine*. Feb 2018;24(2):154-164. doi:10.1038/nm.4456

95. Song TL, Nairismagi ML, Laurensia Y, et al. Oncogenic activation of the STAT3 pathway drives PD-L1 expression in natural killer/T-cell lymphoma. *Blood*. Sep 13 2018;132(11):1146-1158. doi:10.1182/blood-2018-01-829424

96. Li Z, Zhang X, Xue W, et al. Recurrent GNAQ mutation encoding T96S in natural killer/T cell lymphoma. *Nat Commun*. Sep 16 2019;10(1):4209. doi:10.1038/s41467-019-12032-9

97. Sim SH, Kim S, Kim TM, et al. Novel JAK3-Activating Mutations in Extranodal NK/T-Cell Lymphoma, Nasal Type. *Am J Pathol*. May 2017;187(5):980-986. doi:10.1016/j.ajpath.2017.01.004

98. Shen L, Liang AC, Lu L, et al. Frequent deletion of Fas gene sequences encoding death and transmembrane domains in nasal natural killer/T-cell lymphoma. *Am J Pathol*. Dec 2002;161(6):2123-31. doi:10.1016/S0002-9440(10)64490-2

99. Takakuwa T, Dong Z, Nakatsuka S, et al. Frequent mutations of Fas gene in nasal NK/T cell lymphoma. *Oncogene*. Jul 11 2002;21(30):4702-5. doi:10.1038/sj.onc.1205571

100. Xiong J, Zhao W-L. Advances in multiple omics of natural-killer/T cell lymphoma. *Journal of hematology & oncology*. 2018/12/04 2018;11(1):134. doi:10.1186/s13045-018-0678-1

101. de Mel S, Hue SS-S, Jeyasekharan AD, Chng W-J, Ng S-B. Molecular pathogenic pathways in extranodal NK/T cell lymphoma. *Journal of hematology & oncology*. 2019/04/02 2019;12(1):33. doi:10.1186/s13045-019-0716-7

102. Karube K, Nakagawa M, Tsuzuki S, et al. Identification of FOXO3 and PRDM1 as tumor-suppressor gene candidates in NK-cell neoplasms by genomic and functional analyses. *Blood*. Sep 22 2011;118(12):3195-204. doi:10.1182/blood-2011-04-346890

103. Iqbal J, Kucuk C, deLeeuw RJ, et al. Genomic analyses reveal global functional alterations that promote tumor growth and novel tumor suppressor genes in natural killer-cell malignancies. *Leukemia*. 2009/06/01 2009;23(6):1139-1151. doi:10.1038/leu.2009.3

104. Ko YH, Choi KE, Han JH, Kim JM, Ree HJ. Comparative genomic hybridization study of nasal-type NK/T-cell lymphoma. *Cytometry*. 2001;46(2):85-91. doi:10.1002/cyto.1069

105. Sun L, Li M, Huang X, Xu J, Gao Z, Liu C. High-resolution genome-wide analysis identified recurrent genetic alterations in NK/T-cell lymphoma, nasal type, which are associated with disease progression. *Medical Oncology*. 2014/06/22 2014;31(7):71. doi:10.1007/s12032-014-0071-z

106. Nakashima Y, Tagawa H, Suzuki R, et al. Genome-wide array-based comparative genomic hybridization of natural killer cell lymphoma/leukemia: different genomic alteration patterns of aggressive NK-cell leukemia and extranodal Nk/T-cell lymphoma, nasal type. *Genes Chromosomes Cancer*. Nov 2005;44(3):247-55. doi:10.1002/gcc.20245

107. Yang CF, Hsu CY, Ho DM. Aggressive natural killer (NK)-cell leukaemia and extranodal NK/T-cell lymphoma are two distinct diseases that differ in their clinical presentation and cytogenetic findings. *Histopathology*. May 2018;72(6):955-964. doi:10.1111/his.13463

108. Ng SB, Chung TH, Kato S, et al. Epstein-Barr virus-associated primary nodal T/NK-cell lymphoma shows a distinct molecular signature and copy number changes. *Haematologica*. Feb 2018;103(2):278-287. doi:10.3324/haematol.2017.180430

109. Rawlings JS, Rosler KM, Harrison DA. The JAK/STAT signaling pathway. *Journal of cell science*. Mar 15 2004;117(Pt 8):1281-3. doi:10.1242/jcs.00963

110. Bousoik E, Montazeri Aliabadi H. “Do We Know Jack” About JAK? A Closer Look at JAK/STAT Signaling Pathway. Review. *Frontiers in Oncology*. 2018-July-31 2018;8(287)doi:10.3389/fonc.2018.00287

111. Jerez A, Clemente MJ, Makishima H, et al. STAT3 mutations unify the pathogenesis of chronic lymphoproliferative disorders of NK cells and T-cell large granular lymphocyte leukemia. *Blood*. Oct 11 2012;120(15):3048-57. doi:10.1182/blood-2012-06-435297

112. Koskela HL, Eldfors S, Ellonen P, et al. Somatic STAT3 mutations in large granular lymphocytic leukemia. *N Engl J Med*. May 17 2012;366(20):1905-13. doi:10.1056/NEJMoa1114885

113. Perez-Garcia A, Ambesi-Impiombato A, Hadler M, et al. Genetic loss of SH2B3 in acute lymphoblastic leukemia. *Blood*. Oct 3 2013;122(14):2425-32. doi:10.1182/blood-2013-05-500850

114. Muromoto R, Ikeda O, Okabe K, et al. Epstein-Barr virus-derived EBNA2 regulates STAT3 activation. *Biochem Biophys Res Commun*. Jan 16 2009;378(3):439-43. doi:10.1016/j.bbrc.2008.11.053

115. Shair KH, Bendt KM, Edwards RH, Bedford EC, Nielsen JN, Raab-Traub N. EBV latent membrane protein 1 activates Akt, NFkappaB, and Stat3 in B cell lymphomas. *PLoS Pathog*. Nov 2007;3(11):e166. doi:10.1371/journal.ppat.0030166

116. Huang X, Meng B, Iqbal J, et al. Activation of the STAT3 signaling pathway is associated with poor survival in diffuse large B-cell lymphoma treated with R-CHOP. *Journal of clinical oncology : official journal of the American Society of Clinical Oncology*. Dec 20 2013;31(36):4520-8. doi:10.1200/jco.2012.45.6004

117. Koo GC, Tan SY, Tang T, et al. Janus kinase 3-activating mutations identified in natural killer/T-cell lymphoma. *Cancer discovery*. Jul 2012;2(7):591-7. doi:10.1158/2159-8290.CD-12-0028

118. Huynh KD, Fischle W, Verdin E, Bardwell VJ. BCoR, a novel corepressor involved in BCL-6 repression. *Genes Dev*. 2000;14(14):1810-1823.

119. Sakano D, Kato A, Parikh N, et al. BCL6 canalizes Notch-dependent transcription, excluding Mastermind-like1 from selected target genes during left-right patterning. *Dev Cell*. 2010;18(3):450-462. doi:10.1016/j.devcel.2009.12.023

120. Damm F, Chesnais V, Nagata Y, et al. BCOR and BCORL1 mutations in myelodysplastic syndromes and related disorders. *Blood*. Oct 31 2013;122(18):3169-77. doi:10.1182/blood-2012-11-469619

121. Grossmann V, Tiacci E, Holmes AB, et al. Whole-exome sequencing identifies somatic mutations of BCOR in acute myeloid leukemia with normal karyotype. *Blood*. Dec 1 2011;118(23):6153-63. doi:10.1182/blood-2011-07-365320

122. Olivier M, Hollstein M, Hainaut P. TP53 mutations in human cancers: origins, consequences, and clinical use. *Cold Spring Harb Perspect Biol*. 2010;2(1):a001008-a001008. doi:10.1101/cshperspect.a001008

123. Yin Y, Stephen CW, Luciani MG, Fahraeus R. p53 Stability and activity is regulated by Mdm2-mediated induction of alternative p53 translation products. *Nature cell biology*. Jun 2002;4(6):462-7. doi:10.1038/ncb801

124. Perri F, Pisconti S, Della Vittoria Scarpati G. P53 mutations and cancer: a tight linkage. *Ann Transl Med*. 2016;4(24):522-522. doi:10.21037/atm.2016.12.40

125. El-Deiry WS. The role of p53 in chemosensitivity and radiosensitivity. *Oncogene*. Oct 20 2003;22(47):7486-95. doi:10.1038/sj.onc.1206949

126. Alarcon-Vargas D, Ronai Z. p53-Mdm2--the affair that never ends. *Carcinogenesis*. Apr 2002;23(4):541-7. doi:10.1093/carcin/23.4.541

127. Kurniawan A, Hongyo T, Hardjolukito E, et al. Gene mutation analysis of sinonasal lymphomas in Indonesia. *Oncology reports*. 06/01 2006;15:1257-63. doi:10.3892/or.15.5.1257

128. Takahara M, Kishibe K, Bandoh N, Nonaka S, Harabuchi Y. P53, N- and K-Ras, and beta-catenin gene mutations and prognostic factors in nasal NK/T-cell lymphoma from Hokkaido, Japan. *Hum Pathol*. Jan 2004;35(1):86-95. doi:10.1016/j.humpath.2003.08.025

129. Muller PA, Vousden KH. p53 mutations in cancer. *Nature cell biology*. Jan 2013;15(1):2-8. doi:10.1038/ncb2641

130. Guedes LB, Almutairi F, Haffner MC, et al. Analytic, Preanalytic, and Clinical Validation of p53 IHC for Detection of TP53 Missense Mutation in Prostate Cancer. *Clin Cancer Res*. 2017;23(16):4693-4703. doi:10.1158/1078-0432.CCR-17-0257

131. Liu J, Li W, Deng M, Liu D, Ma Q, Feng X. Immunohistochemical Determination of p53 Protein Overexpression for Predicting p53 Gene Mutations in Hepatocellular Carcinoma: A Meta-Analysis. *PloS one*. 2016;11(7):e0159636. doi:10.1371/journal.pone.0159636

132. Gulley ML, Burton MP, Allred DC, et al. Epstein-Barr virus infection is associated with p53 accumulation in nasopharyngeal carcinoma. *Hum Pathol*. Mar 1998;29(3):252-9. doi:10.1016/s0046-8177(98)90044-2

133. Gomez-Manzano C, Fueyo J, Kyritsis AP, et al. Characterization of p53 and p21 functional interactions in glioma cells en route to apoptosis. *J Natl Cancer Inst*. Jul 16 1997;89(14):1036-44. doi:10.1093/jnci/89.14.1036

134. Chen W, Cooper NR. Epstein-Barr virus nuclear antigen 2 and latent membrane protein independently transactivate p53 through induction of NF-kappaB activity. *J Virol*. Jul 1996;70(7):4849-53. doi:10.1128/jvi.70.7.4849-4853.1996

135. Szekely L, Selivanova G, Magnusson KP, Klein G, Wiman KG. EBNA-5, an Epstein-Barr virus-encoded nuclear antigen, binds to the retinoblastoma and p53 proteins. *Proceedings of the National Academy of Sciences of the United States of America*. Jun 15 1993;90(12):5455-9. doi:10.1073/pnas.90.12.5455

136. Dreyfus DH, Nagasawa M, Kelleher CA, Gelfand EW. Stable expression of Epstein-Barr virus BZLF-1-encoded ZEBRA protein activates p53-dependent transcription in human Jurkat T-lymphoblastoid cells. *Blood*. Jul 15 2000;96(2):625-34.

137. Brandimarte L, La Starza R, Gianfelici V, et al. DDX3X-MLLT10 fusion in adults with NOTCH1 positive T-cell acute lymphoblastic leukemia. *Haematologica*. May 2014;99(5):64-6. doi:10.3324/haematol.2013.101725

138. Ojha J, Secreto CR, Rabe KG, et al. Identification of recurrent truncated DDX3X mutations in chronic lymphocytic leukaemia. *British journal of haematology*. May 2015;169(3):445-8. doi:10.1111/bjh.13211

139. Bol GM, Vesuna F, Xie M, et al. Targeting DDX3 with a small molecule inhibitor for lung cancer therapy. *EMBO molecular medicine*. May 2015;7(5):648-69. doi:10.15252/emmm.201404368

140. Stransky N, Egloff AM, Tward AD, et al. The mutational landscape of head and neck squamous cell carcinoma. *Science*. 2011;333(6046):1157-1160. doi:10.1126/science.1208130

141. Kandoth C, McLellan MD, Vandin F, et al. Mutational landscape and significance across 12 major cancer types. *Nature*. Oct 17 2013;502(7471):333-339. doi:10.1038/nature12634

142. Jones DT, Jager N, Kool M, et al. Dissecting the genomic complexity underlying medulloblastoma. *Nature*. Aug 2 2012;488(7409):100-5. doi:10.1038/nature11284

143. Valentin-Vega YA, Wang Y-D, Parker M, et al. Cancer-associated DDX3X mutations drive stress granule assembly and impair global translation. *Scientific Reports*. 2016/05/16 2016;6(1):25996. doi:10.1038/srep25996

144. Pugh TJ, Weeraratne SD, Archer TC, et al. Medulloblastoma exome sequencing uncovers subtype-specific somatic mutations. *Nature*. Aug 2 2012;488(7409):106-10. doi:10.1038/nature11329

145. Wu DW, Lee MC, Wang J, Chen CY, Cheng YW, Lee H. DDX3 loss by p53 inactivation promotes tumor malignancy via the MDM2/Slug/E-cadherin pathway and poor patient outcome in non-small-cell lung cancer. *Oncogene*. Mar 20 2014;33(12):1515-26. doi:10.1038/onc.2013.107

146. Hurlin PJ, Steingrìmsson E, Copeland NG, Jenkins NA, Eisenman RN. Mga, a dual-specificity transcription factor that interacts with Max and contains a T-domain DNA-binding motif. *Embo j*. Dec 15 1999;18(24):7019-28. doi:10.1093/emboj/18.24.7019

147. Romero OA, Torres-Diz M, Pros E, et al. MAX inactivation in small cell lung cancer disrupts MYC-SWI/SNF programs and is synthetic lethal with BRG1. *Cancer discovery*. Mar 2014;4(3):292-303. doi:10.1158/2159-8290.Cd-13-0799

148. Jo YS, Kim MS, Yoo NJ, Lee SH. Somatic mutation of a candidate tumour suppressor MGA gene and its mutational heterogeneity in colorectal cancers. *Pathology*. Aug 2016;48(5):525-7. doi:10.1016/j.pathol.2016.04.010

149. Edelmann J, Holzmann K, Miller F, et al. High-resolution genomic profiling of chronic lymphocytic leukemia reveals new recurrent genomic alterations. *Blood*. Dec 6 2012;120(24):4783-94. doi:10.1182/blood-2012-04-423517

150. Liang L, Dong M, Cong K, Chen Y, Ma Z. Correlations of Moesin expression with the pathological stage, nerve infiltration, tumor location and pain severity in patients with pancreatic cancer. *J BUON*. May-Jun 2019;24(3):1225-1232.

151. Rey-Gallardo A, Tomlins H, Joachim J, et al. Sequential binding of ezrin and moesin to L-selectin regulates monocyte protrusive behaviour during transendothelial migration. *Journal of cell science*. Jul 4 2018;131(13)doi:10.1242/jcs.215541

152. Berryman M, Franck Z, Bretscher A. Ezrin is concentrated in the apical microvilli of a wide variety of epithelial cells whereas moesin is found primarily in endothelial cells. *Journal of cell science*. Aug 1993;105 (Pt 4):1025-43.

153. Shcherbina A, Bretscher A, Kenney DM, Remold-O'Donnell E. Moesin, the major ERM protein of lymphocytes and platelets, differs from ezrin in its insensitivity to calpain. *FEBS Lett*. Jan 22 1999;443(1):31-6. doi:10.1016/s0014-5793(98)01674-3

154. Tse E, Kwong YL. How I treat NK/T-cell lymphomas. *Blood*. Jun 20 2013;121(25):4997-5005. doi:10.1182/blood-2013-01-453233

155. Kim SJ, Yang DH, Kim JS, et al. Concurrent chemoradiotherapy followed by L-asparaginase-containing chemotherapy, VIDL, for localized nasal extranodal NK/T cell lymphoma: CISL08-01 phase II study. *Ann Hematol*. Nov 2014;93(11):1895-901. doi:10.1007/s00277-014-2137-6

156. Loong HH, Winquist E, Waldron J, et al. Phase 1 study of nab-paclitaxel, cisplatin and 5-fluorouracil as induction chemotherapy followed by concurrent chemoradiotherapy in locoregionally advanced squamous cell carcinoma of the oropharynx. *Eur J Cancer*. Sep 2014;50(13):2263-70. doi:10.1016/j.ejca.2014.05.021

157. Yamaguchi M, Tobinai K, Oguchi M, et al. Phase I/II study of concurrent chemoradiotherapy for localized nasal natural killer/T-cell lymphoma: Japan Clinical Oncology Group Study JCOG0211. *Journal of clinical oncology : official journal of the American Society of Clinical Oncology*. Nov 20 2009;27(33):5594-600. doi:10.1200/JCO.2009.23.8295

158. Kim SJ, Kim K, Kim BS, et al. Phase II trial of concurrent radiation and weekly cisplatin followed by VIPD chemotherapy in newly diagnosed, stage IE to IIE, nasal, extranodal NK/T-Cell Lymphoma: Consortium for Improving Survival of Lymphoma study. *Journal of clinical oncology : official journal of the American Society of Clinical Oncology*. Dec 10 2009;27(35):6027-32. doi:10.1200/JCO.2009.23.8592

159. Dong LH, Zhang LJ, Wang WJ, et al. Sequential DICE combined with l-asparaginase chemotherapy followed by involved field radiation in newly diagnosed, stage IE to IIE, nasal and extranodal NK/T-cell lymphoma. *Leuk Lymphoma*. Jul 2016;57(7):1600-6. doi:10.3109/10428194.2015.1108415

160. Li YX, Fang H, Liu QF, et al. Clinical features and treatment outcome of nasal-type NK/T-cell lymphoma of Waldeyer ring. *Blood*. Oct 15 2008;112(8):3057-64. doi:10.1182/blood-2008-05-160176

161. Kim SJ, Yoon DH, Jaccard A, et al. A prognostic index for natural killer cell lymphoma after non-anthracycline-based treatment: a multicentre, retrospective analysis. *Lancet Oncol*. Mar 2016;17(3):389-400. doi:10.1016/S1470-2045(15)00533-1

162. Lee J, Suh C, Park YH, et al. Extranodal natural killer T-cell lymphoma, nasal-type: a prognostic model from a retrospective multicenter study. *Journal of clinical oncology : official journal of the American Society of Clinical Oncology*. Feb 1 2006;24(4):612-8. doi:10.1200/JCO.2005.04.1384

163. Montes-Mojarro IA, Chen BJ, Ramirez-Ibarguen AF, et al. Mutational profile and EBV strains of extranodal NK/T-cell lymphoma, nasal type in Latin America. *Mod Pathol*. May 2020;33(5):781-791. doi:10.1038/s41379-019-0415-5

164. van Dongen JJ, Langerak AW, Bruggemann M, et al. Design and standardization of PCR primers and protocols for detection of clonal immunoglobulin and T-cell receptor gene recombinations in suspect lymphoproliferations: report of the BIOMED-2 Concerted Action BMH4-CT98-3936. *Leukemia*. Dec 2003;17(12):2257-317. doi:10.1038/sj.leu.2403202

165. Quintanilla-Martinez L, Lome-Maldonado C, Schwarzmann F, et al. Post-transplantation lymphoproliferative disorders in Mexico: an aggressive clonal disease associated with Epstein-Barr virus type A. *Modern pathology : an official journal of the United States and Canadian Academy of Pathology, Inc*. Feb 1998;11(2):200-8.

166. Kim WY, Montes-Mojarro IA, Fend F, Quintanilla-Martinez L. Epstein-Barr Virus-Associated T and NK-Cell Lymphoproliferative Diseases. *Front Pediatr*. 2019;7:71. doi:10.3389/fped.2019.00071

167. Montes-Mojarro IA, Kim WY, Fend F, Quintanilla-Martinez L. Epstein - Barr virus positive T and NK-cell lymphoproliferations: Morphological features and differential diagnosis. *Semin Diagn Pathol*. Jan 2020;37(1):32-46. doi:10.1053/j.semdp.2019.12.004

168. Coppo P, Gouilleux-Gruart V, Huang Y, et al. STAT3 transcription factor is constitutively activated and is oncogenic in nasal-type NK/T-cell lymphoma. *Leukemia*. Sep 2009;23(9):1667-78. doi:10.1038/leu.2009.91

169. Zhang HF, Lai R. STAT3 in Cancer-Friend or Foe? *Cancers (Basel)*. Jul 3 2014;6(3):1408-40. doi:10.3390/cancers6031408

170. Calò V, Migliavacca M, Bazan V, et al. STAT proteins: from normal control of cellular events to tumorigenesis. *Journal of cellular physiology*. Nov 2003;197(2):157-68. doi:10.1002/jcp.10364

171. Siavash H, Nikitakis NG, Sauk JJ. Signal transducers and activators of transcription: insights into the molecular basis of oral cancer. *Crit Rev Oral Biol Med*. Sep 1 2004;15(5):298-307. doi:10.1177/154411130401500505

172. Shahmarvand N, Nagy A, Shahryari J, Ohgami RS. Mutations in the signal transducer and activator of transcription family of genes in cancer. *Cancer Sci*. Apr 2018;109(4):926-933. doi:10.1111/cas.13525

173. Tsuruta-Kishino T, Koya J, Kataoka K, et al. Loss of p53 induces leukemic transformation in a murine model of Jak2 V617F-driven polycythemia vera. *Oncogene*. Jun 8 2017;36(23):3300-3311. doi:10.1038/onc.2016.478

174. Rampal R, Ahn J, Abdel-Wahab O, et al. Genomic and functional analysis of leukemic transformation of myeloproliferative neoplasms. *Proceedings of the National Academy of Sciences of the United States of America*. Dec 16 2014;111(50):E5401-10. doi:10.1073/pnas.1407792111

175. Martinez GS, Ross JA, Kirken RA. Transforming Mutations of Jak3 (A573V and M511I) Show Differential Sensitivity to Selective Jak3 Inhibitors. *Clin Cancer Drugs*. 2016;3(2):131-137. doi:10.2174/2212697X03666160610085943

176. Hanissian SH, Geha RS. Jak3 is associated with CD40 and is critical for CD40 induction of gene expression in B cells. *Immunity*. Apr 1997;6(4):379-87.

177. Vaysberg M, Lambert SL, Krams SM, Martinez OM. Activation of the JAK/STAT pathway in Epstein Barr virus+-associated posttransplant lymphoproliferative disease: role of interferon-gamma. *Am J Transplant*. Oct 2009;9(10):2292-302. doi:10.1111/j.1600-6143.2009.02781.x

178. Hatzivassiliou E, Mosialos G. Cellular signaling pathways engaged by the Epstein-Barr virus transforming protein LMP1. *Front Biosci*. Jan 1 2002;7:d319-29. doi:10.2741/hatziva

179. Kobayashi H, Sagara J, Masumoto J, Kurita H, Kurashina K, Taniguchi S. Shifts in cellular localization of moesin in normal oral epithelium, oral epithelial dysplasia, verrucous carcinoma and oral squamous cell carcinoma. *J Oral Pathol Med*. Jul 2003;32(6):344-9. doi:10.1034/j.1600-0714.2003.00111.x

180. Li YY, Zhou CX, Gao Y. Moesin regulates the motility of oral cancer cells via MT1-MMP and E-cadherin/p120-catenin adhesion complex. *Oral Oncol*. Oct 2015;51(10):935-43. doi:10.1016/j.oraloncology.2015.07.003

181. Assao A, Yoshino PM, Medeiros MCM, et al. Moesin Involvement in Oral Carcinogenesis of the Lower Lip. *Anticancer Res*. May 2018;38(5):2755-2760. doi:10.21873/anticanres.12518

182. Lagresle-Peyrou C, Luce S, Ouchani F, et al. X-linked primary immunodeficiency associated with hemizygous mutations in the moesin (MSN) gene. *Journal of Allergy and Clinical Immunology*. 2016/12/01/ 2016;138(6):1681-1689.e8. doi:10.1016/j.jaci.2016.04.032

183. Tort F, Pinyol M, Pulford K, et al. Molecular characterization of a new ALK translocation involving moesin (MSN-ALK) in anaplastic large cell lymphoma. *Lab Invest*. Mar 2001;81(3):419-26. doi:10.1038/labinvest.3780249

184. Astolfi A, Fiore M, Melchionda F, Indio V, Bertuccio SN, Pession A. BCOR involvement in cancer. *Epigenomics*. May 2019;11(7):835-855. doi:10.2217/epi-2018-0195

185. Abuhadra N, Al-Issa K, Mukherjee S, et al. BCOR Mutations in Myelodysplastic Syndromes (MDS): Mutation Characteristics Impact Clinical

Outcomes. *Blood*. 2017;130(Supplement 1):5304-5304. doi:10.1182/blood.V130.Suppl_1.5304.5304

186. Martinez N, Almaraz C, Vaque JP, et al. Whole-exome sequencing in splenic marginal zone lymphoma reveals mutations in genes involved in marginal zone differentiation. *Leukemia*. Jun 2014;28(6):1334-40. doi:10.1038/leu.2013.365
187. Jallades L, Baseggio L, Sujobert P, et al. Exome sequencing identifies recurrent BCOR alterations and the absence of KLF2, TNFAIP3 and MYD88 mutations in splenic diffuse red pulp small B-cell lymphoma. *Haematologica*. Oct 2017;102(10):1758-1766. doi:10.3324/haematol.2016.160192
188. Sakano D, Kato A, Parikh N, et al. BCL6 canalizes Notch-dependent transcription, excluding Mastermind-like1 from selected target genes during left-right patterning. *Dev Cell*. Mar 16 2010;18(3):450-62. doi:10.1016/j.devcel.2009.12.023
189. Tanaka T, Nakajima-Takagi Y, Aoyama K, et al. Internal deletion of BCOR reveals a tumor suppressor function for BCOR in T lymphocyte malignancies. *J Exp Med*. Oct 2 2017;214(10):2901-2913. doi:10.1084/jem.20170167
190. Pugh TJ, Weeraratne SD, Archer TC, et al. Medulloblastoma exome sequencing uncovers subtype-specific somatic mutations. *Nature*. 2012/08/01 2012;488(7409):106-110. doi:10.1038/nature11329
191. Takahashi K, Hu B, Wang F, et al. Clinical implications of cancer gene mutations in patients with chronic lymphocytic leukemia treated with lenalidomide. *Blood*. Apr 19 2018;131(16):1820-1832. doi:10.1182/blood-2017-11-817296
192. Sun M, Zhou T, Jonasch E, Jope RS. DDX3 regulates DNA damage-induced apoptosis and p53 stabilization. *Biochim Biophys Acta*. Jun 2013;1833(6):1489-97. doi:10.1016/j.bbamcr.2013.02.026
193. Huang HS, Liao CK, Liu TT, You HL, Wang MC, Huang WT. TP53 mutations in peripheral mature T and NK cell lymphomas: a whole-exome sequencing study with correlation to p53 expression. *Hum Pathol*. Jun 6 2018;doi:10.1016/j.humpath.2018.05.026
194. Velculescu VE, El-Deiry WS. Biological and clinical importance of the p53 tumor suppressor gene. *Clin Chem*. Jun 1996;42(6 Pt 1):858-68.
195. Végran F, Rebucci M, Chevrier S, Cadouot M, Boidot R, Lizard-Nacol S. Only missense mutations affecting the DNA binding domain of p53 influence outcomes in patients with breast carcinoma. *PloS one*. 2013;8(1):e55103. doi:10.1371/journal.pone.0055103
196. Zain JM. Aggressive T-cell lymphomas: 2019 updates on diagnosis, risk stratification, and management. *American Journal of Hematology*. 2019;94(8):929-946. doi:10.1002/ajh.25513
197. Herrero AB, Rojas EA, Misiewicz-Krzeminska I, Krzeminski P, Gutiérrez NC. Molecular Mechanisms of p53 Deregulation in Cancer: An Overview in Multiple Myeloma. *Int J Mol Sci*. Nov 30 2016;17(12)doi:10.3390/ijms17122003

198. Ott G, Rosenwald A, Campo E. Understanding MYC-driven aggressive B-cell lymphomas: pathogenesis and classification. *Blood*. 2013;122(24):3884-3891. doi:10.1182/blood-2013-05-498329

199. Sanchez-Martin M, Ferrando A. The NOTCH1-MYC highway toward T-cell acute lymphoblastic leukemia. *Blood*. 2017;129(9):1124-1133. doi:10.1182/blood-2016-09-692582

200. Ng SB, Selvarajan V, Huang G, et al. Activated oncogenic pathways and therapeutic targets in extranodal nasal-type NK/T cell lymphoma revealed by gene expression profiling. *J Pathol*. Mar 2011;223(4):496-510. doi:10.1002/path.2823

201. Nagamine M, Takahara M, Kishibe K, et al. Sequence variations of Epstein-Barr virus LMP1 gene in nasal NK/T-cell lymphoma. *Virus Genes*. Jan 2007;34(1):47-54. doi:10.1007/s11262-006-0008-5

202. Correia S, Bridges R, Wegner F, et al. Sequence Variation of Epstein-Barr Virus: Viral Types, Geography, Codon Usage, and Diseases. *J Virol*. Nov 15 2018;92(22)doi:10.1128/JVI.01132-18

203. Gantuz M, Lorenzetti MA, Chabay PA, Preciado MV. A novel recombinant variant of latent membrane protein 1 from Epstein Barr virus in Argentina denotes phylogeographical association. *PloS one*. 2017;12(3):e0174221. doi:10.1371/journal.pone.0174221

204. Correia S, Palser A, Elgueta Karstegl C, et al. Natural Variation of Epstein-Barr Virus Genes, Proteins, and Primary MicroRNA. *J Virol*. 2017;91(15):e00375-17. doi:10.1128/jvi.00375-17

205. Zanella L, Riquelme I, Buchegger K, Abanto M, Ili C, Brebi P. A reliable Epstein-Barr Virus classification based on phylogenomic and population analyses. *Scientific Reports*. 2019/07/08 2019;9(1):9829. doi:10.1038/s41598-019-45986-3

206. Epstein MA, Rickinson AB, Weiss RA, McGeoch DJ. Molecular evolution of the Herpesvirinae. *Philosophical Transactions of the Royal Society of London Series B: Biological Sciences*. 2001;356(1408):421-435. doi: 10.1098/rstb.2000.0775

207. Zeng L, Huang W, Cao Z, et al. The correlation of clinicopathological features and prognosis in extranodal natural killer/T cell lymphoma: a report of 42 cases in the early stage. *Ann Hematol*. Jun 2019;98(6):1467-1476. doi:10.1007/s00277-019-03643-9

7. Declaration of contribution of others

Statutory Declaration

Hereby I affirm that I wrote this Doctoral thesis independently with the topic

“Molecular analysis and EBV strains of extranodal NK/T-cell lymphoma, nasal type in Latin America”

and that I used no other aids than those cited. In each individual case, I have clearly identified the source of the passages that are taken paraphrased from other works and the linked manuscript. The work was carried out in the Institute of Pathology and Neuropathology under the supervision of the Prof. Leticia Quintanilla-Fend. The study was designed by Prof. Quintanilla-Fends and her working group in collaboration with the Latin American Society of Hematopathology. All experiments were performed by me, following the advices of other laboratory members, specifically Dr. Julia Steinhilber and with the assistance of Biol. Esther Köhler. The statistical analysis was performed by me with the guidance of M.D.Lina Maria Serna-Higuita, as part of the consultation with the Institute of Biometry. I acknowledge the work done by collaborators.
I affirm to have completed the manuscript independently and I performed the scientific studies according to the principles of good scientific practice.

Ivonne A. Montes-Mojarro

_____

Tübingen, Germany

8. Publications

Publications related to this thesis:

- **Modern Pathology (IF: 6.36)**

Montes-Mojarro IA, Chen BJ, Ramirez-Ibarguen AF, Quezada-Fiallos CM, Pérez-Báez WB, Dueñas D, Casavilca-Zambrano S, Ortiz-Mayor M, Rojas-Bilbao E, García-Rivello H, Metrebian MF, Narbaitz M, Barrionuevo C, Lome-Maldonado C, Bonzheim I, Fend F, Steinhilber J, Quintanilla-Martinez L. Mutational profile and EBV strains of extranodal NK/T-cell lymphoma, nasal type in Latin America. *Mod Pathol* **2020** May; 33(5):781-791. doi: 10.1038/s41379-019-0415-5.

- **Seminars in diagnostic pathology (IF: 3.46)**

Montes-Mojarro IA, Kim WY, Fend F, Quintanilla-Martinez L. Epstein - Barr virus positive T and NK-cell lymphoproliferations: Morphological features and differential diagnosis. *Semin Diagn Pathol* 2020 Jan; **37**(1)**:** 32-46.

- **Cancers (IF: 6. 13)**

Montes-Mojarro IA, Fend F, Quintanilla-Martinez L. EBV and the Pathogenesis of NK/T Cell Lymphoma. *Cancers (Basel)* 2021 Mar 19; **13**(6).

Publications not related to this thesis:

- **Leukemia (IF: 11.58)**

Lobello, C.; Tichy, B.; Bystry, V.; Radova, L.; Filip, D.; Mraz, M.; **Montes-Mojarro, I.A.;** Prokoph, N.; Larose, H.; Liang, H.C., et al. STAT3 and TP53 mutations associate with poor prognosis in anaplastic large cell lymphoma. *Leukemia* **2021**, *35*, 1500-1505, doi:10.1038/s41375-020-01093-1.

- **Nature Communications (14.91)**

Liang, H.C.; Costanza, M.; Prutsch, N.; Zimmerman, M.W.; Gurnhofer, E.; **Montes-Mojarro, I.A.**; Abraham, B.J.; Prokoph, N.; Stoiber, S.; Tangermann, S., et al. Super-enhancer-based identification of a BATF3/IL-2R-module reveals vulnerabilities in anaplastic large cell lymphoma. *Nat Commun* **2021**, *12*, 5577, doi:10.1038/s41467-021-25379-9.

- **Blood (IF:23.62)**

Prokoph, N.; Probst, N.A.; Lee, L.C.; Monahan, J.M.; Matthews, J.D.; Liang, H.C.; Bahnsen, K.; **Montes-Mojarro, I.A**.; Karaca-Atabay, E.; Sharma, G.G., et al. IL10RA modulates crizotinib sensitivity in NPM1-ALK+ anaplastic large cell lymphoma. *Blood* **2020**, *136*, 1657-1669, doi:10.1182/blood.2019003793.

- **Frontiers in Pediatrics (3.42)**

Kim, W.Y.; **Montes-Mojarro, I.A.;** Fend, F.; Quintanilla-Martinez, L. Epstein-Barr Virus-Associated T and NK-Cell Lymphoproliferative Diseases. *Front Pediatr* **2019**, *7*, 71, doi:10.3389/fped.2019.00071.

- **Cancers (IF: 6.64)**

Montes-Mojarro, I.A.; Steinhilber, J.; Bonzheim, I.; Quintanilla-Martinez, L.; Fend, F. The Pathological Spectrum of Systemic Anaplastic Large Cell Lymphoma (ALCL). *Cancers (Basel)* **2018**, *10*, doi:10.3390/cancers10040107.

- **Blood (IF:23.62)**

Schmidt, J.; Ramis-Zaldivar, J.E.; Nadeu, F.; Gonzalez-Farre, B.; Navarro, A.; Egan, C.; **Montes-Mojarro, I.A.**; Marafioti, T.; Cabecadas, J.; van der Walt, J., et al. Mutations of MAP2K1 are frequent in pediatric-type follicular lymphoma and result in ERK pathway activation. *Blood* **2017**, *130*, 323-327, doi:10.1182/blood-2017-03-776278.

Acknowledgments

I would also like to acknowledge Professors Fend and Quintanilla-Fend, who are the real creators of this work, who gave me the opportunity to work in Tübingen and who also lead and help me to develop as a researcher. I would specially like to thank Professor Quintanilla-Fend, because of her time and her great interest in the work and my academic development.

I would like to thank all the people who worked very hard to accomplish this work, Irina Bonzheim, Julia Steinhilber, Wendy Perez and Bo-Jung Chen. To the Latin American Society of Hematopathology for their great effort to collect this series of ENKTCL cases. I would also like to thank Claudia Hermann and Esther Kohler for their excellent technical assistance.

To my dear colleagues Franzi Otto, Achim Rau, Antonio Vogelsberg, Vanessa Borgmann, Inga Müller and Leonie Frauenfeld, thanks for their cheers and their care. To my friends Monica García, Gloria Madrid; Yamel Cardona and Lina Serna-Higuita because of their affection and laughs that make my life happier.

During this work, I was supported by funding from the European Union's Horizon 2020 research and innovative Programme under the Marie Sklodowska-Curie grant agreement No. 675712.